

# MediEncoder: Nonlinear Representation Learning for High-Dimensional Causal Mediation Analysis

Shi Bo, Debarghya Mukherjee<sup>†</sup>, and AmirEmad Ghassami<sup>†</sup>  
 Department of Mathematics and Statistics, Boston University

## Abstract

Causal mediation analysis decomposes a treatment effect into indirect pathways through mediators and direct pathways not operating through them. Modern biomedical studies often involve high-dimensional covariates and mediators that are noisy proxies for lower-dimensional latent biological processes. Existing methods typically rely on sparsity, linear factor models, or ignore the connection among variables in the learned representations, which can be restrictive when measurements are nonlinear and covariate and mediator factors are structurally dependent. We propose **MediEncoder**, a representation-learning framework for nonlinear high-dimensional mediation analysis. MediEncoder jointly learns low-dimensional covariate and mediator representations using a coupled encoder–decoder architecture with a cross-factor network that links treatment and covariate representations to mediator representations. The learned features are then used in a cross-fitted efficient influence function-based estimator of natural direct and indirect effects. The resulting estimator is multiply robust and asymptotically normal under suitable regularity conditions. Simulations show that MediEncoder improves estimation accuracy over competing dimension-reduction approaches, and an application to Alzheimer’s Disease Neuroimaging Initiative data illustrates its utility in high-dimensional biomedical causal mediation analysis.

**Keywords**— Causal Inference; Dimension Reduction; Factor Models; High-Dimensional Data; Auto-encoder

## 1 Introduction

Causal mediation analysis seeks to explain how a treatment affects an outcome by decomposing the total effect into pathways operating through intermediate variables, or mediators (Baron and Kenny, 1986; Pearl, 2001; Imai et al., 2010; VanderWeele and Vansteelandt, 2014). In the potential-outcomes framework (Rubin, 1974), this amounts to studying counterfactual means whose contrasts yield the natural indirect effect, natural direct effect, and total effect. Classical methods typically assume that the relevant covariates and mediators are directly observed and low-dimensional. Modern biomedical studies often violate both assumptions: the causal mechanisms of interest are latent, while the available measurements are noisy, high-dimensional proxies. This setting arises across genomics and multi-omics applications. High-dimensional molecular measurements, such as metabolomic or multi-omics profiles, are often indirect views of lower-dimensional biological states (Wörheide et al., 2021; Rahnenführer et al., 2023). For example, oxidative stress has been proposed as a pathway linking depression to Alzheimer’s disease (Livingston et al., 2024; Buccellato et al., 2021), but reactive oxygen species are short-lived and difficult to measure directly (Katerji et al., 2019). Researchers therefore rely on downstream molecular signatures, including DNA damage and DNA methylation changes (Pandya

---

<sup>†</sup> Corresponding authors.

et al., 2013; Black et al., 2015; Miranda et al., 2000). Such measurements may be nonlinear functions of latent biological processes (Johnson et al., 2017; Verшинina et al., 2021); moreover, upstream covariate factors, treatments, and mediator factors can interact in ways that complicate causal identification and estimation (VanderWeele, 2015). These features motivate a mediation framework that can handle latent structure, high dimensionality, nonlinear measurement maps, and treatment–covariate–mediator interactions simultaneously.

Existing high-dimensional mediation methods address only parts of this problem. Sparse and variable-selection approaches can screen many candidate mediators (Zhang, 2022; Zhao and Luo, 2021; Bo et al., 2024; Jones et al., 2025), but they usually treat the observed variables as the mediators and do not model latent structure. Dimension-reduction methods based on PCA or linear factor models provide low-dimensional summaries (Derkach et al., 2019; Fan et al., 2025), but linear measurement maps can be restrictive in complex biological systems (Angermueller et al., 2016). Autoencoders and related deep models can learn nonlinear representations (Hinton and Salakhutdinov, 2006; Goodfellow et al., 2016), yet applying them separately to covariates and mediators ignores the structural dependence between the two latent systems. Deep mediation estimators such as (Xu et al., 2022) improve robustness to nuisance model misspecification, but do not explicitly target nonlinear high-dimensional latent-factor settings. Variational autoencoder approaches for indirectly observed mediators (Jiang et al., 2023) model latent mediators, but do not jointly accommodate latent nonlinear covariate structure, structural dependence between covariate and mediator representations, and interaction effects; see Appendix A for further discussion. Overall, existing methods address individual aspects of the problem but do not simultaneously address all the aforementioned challenges. The key missing ingredient is a framework that learns nonlinear covariate and mediator representations jointly, aligns them with the latent mediation structure, and then uses these representations in a statistically valid causal estimator.

To bridge this gap, we propose **MediEncoder**, a nonlinear representation-learning framework for high-dimensional causal mediation analysis. The method jointly learns low-dimensional representations of covariates and mediators through a structured encoder–decoder architecture. A cross-factor network links the treatment and covariate representation to the mediator representation, encouraging the learned features to respect the causal structure of the latent mediation problem. Exact recovery of the original latent factors is not required: it suffices to learn representations that preserve the information needed for the mediation functional, and our theory formalizes invariance under left-invertible transformations of the latent factors.

Our contributions are fourfold. **(i)** First, we introduce a nonlinear latent-factor framework for mediation analysis with high-dimensional covariates and mediators, avoiding linearity and sparsity requirements. **(ii)** Second, we develop MediEncoder, a coupled representation-learning algorithm that uses a cross-factor network to capture structural dependence between covariate and mediator representations. **(iii)** Third, we develop a modular asymptotic theory for the resulting cross-fitted efficient influence-function estimator. The theory formalizes that exact factor recovery is unnecessary: it suffices for the learned representation to approximate a left-invertible transformation of the latent factors, and the resulting inference remains valid under high-level factor-recovery and nuisance-rate conditions. **(iv)** Fourth, we demonstrate the empirical performance of MediEncoder in extensive simulations and in a biomedical application using data from the Alzheimer’s Disease Neuroimaging Initiative (ADNI).

## 2 Model Description

We consider a binary treatment (or exposure)  $A \in \{0, 1\}$  and a real-valued outcome  $Y \in \mathbb{R}$ . Let  $\mathbf{f}_X \in \mathbb{R}^p$  denote a vector of pre-treatment latent covariate factors and let  $\mathbf{f}_M \in \mathbb{R}^q$  denote a vector of latent mediator factors. The covariate factors may confound the treatment–mediator, treatment–outcome, and mediator–outcome relationships, whereas the mediator factors are the mechanisms through which part of the effect of  $A$  on  $Y$  may be transmitted. We use boldface notation for random latent vectors and write  $f_X$  and  $f_M$  for their generic values.

A compact structural representation of the latent mediation model is

$$\begin{aligned} \mathbf{f}_M &= (1 - A)\{\mu_0^*(\mathbf{f}_X) + \mathbf{u}_{XM}\} + A\{\mu_1^*(\mathbf{f}_X) + \mathbf{u}'_{XM}\}, \\ Y &= (1 - A)\{\mu_0(\mathbf{f}_X, \mathbf{f}_M) + \epsilon'\} + A\{\mu_1(\mathbf{f}_X, \mathbf{f}_M) + \epsilon\}, \end{aligned} \tag{2.1}$$

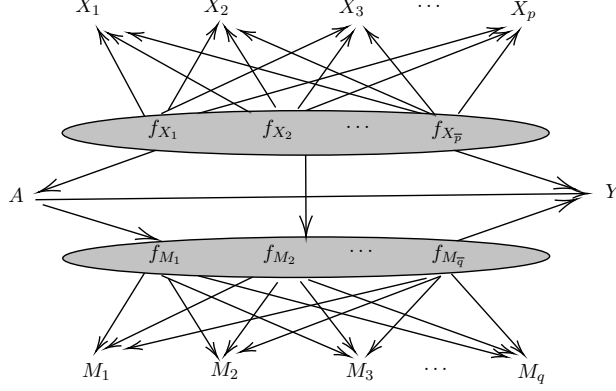


Figure 1: Causal relationship in the presence of latent factors  $\mathbf{f}_X$  and  $\mathbf{f}_M$

where  $\mu_0^*, \mu_1^* : \mathbb{R}^{\bar{p}} \rightarrow \mathbb{R}^{\bar{q}}$  and  $\mu_0, \mu_1 : \mathbb{R}^{\bar{p}+\bar{q}} \rightarrow \mathbb{R}$  are unknown structural functions and  $\epsilon, \epsilon', \mathbf{u}_{XM} \in \mathbb{R}^{\bar{q}}$ , and  $\mathbf{u}'_{XM} \in \mathbb{R}^{\bar{q}}$  are centered noise terms.

In the applications motivating this work,  $\mathbf{f}_X$  and  $\mathbf{f}_M$  are not directly observed. Instead, we observe high-dimensional measurements  $X \in \mathbb{R}^p$  and  $M \in \mathbb{R}^q$ , with  $p \gg \bar{p}$  and  $q \gg \bar{q}$ , that serve as noisy proxies for the latent factors; see Figure 1. We assume the measurement model

$$X = \phi_X(\mathbf{f}_X) + \mathbf{u}_X, \quad M = \phi_M(\mathbf{f}_M) + \mathbf{u}_M, \quad (2.2)$$

where  $\phi_X : \mathbb{R}^{\bar{p}} \rightarrow \mathbb{R}^p$  and  $\phi_M : \mathbb{R}^{\bar{q}} \rightarrow \mathbb{R}^q$  are unknown loading functions, and  $\mathbf{u}_X$  and  $\mathbf{u}_M$  are centered idiosyncratic errors. The classical linear factor model is a special case of (2.2), obtained by taking  $\phi_X(\mathbf{f}_X) = \Gamma_X \mathbf{f}_X$  and  $\phi_M(\mathbf{f}_M) = \Gamma_M \mathbf{f}_M$  for loading matrices  $\Gamma_X \in \mathbb{R}^{p \times \bar{p}}$  and  $\Gamma_M \in \mathbb{R}^{q \times \bar{q}}$ .

We next define the causal estimands at the latent-factor level. Let  $\mathbf{f}_M^{(a)}$  denote the mediator factors that would be observed if the treatment were set to  $a$ , and let  $Y^{(a, \mathbf{f}_M)}$  denote the potential outcome if the treatment were set to  $a$  and the mediator factors were set to the value  $\mathbf{f}_M$ . We use the shorthand  $Y^{(a)} = Y^{(a, \mathbf{f}_M^{(a)})}$ . For treatment level 1 relative to 0, the total effect decomposes as

$$\underbrace{\mathbb{E}\{Y^{(1)} - Y^{(0)}\}}_{\text{Total effect}} = \underbrace{\mathbb{E}\left[Y^{(1, \mathbf{f}_M^{(1)})} - Y^{(1, \mathbf{f}_M^{(0)})}\right]}_{\text{Natural indirect effect}} + \underbrace{\mathbb{E}\left[Y^{(1, \mathbf{f}_M^{(0)})} - Y^{(0, \mathbf{f}_M^{(0)})}\right]}_{\text{Natural direct effect}}. \quad (2.3)$$

Identification of parameters of the form  $\theta(a, a') = \mathbb{E}\{Y^{(a, \mathbf{f}_M^{(a')})}\}$  for any  $a, a' \in \{0, 1\}$  yields identifying the natural indirect effect, natural direct effect, and total effect through (2.3). Specifically, NIE =  $\theta(1, 1) - \theta(1, 0)$ , NDE =  $\theta(1, 0) - \theta(0, 0)$ , and TE =  $\theta(1, 1) - \theta(0, 0)$ . Hence, in what follows, we focus on the cross-world mean

$$\theta_0 := \theta(1, 0) = \mathbb{E}[Y^{(1, \mathbf{f}_M^{(0)})}].$$

To identify  $\theta_0$ , we impose the following standard causal assumptions.

**Assumption 2.1** (Consistency). *For all  $a \in \{0, 1\}$  and all mediator values  $f_M$ , if  $A = a$  and  $\mathbf{f}_M = f_M$ , then  $Y = Y^{(a, \mathbf{f}_M)}$ . In addition, if  $A = a$ , then  $\mathbf{f}_M = \mathbf{f}_M^{(a)}$ .*

**Assumption 2.2** (Positivity). *For every value  $f_X$  in the support of  $\mathbf{f}_X$ ,  $0 < \mathbb{P}(A = 1 \mid \mathbf{f}_X = f_X) < 1$ . Moreover, the conditional density of the mediator is positive, i.e.,  $0 < p(f_M \mid A = a, \mathbf{f}_X = f_X)$  for all  $A, f_X$ , and  $f_M$ .*

**Assumption 2.3** (Sequential exchangeability). *Let  $U \perp\!\!\!\perp V \mid W$  denote conditional independence of  $U$  and  $V$  given  $W$ . For all  $a, a' \in \{0, 1\}$  and all mediator values  $f_M$ ,*

1.  $\{Y^{(a, \mathbf{f}_M)}, \mathbf{f}_M^{(a)}\} \perp\!\!\!\perp A \mid \mathbf{f}_X$ ;
2.  $Y^{(a, \mathbf{f}_M)} \perp\!\!\!\perp \mathbf{f}_M^{(a')} \mid \mathbf{f}_X$ .

The first part rules out unmeasured confounding of the treatment–outcome and treatment–mediator relationships after conditioning on the latent covariate factors. The second part is the usual cross-world condition for natural direct and indirect effects; it rules out unmeasured mediator–outcome confounding not captured by  $\mathbf{f}_X$  and excludes treatment-induced mediator–outcome confounders.

Under Assumptions 2.1–2.3, the mediation functional is identified by the mediation formula (Pearl, 2001; Imai et al., 2010). Let  $\mu_1(\mathbf{f}_X, \mathbf{f}_M) := \mathbb{E}\{Y \mid A = 1, \mathbf{f}_X = \mathbf{f}_X, \mathbf{f}_M = \mathbf{f}_M\}$ . Then

$$\theta_0 = \mathbb{E}[\mathbb{E}\{\mathbb{E}(Y \mid A = 1, \mathbf{f}_X, \mathbf{f}_M) \mid A = 0, \mathbf{f}_X\}]. \quad (2.4)$$

A direct plug-in estimator based on (2.4) can be sensitive to nuisance-model misspecification. Following the semiparametric theory of Tchetgen Tchetgen and Shpitser (2012), we instead use the efficient influence function-based estimator of  $\theta_0$ . Define the nuisance functions

$$\begin{aligned} \pi_1(\mathbf{f}_X) &:= \mathbb{P}(A = 1 \mid \mathbf{f}_X = \mathbf{f}_X), & \mu_1(\mathbf{f}_X, \mathbf{f}_M) &:= \mathbb{E}\{Y \mid A = 1, \mathbf{f}_X = \mathbf{f}_X, \mathbf{f}_M = \mathbf{f}_M\}, \\ \pi_2(\mathbf{f}_X, \mathbf{f}_M) &:= \frac{p(\mathbf{f}_M \mid A = 0, \mathbf{f}_X)}{p(\mathbf{f}_M \mid A = 1, \mathbf{f}_X)}, & \mu_{10}(\mathbf{f}_X) &:= \mathbb{E}\{\mu_1(\mathbf{f}_X, \mathbf{f}_M) \mid A = 0, \mathbf{f}_X = \mathbf{f}_X\}. \end{aligned} \quad (2.5)$$

With these definitions,  $\theta_0 = \mathbb{E}\{\mu_{10}(\mathbf{f}_X)\}$ , and the efficient influence function is

$$\begin{aligned} \psi_0(O) &= \mu_{10}(\mathbf{f}_X) - \theta_0 + \frac{A}{\pi_1(\mathbf{f}_X)} \pi_2(\mathbf{f}_X, \mathbf{f}_M) \{Y - \mu_1(\mathbf{f}_X, \mathbf{f}_M)\} \\ &\quad + \frac{1 - A}{1 - \pi_1(\mathbf{f}_X)} \{\mu_1(\mathbf{f}_X, \mathbf{f}_M) - \mu_{10}(\mathbf{f}_X)\}, \end{aligned} \quad (2.6)$$

where  $O = (Y, A, \mathbf{f}_X, \mathbf{f}_M)$ . In the oracle setting where  $(\mathbf{f}_X, \mathbf{f}_M)$  are observed, replacing the nuisance functions in (2.6) by estimates and solving the corresponding estimating equation gives

$$\begin{aligned} \hat{\theta}_0^{\text{IF}} &= \mathbb{P}_n \left[ \hat{\mu}_{10}(\mathbf{f}_X) + \frac{A}{\hat{\pi}_1(\mathbf{f}_X)} \hat{\pi}_2(\mathbf{f}_X, \mathbf{f}_M) \{Y - \hat{\mu}_1(\mathbf{f}_X, \mathbf{f}_M)\} \right. \\ &\quad \left. + \frac{1 - A}{1 - \hat{\pi}_1(\mathbf{f}_X)} \{\hat{\mu}_1(\mathbf{f}_X, \mathbf{f}_M) - \hat{\mu}_{10}(\mathbf{f}_X)\} \right], \end{aligned} \quad (2.7)$$

where  $\mathbb{P}_n$  denotes the empirical average. However, in reality, we only observe  $(X, M)$ , (ultra)-high-dimensional proxies of  $(\mathbf{f}_X, \mathbf{f}_M)$ , and the latent factors in this oracle estimator are replaced by learned representations, as elaborated in the next section.

### 3 Proposed Method: MediEncoder

We now describe MediEncoder, a cross-fitted procedure for estimating the mediation functional  $\theta_0 = \theta(1, 0) = \mathbb{E}\{Y^{(1, \mathbf{f}_M^{(0)})}\}$ . The method has two main components. First, it learns low-dimensional nonlinear representations of the high-dimensional covariates and mediators through a coupled autoencoder. Second, it uses these learned representations to estimate the nuisance functions in the efficient-influence function estimator from Section 2.

**Coupled representation learning.** Let  $z_{XM} = (g_X, g_M, g_{XM}, h_X, h_M) \in \mathcal{Z}_{\text{NN}}$ , where  $g_X : \mathbb{R}^p \rightarrow \mathbb{R}^{\tilde{p}}$  and  $h_X : \mathbb{R}^{\tilde{p}} \rightarrow \mathbb{R}^p$  are the covariate encoder and decoder,  $g_M : \mathbb{R}^q \rightarrow \mathbb{R}^{\tilde{q}}$  and  $h_M : \mathbb{R}^{\tilde{q}} \rightarrow \mathbb{R}^q$  are the mediator encoder and decoder, and  $g_{XM} : \{0, 1\} \times \mathbb{R}^{\tilde{p}} \rightarrow \mathbb{R}^{\tilde{q}}$  maps the treatment and covariate representation to the mediator-representation space. For a training index set  $\mathcal{I}$ , define the empirical loss

$$\begin{aligned} \mathcal{L}_\lambda(z_{XM}; \mathcal{I}) &= \frac{1}{|\mathcal{I}|} \sum_{i \in \mathcal{I}} \left[ \lambda_1 \|X_i - h_X(g_X(X_i))\|_2^2 + \lambda_2 \|M_i - h_M(g_M(M_i))\|_2^2 \right. \\ &\quad \left. + \lambda_3 \|g_M(M_i) - g_{XM}(A_i, g_X(X_i))\|_2^2 \right], \end{aligned} \quad (3.1)$$

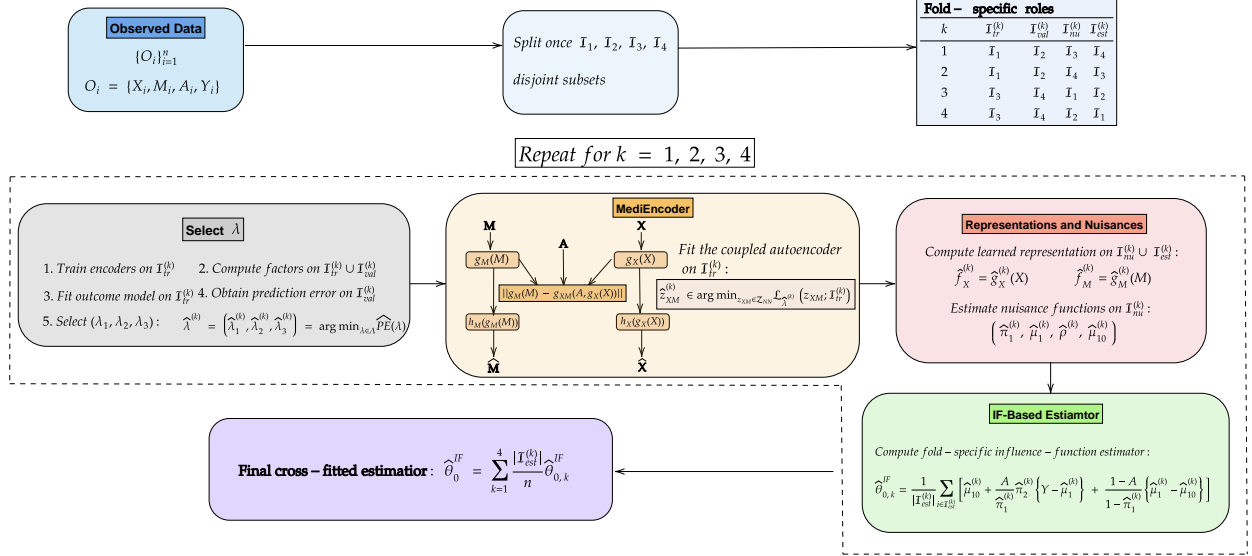


Figure 2: Schematic overview of MediEncoder. The observed data are split into disjoint subsets for representation learning, tuning, nuisance estimation, and final evaluation.

where  $\lambda = (\lambda_1, \lambda_2, \lambda_3)$  consists of nonnegative tuning parameters. The first two terms are reconstruction losses for  $X$  and  $M$ . The third term couples the two representations by encouraging the mediator representation to be predictable from the treatment and the covariate representation, matching the structural dependence of the latent mediator factors on  $(A, \mathbf{f}_X)$ . Unlike a standard multi-view autoencoder, the coupling is *directional and treatment-aware*: the mediator representation is encouraged to be predictable from  $(A, g_X(X))$ , obeying the latent structural equation for  $\mathbf{f}_M$ . After representation learning, only the encoders  $\hat{g}_X$  and  $\hat{g}_M$  are used in the influence function-based estimator; the decoders and  $g_{XM}$  act as regularizers during training.

The working dimensions  $(\tilde{p}, \tilde{q})$  need not equal the true latent dimensions  $(\bar{p}, \bar{q})$ . The theoretical results in Section 4 require the learned representation to approximate a sufficiently informative, left-invertible transformation of the latent factors. Thus, exact recovery of the original factors is not required, but the chosen representation dimensions must be large enough to retain the information relevant for the mediation functional.

**Cross-fitted estimation.** Algorithm 1 gives the full procedure for estimating  $\theta_0$ . The data are split into four disjoint subsets. In each fold, these subsets play four distinct roles: representation training, tuning, nuisance estimation, and final evaluation. This separation ensures that the summands used to evaluate the influence function-based estimator are not used to train either the representation or the nuisance functions. The particular rotations below are one convenient choice; any rotations with the same disjointness property can be used.

The estimator in (3.4) is the empirical analogue of the efficient influence function representation in Section 2, with the latent factors replaced by fold-specific learned representations. The auxiliary propensity score  $\rho(f_X, f_M) = \mathbb{P}(A = 1 \mid \mathbf{f}_X = f_X, \mathbf{f}_M = f_M)$  is used only to estimate the mediator density ratio  $\pi_2$ . Indeed,

$$\frac{\rho(f_M \mid A = 0, f_X)}{\rho(f_M \mid A = 1, f_X)} = \frac{\mathbb{P}(A = 0 \mid f_X, f_M) \mathbb{P}(A = 1 \mid f_X)}{\mathbb{P}(A = 1 \mid f_X, f_M) \mathbb{P}(A = 0 \mid f_X)}, \quad (3.2)$$

which yields (C.2) after substituting  $\rho$  and  $\pi_1$ .

The same construction estimates any mediation functional  $\theta(a, a') = \mathbb{E}\{Y^{(a, \mathbf{f}_M^{(a')})}\}$ . Consequently,

$$\widehat{\text{NIE}} = \hat{\theta}^{\text{IF}}(1, 1) - \hat{\theta}^{\text{IF}}(1, 0), \quad \widehat{\text{NDE}} = \hat{\theta}^{\text{IF}}(1, 0) - \hat{\theta}^{\text{IF}}(0, 0), \quad \widehat{\text{TE}} = \hat{\theta}^{\text{IF}}(1, 1) - \hat{\theta}^{\text{IF}}(0, 0).$$

Section 4 establishes conditions under which  $\hat{\theta}_0^{\text{IF}}$  is  $\sqrt{n}$ -consistent and asymptotically normal.

**Remark 3.1** (Capacity of the cross-factor network  $g_{XM}$ ). *The cross-factor network  $g_{XM}$  should have moderate capacity. If it is overly expressive, it can approximate an arbitrary mapping from  $(A, g_X(X))$  to  $g_M(M)$ , driving the alignment loss in (3.1) close to zero regardless of the quality of  $g_X$  and  $g_M$ . In that case,  $g_{XM}$  absorbs discrepancies between the two representations, and the alignment term no longer enforces a meaningful structural relationship. Conversely, if  $g_{XM}$  is too restrictive, it may fail to capture the dependence of the mediator factors on the treatment and covariate factors. In practice, we use a lower- or moderate-capacity architecture for  $g_{XM}$ , relative to the encoders and decoders, so that the alignment term couples the representations without allowing the cross-factor network to overfit.*

---

**Algorithm 1** MediEncoder: Estimating  $\theta_0$  with cross-fitting

---

**Require:** Data  $\{(X_i, A_i, M_i, Y_i)\}_{i=1}^n$ ; representation dimensions  $(\tilde{p}, \tilde{q})$ ; tuning grid  $\Lambda$

**Ensure:** Cross-fitted estimator  $\hat{\theta}_0^{\text{IF}}$

- 1: Split  $\{1, \dots, n\}$  into four disjoint subsets  $\mathcal{I}_1, \dots, \mathcal{I}_4$ , each of size approximately  $n/4$ . Use the following fold assignments, where the four columns denote the representation-training, validation, nuisance-estimation, and final-evaluation sets:

$k$	$\mathcal{I}_{\text{tr}}^{(k)}$	$\mathcal{I}_{\text{val}}^{(k)}$	$\mathcal{I}_{\text{nu}}^{(k)}$	$\mathcal{I}_{\text{est}}^{(k)}$
1	$\mathcal{I}_1$	$\mathcal{I}_2$	$\mathcal{I}_3$	$\mathcal{I}_4$
2	$\mathcal{I}_1$	$\mathcal{I}_2$	$\mathcal{I}_4$	$\mathcal{I}_3$
3	$\mathcal{I}_3$	$\mathcal{I}_4$	$\mathcal{I}_1$	$\mathcal{I}_2$
4	$\mathcal{I}_3$	$\mathcal{I}_4$	$\mathcal{I}_2$	$\mathcal{I}_1$

- 2: **for**  $k = 1, \dots, 4$  **do**

- 3: Set  $\mathcal{I}_{\text{tr}}^{(k)}, \mathcal{I}_{\text{val}}^{(k)}, \mathcal{I}_{\text{nu}}^{(k)}, \mathcal{I}_{\text{est}}^{(k)}$  according to the  $k$ -th row above.

- 4: Select  $\hat{\lambda}^{(k)} = (\hat{\lambda}_1^{(k)}, \hat{\lambda}_2^{(k)}, \hat{\lambda}_3^{(k)}) \in \Lambda$  using the training and validation sets  $(\mathcal{I}_{\text{tr}}^{(k)}, \mathcal{I}_{\text{val}}^{(k)})$  via Algorithm 2.

- 5: Fit the coupled autoencoder on  $\mathcal{I}_{\text{tr}}^{(k)}$ :

$$\hat{z}_{XM}^{(k)} = (\hat{g}_X^{(k)}, \hat{g}_M^{(k)}, \hat{g}_{XM}^{(k)}, \hat{h}_X^{(k)}, \hat{h}_M^{(k)}) \in \arg \min_{z_{XM} \in \mathcal{Z}_{\text{NN}}} \mathcal{L}_{\hat{\lambda}^{(k)}}(z_{XM}; \mathcal{I}_{\text{tr}}^{(k)}). \quad (3.3)$$

- 6: Compute learned representations for all  $i \in \mathcal{I}_{\text{nu}}^{(k)} \cup \mathcal{I}_{\text{est}}^{(k)}$ :

$$\hat{\mathbf{f}}_{X,i}^{(k)} = \hat{g}_X^{(k)}(X_i), \quad \hat{\mathbf{f}}_{M,i}^{(k)} = \hat{g}_M^{(k)}(M_i).$$

- 7: Estimate nuisance functions via  $\hat{\pi}_1^{(k)}, \hat{\mu}_1^{(k)}, \hat{\mu}_{10}^{(k)}$ , and  $\hat{\rho}^{(k)}$  on  $\mathcal{I}_{\text{nu}}^{(k)}$  using the learners provided in Appendix C. Set  $\hat{\pi}_2^{(k)}$  as per Equation (3.2).

- 8: Compute the fold-specific influence-function estimator:

$$\begin{aligned} \hat{\theta}_{0,k}^{\text{IF}} = & \frac{1}{|\mathcal{I}_{\text{est}}^{(k)}|} \sum_{i \in \mathcal{I}_{\text{est}}^{(k)}} \left[ \hat{\mu}_{10}^{(k)}(\hat{\mathbf{f}}_{X,i}^{(k)}) + \frac{A_i}{\hat{\pi}_1^{(k)}(\hat{\mathbf{f}}_{X,i}^{(k)})} \hat{\pi}_2^{(k)}(\hat{\mathbf{f}}_{X,i}^{(k)}, \hat{\mathbf{f}}_{M,i}^{(k)}) \{Y_i - \hat{\mu}_1^{(k)}(\hat{\mathbf{f}}_{X,i}^{(k)}, \hat{\mathbf{f}}_{M,i}^{(k)})\} \right. \\ & \left. + \frac{1 - A_i}{1 - \hat{\pi}_1^{(k)}(\hat{\mathbf{f}}_{X,i}^{(k)})} \left\{ \hat{\mu}_1^{(k)}(\hat{\mathbf{f}}_{X,i}^{(k)}, \hat{\mathbf{f}}_{M,i}^{(k)}) - \hat{\mu}_{10}^{(k)}(\hat{\mathbf{f}}_{X,i}^{(k)}) \right\} \right]. \end{aligned} \quad (3.4)$$

- 9: **end for**

- 10: Return the weighted cross-fitted estimator

$$\hat{\theta}_0^{\text{IF}} = \sum_{k=1}^4 \frac{|\mathcal{I}_{\text{est}}^{(k)}|}{n} \hat{\theta}_{0,k}^{\text{IF}}.$$


---

## 4 Theoretical Analysis

In this section, we present theoretical results establishing the  $\sqrt{n}$ -consistency and asymptotic normality of the proposed estimator  $\hat{\theta}_0^{\text{IF}}$ . As is clear from Algorithm 1, the estimation procedure relies on two key ingredients: (i) constructing  $(\hat{\mathbf{f}}_X, \hat{\mathbf{f}}_M)$ , a surrogate of the latent factors  $(\mathbf{f}_X, \mathbf{f}_M)$ , from the high-dimensional observations  $(X, M)$ ; and (ii) estimating the nuisance functions that enter the influence function representation by regressing either  $Y$  or  $A$  on these learned representations. Moreover, as discussed in the Section 1, we do not assume that the true factor dimensions are known. Instead, we only require an upper bound on them, and our theoretical framework is flexible enough to accommodate this setting. We impose the following regularity condition on the data-generating process, in addition to the standard causal identification assumptions in Assumptions 2.1–2.3.

**Assumption 4.1.** *There exists a constant  $C < \infty$  such that  $\mathbb{E}[(Y - \mu_1(\mathbf{f}_X, \mathbf{f}_M))^2 \mid A = 1, \mathbf{f}_X, \mathbf{f}_M] \leq C$  and  $\mathbb{E}[(\mu_1(\mathbf{f}_X, \mathbf{f}_M) - \mu_{10}(\mathbf{f}_X))^2 \mid A = 0, \mathbf{f}_X] \leq C$ .*

Assumption 4.1 is mild. It requires the outcome noise and the relevant conditional mean contrast to have finite conditional second moments, which is a basic regularity requirement for establishing a central limit theorem. We further have the following requirement on the estimated factor surrogates.

**Assumption 4.2.** *The estimated factors  $\hat{\mathbf{f}} = (\hat{\mathbf{f}}_X, \hat{\mathbf{f}}_M)$  satisfy:*

$$\|\hat{\mathbf{f}} - \nu(\mathbf{f})\|_{L_2(P)} = O_p(\delta_{n,f}), \quad \delta_{n,f} \downarrow 0 \text{ as } n \uparrow \infty, \quad (4.1)$$

for some  $\nu : \mathbb{R}^{\bar{p}+\bar{q}} \mapsto \mathbb{R}^{\bar{p}+\bar{q}}$ , where  $\nu = (\nu_X, \nu_M)$  admits a Lipschitz left inverse  $\nu^{-1} : \mathbb{R}^{\bar{p}+\bar{q}} \mapsto \mathbb{R}^{\bar{p}+\bar{q}}$ .

In Appendix H (Proposition H.1), we give a sufficient condition showing that Equation (4.1) follows from three interpretable ingredients: (i) the existence of oracle encoders that recover a left-invertible transformation of the latent factors up to denoising error; (ii) a local stability, or quadratic-growth, condition for the population MediEncoder objective around the oracle representation; and (iii) a small excess-risk bound for the fitted MediEncoder. This result shows that the factor condition is not tied to a particular algorithm, but can be verified whenever the representation learning objective is stable, and the learned encoder has small population excess risk. In linear factor models with pervasive factors, diversified projection provides one such example Fan et al. (2013); Fan and Gu (2023); Fan and Liao (2022). For nonlinear factor models, recent autoencoder theory Xiu and Shen (2024) provides related recovery guarantees up to functional transformations. Translating these guarantees into (4.1) requires additional stability conditions on the learned bottleneck map; we discuss this connection in Appendix H.

We now present our first main result which shows that if the estimated factor surrogates and the nuisance estimators converge at appropriate rates, then the final estimator  $\hat{\theta}^{\text{IF}}$  is  $\sqrt{n}$ -consistent and asymptotically normal.

**Theorem 4.3.** *Suppose Assumptions 2.1–4.2 hold and the nuisance estimators from Line 7 of Algorithm 1 are Lipschitz continuous, and  $(\pi_1, \hat{\pi}_1, \rho, \hat{\rho})$  are uniformly bounded away from 0 and 1, and*

$$\begin{aligned} \|\hat{\pi}_1 - \pi_1 \circ \nu_X^{-1}\|_{L_2(P)} &= O_p(\delta_{n,\pi_1}), & \|\hat{\mu}_1 - \mu_1 \circ \nu^{-1}\|_{L_2(P)} &= O_p(\delta_{n,\mu_1}), \\ \|\hat{\mu}_{10} - \mu_{10} \circ \nu_X^{-1}\|_{L_2(P)} &= O_p(\delta_{n,\mu_{10}}), & \|\hat{\rho} - \rho \circ \nu^{-1}\|_{L_2(P)} &= O_p(\delta_{n,\rho}). \end{aligned} \quad (4.2)$$

for some rates  $\{\delta_{n,\eta} : \eta \in \Xi\} \downarrow 0$  as  $n \uparrow \infty$ , that satisfy:

$$\begin{aligned} \sqrt{n}(\delta_{n,\pi_1} + \delta_{n,\rho} + \delta_{n,f} + n^{-1/2})(\delta_{n,\mu_1} + \delta_{n,f} + n^{-1/2}) &= o(1), \\ \sqrt{n}(\delta_{n,\pi_1} + \delta_{n,f} + n^{-1/2})(\delta_{n,\mu_{10}} + \delta_{n,f} + n^{-1/2}) &= o(1). \end{aligned} \quad (4.3)$$

Then, the estimator  $\hat{\theta}_0^{\text{IF}}$  satisfies  $\sqrt{n}(\hat{\theta}_0^{\text{IF}} - \theta_0) \xrightarrow{\mathcal{L}} \mathcal{N}(0, \sigma_{\text{eff}}^2)$ , where  $\sigma_{\text{eff}}^2$  is the semiparametrically efficient variance of the oracle latent-factor model. A sufficient condition for Equation (4.3) is  $\max\{\delta_{n,\pi_1}, \delta_{n,\rho}, \delta_{n,\mu_1}, \delta_{n,\mu_{10}}, \delta_{n,f}\} = o(n^{-1/4})$ .

**Remark 4.4.** It is important to note that the transformation  $\nu$  is an unknown population-level map and is not estimated by our procedure. It is used only to formalize the class of latent representations under which the mediation functional remains estimable at root- $n$  rate. Thus, our theory does not require recovering the true factors themselves; it only requires the learned representation to be close to some left-invertible transformation of them.

Theorem 4.3 only requires weak rate requirements on the learned representation and nuisance functions irrespective of what algorithm is being used. We now verify these rates under a compositional smoothness assumption for DNN-based estimators as used in Algorithm 1. However, the nuisances are estimated using learned representation  $\widehat{\mathbf{f}}$ , but their population targets are functions of  $\mathbf{f}$  or equivalently  $\nu(\mathbf{f})$  as  $\nu$  is left-invertible; hence, the factor learning error  $\delta_{n,f}$  contributes to the nuisance parameter estimation. We start with a definition of the compositional function class, namely Hierarchical Compositional Model (HCM):

**Definition 4.5** (Hierarchical Composition Model). Let  $\mathcal{P} \subset [1, \infty) \times \mathbb{N}$ . For  $\ell = 1$ , define a collection  $\mathcal{H}(d, 1, \mathcal{P})$  consisting of functions  $h(x) = g(x_{\pi(1)}, \dots, x_{\pi(t)})$ , where  $g : \mathbb{R}^t \rightarrow \mathbb{R}$  is  $(\beta, C)$  Hölder-smooth for some  $(\beta, t) \in \mathcal{P}$ . For  $\ell > 1$ ,  $\mathcal{H}(d, \ell, \mathcal{P})$  is defined recursively by  $h(x) = g(h_1(x), \dots, h_t(x))$ , where  $g : \mathbb{R}^t \rightarrow \mathbb{R}$  is  $(\beta, C)$  Hölder-smooth for some  $(\beta, t) \in \mathcal{P}$ , and each  $h_j \in \mathcal{H}(d, \ell - 1, \mathcal{P})$ . The dimensional-adjusted smoothness (DAS) is defined as  $\gamma^* := \inf_{(\beta, t) \in \mathcal{P}} (\beta/t)$ .

HCM includes ordinary Hölder classes as well as additive, single-index, and other low-dimensional compositional models. For instance, if  $h(x) = \sum_{j=1}^d h_j(x_j)$  or  $h(x) = g(x^\top \beta_0)$  with  $\beta$ -smooth univariate components or link functions, then the effective index is  $\gamma^* = \beta$  up to smooth linear and aggregation maps, whereas a generic  $d$ -variate Hölder function has  $\gamma^* = \beta/d$ . Thus  $\gamma^*$  can be much larger than the ambient smoothness index, and DNN-based estimators adaptively achieve faster rates than those dictated by the ambient dimension. To that end, we require the following condition.

**Assumption 4.6.** The mean functions  $\mu_1$  and  $\mu_{10}$  are uniformly bounded, and  $(\epsilon, \epsilon', \mathbf{u}_X, \mathbf{u}_M)$  in Equation (2.1) are independent of  $(\mathbf{f}_X, \mathbf{f}_M)$  and centered sub-Gaussian random variables.

**Theorem 4.7.** Suppose Assumptions 2.1-2.3, 4.2, and 4.6 hold. Define the transformed nuisances as  $\eta_{\mu_1} := \mu_1 \circ \nu^{-1}$ ,  $\eta_{10} := \mu_{10} \circ \nu_X^{-1}$ ,  $\eta_{\pi_1} := \pi_1 \circ \nu_X^{-1}$  and  $\eta_\rho := \rho \circ \nu^{-1}$ . Assume that each of these  $\eta_j$  admits a bounded Lipschitz HCM extension with DAS  $\gamma_j^*$  to a compact neighborhood containing both the transformed  $(\nu(\mathbf{f}))$  and learned representations  $(\widehat{\mathbf{f}})$ . Assume also the overlap conditions that  $\pi_1$  and  $\rho$  are bounded away from 0 and 1. Then, under a proper choice of width and depth (see Appendix G for details) of deep ReLU networks, the estimators obtained in Line 7 of Algorithm 1 satisfy:

$$\|\widehat{\eta}_j(\widehat{\mathbf{f}}) - \eta_j(\nu(\mathbf{f}))\|_{L_2(P)}^2 = O_p(\delta_{n,j}^2), \quad \text{with } \delta_{n,j}^2 = n^{-2\gamma_j^*/(2\gamma_j^*+1)}(\log n)^{a_j} + \delta_{n,f}^2,$$

for  $j \in \{\pi_1, \rho, \mu_1\}$ , and  $a_j > 0$  fixed constant. Further  $\widehat{\eta}_{10}$  satisfies:

$$\|\widehat{\eta}_{10}(\widehat{\mathbf{f}}_X) - \eta_{10}(\nu_X(\mathbf{f}_X))\|_{L_2(P)}^2 = O_p(\delta_{n,10}^2), \quad \delta_{n,10}^2 = n^{-2\gamma_{10}^*/(2\gamma_{10}^*+1)}(\log n)^{a_{10}} + \delta_{n,f}^2 + \delta_{n,\mu_1}^2.$$

Theorem 4.7 implies that, if  $\gamma_j^* > 1/2$  and  $\delta_{n,f} = o(n^{-1/4})$ , then all nuisance functions are estimable at rates faster than  $n^{-1/4}$ . Consequently, Equation (4.3) in Theorem 4.3 holds, and  $\widehat{\theta}^{\text{IF}}$  is  $\sqrt{n}$ -CAN. The rate for  $\mu_{10}$  additionally depends on the rate for  $\mu_1$ , because  $\mu_{10}$  is estimated by regressing the estimated responses  $\widehat{\mu}_1(\widehat{\mathbf{f}}_X, \widehat{\mathbf{f}}_M)$  on  $\widehat{\mathbf{f}}_X$ . Our theory extends the results of Fan and Gu (2024) to nonlinear factor estimation and nuisance estimation under logistic-link losses.

## 5 Experiments

### 5.1 Simulation and Ablation Study

We evaluate MediEncoder in nonlinear high-dimensional settings generated from the latent mediation model in Section 2. The target is  $\theta_0 = \theta(1, 0)$ , estimated by the cross-fitted efficient influence function-based estimator

$n$	Estimator	SD	RMSE	CI Length	Coverage
300	Projection	1.831	2.011	7.175	0.951
	Autoencoder	1.533	1.672	6.011	0.955
	VAE	0.412	0.423	1.616	0.952
	IMAVAE	0.442	0.733	1.740	0.875
	MediEncoder	0.366	0.388	1.435	0.945
1200	Projection	0.319	0.439	1.251	0.855
	Autoencoder	0.415	0.465	1.626	0.915
	VAE	0.329	0.332	1.290	0.935
	IMAVAE	0.341	0.390	1.337	0.927
	MediEncoder	0.269	0.288	1.056	0.925
3000	Projection	0.262	0.368	1.027	0.862
	Autoencoder	0.331	0.396	1.294	0.885
	VAE	0.331	0.343	1.294	0.930
	IMAVAE	0.344	0.349	1.350	0.947
	MediEncoder	0.270	0.290	1.059	0.955

Table 1: Representative simulation results under the nonlinear wavelet DGP with  $p = 2000$ ,  $q = 1000$ ,  $\sigma_X = 2$ ,  $\sigma_M = 1$ ,  $\sigma_Y = 1$ ,  $\bar{p} = \bar{q} = 5$ ,  $\tilde{p} = \tilde{q} = 7$ , and  $B = 500$  replications.

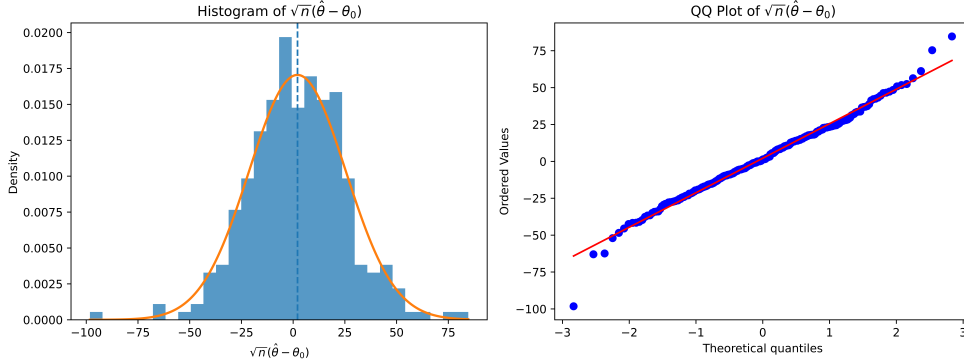


Figure 3: Histogram and Q-Q plot of  $\sqrt{n}(\hat{\theta}_0^{\text{IF}} - \theta_0)$  for  $n = 2000$  and  $p + q = 1000$  under the nonlinear wavelet DGP.

in (2.7). We compare with the baseline representation methods described in Appendix B. Across  $B = 500$  Monte Carlo replications, we report the empirical standard deviation (SD), root mean squared error (RMSE), average length of the nominal 95% confidence interval, and empirical coverage. The full data-generating process is given in Appendix D.

**Simulation settings.** For each replication, we generate  $n \in \{100, 300, 800, 1200, 2000, 3000\}$  observations and consider  $p + q \in \{1000, 3000, 5000, 10000\}$ . The latent dimensions are fixed at  $\bar{p} = \bar{q} = 5$ , while the learned representation dimensions are set to  $\tilde{p} = \tilde{q} = 7$ . The mediator and outcome noise standard deviations are  $\sigma_M = \sigma_Y = 1$ ; the covariate noise level is set to  $\sigma_X = 2$  for the first two dimension settings and  $\sigma_X = 1.5$  for the larger settings. Observed covariates and mediators are generated from nonlinear additive Haar-wavelet loading functions with independent Gaussian idiosyncratic noise.

All representation and nuisance models are multilayer perceptrons with ReLU activations. The encoders  $g_X$  and  $g_M$  use two hidden layers of widths 300 and 200, and the decoders  $h_X$  and  $h_M$  use the reverse architecture. The cross-factor network  $g_{XM}$  uses one hidden layer of width 50, giving it lower capacity than the encoders and decoders. For nuisance estimation, we fit  $\pi_1$ ,  $\rho$ ,  $\mu_1$ , and  $\mu_{10}$  using fully connected networks; the density ratio  $\pi_2$  is then computed from  $\hat{\pi}_1$  and  $\hat{\rho}$  using Bayes' rule as in Algorithm 1. Networks are trained with Adam

Effect	Estimate	Bootstrap Mean	Quantile CI (95%)
Direct	3.2163	2.9623	(0.2268, 5.9212)
Indirect	0.3527	0.2370	(-2.1451, 3.7704)
Total	3.5691	3.1994	(0.7321, 5.5262)

Table 2: Estimated natural direct, natural indirect, and total effects in the ADNI analysis using the binarized threshold  $GDS > 5$ . The selected tuning parameter was  $\hat{\lambda} = (0.5, 0.2, 0.3)$ .

using initial learning rate  $10^{-3}$ , weight decay  $10^{-3}$ , a learning-rate decay factor of 0.5 every 30 epochs, and at most 300 epochs. We use mean squared error for regression losses and binary cross-entropy for classification losses, with early stopping based on validation loss.

**Results.** Table 1 reports a representative setting with  $p + q = 3000$ ; additional results are given in Appendix K. In this setting, **MediEncoder** has the smallest SD, RMSE, and average confidence-interval length for all displayed sample sizes, while maintaining coverage close to the nominal 95% level. The improvement becomes clearer as  $n$  increases: for example, at  $n = 3000$ , **MediEncoder** reduces RMSE from 0.349 for IMAVAE and 0.343 for VAE to 0.290. The appendix results show the same trend for moderate and large sample sizes, although very small samples can favor simpler representation learners because deep representations are harder to train stably. Figure 3 shows that the scaled errors are approximately centered and have nearly linear Q–Q behavior, consistent with the asymptotic normal approximation developed in Section 4.

**Ablation study on  $\lambda_3$ .** To assess the role of the alignment loss, we set  $\lambda_3 = 0$  and compare this ablated version with the fully tuned **MediEncoder**. The ablation results in Appendix K show that removing the alignment term generally increases SD, RMSE, and confidence-interval length, with the largest gap in smaller samples. This supports the use of the cross-factor alignment component for stabilizing the learned mediator representation and improving estimation efficiency, while the advantage naturally becomes less pronounced as the sample size grows.

## 5.2 Real Data Application: Alzheimer’s Disease Neuroimaging Initiative (ADNI)

We apply **MediEncoder** to data from the Alzheimer’s Disease Neuroimaging Initiative (ADNI) (Mueller et al., 2005) to study whether the effect of depressive symptoms on cognitive decline is mediated by DNA methylation. The treatment  $A$  is the binarized Geriatric Depression Scale (GDS), with  $A = 1$  indicating  $GDS > 5$ , a commonly used threshold for elevated depressive symptoms (Greenberg, 2012). The outcome  $Y$  is the Alzheimer’s Disease Assessment Scale–Cognitive Subscale (ADAS-Cog), where higher scores indicate worse cognitive function (Cano et al., 2010; Raghavan et al., 2013). The covariates  $X$  include demographic and clinical variables, and the mediators  $M$  are high-dimensional DNA methylation features.

After preprocessing (Appendix J), the analysis includes  $n = 649$  subjects, with  $\dim(X) = 171$  and  $\dim(M) = 3,206$ . Table 2 reports the estimated natural direct effect (NDE), natural indirect effect (NIE), and total effect (TE). The total effect estimate is positive, suggesting that elevated depressive symptoms are associated, under the causal assumptions in Section 2, with worse cognitive outcomes. The point estimates indicate that most of the effect operates through the direct pathway, while the estimated DNA-methylation-mediated indirect effect is positive but smaller. The bootstrap interval for the total effect excludes zero, whereas the intervals for the direct and indirect effects include zero, so the mediation finding should be interpreted cautiously.

## 6 Conclusion

We introduced **MediEncoder**, a coupled representation-learning framework for high-dimensional causal mediation analysis with nonlinear latent covariate and mediator structures. By combining a structured autoencoder with a cross-fitted efficient influence function-based estimator, the proposed method targets natural direct and indirect effects while accommodating complex high-dimensional measurements. Across simulations, **MediEncoder** achieved lower RMSE and more stable inference than competing methods, and the ablation

study showed that the alignment term improves estimation accuracy and efficiency. In the ADNI application, we found a positive total effect of depressive symptoms on cognitive decline; the point estimates suggested that most of this effect operated through the direct pathway, while the estimated DNA-methylation-mediated indirect effect was smaller and more uncertain.

**Limitations and future work.** The proposed method relies on standard causal assumptions for natural mediation analysis, including no unmeasured mediator–outcome confounding. It is also currently developed for binary treatments, requires tuning representation dimensions and network hyperparameters, and the learned mediator representations may be difficult to interpret biologically. These limitations motivate future work on sensitivity analysis for unmeasured mediator–outcome confounding, extensions to continuous or multi-valued treatments, and methods for improving interpretability of the learned mediator representations.

## References

- Angermueller, C., Pärnamaa, T., Parts, L., and Stegle, O. (2016). Deep learning for computational biology. *Molecular systems biology*, 12(7):MSB156651.
- Aryee, M. J., Jaffe, A. E., Corrada-Bravo, H., Ladd-Acosta, C., Feinberg, A. P., Hansen, K. D., and Irizarry, R. A. (2014). Minfi: a flexible and comprehensive bioconductor package for the analysis of infinium dna methylation microarrays. *Bioinformatics*, 30(10):1363–1369.
- Bai, J. and Ng, S. (2002). Determining the number of factors in approximate factor models. *Econometrica*, 70(1):191–221.
- Bai, J. and Ng, S. (2013). Principal components estimation and identification of static factors. *Journal of econometrics*, 176(1):18–29.
- Baron, R. M. and Kenny, D. A. (1986). The moderator–mediator variable distinction in social psychological research: Conceptual, strategic, and statistical considerations. *Journal of personality and social psychology*, 51(6):1173.
- Bartlett, P. L., Harvey, N., Liaw, C., and Mehrabian, A. (2019). Nearly-tight vc-dimension and pseudodimension bounds for piecewise linear neural networks. *Journal of Machine Learning Research*, 20(63):1–17.
- Battram, T., Yousefi, P., Crawford, G., Prince, C., Babaei, M. S., Sharp, G., Hatcher, C., Vega-Salas, M. J., Khodabakhsh, S., Whitehurst, O., et al. (2022). The ewas catalog: a database of epigenome-wide association studies. *Wellcome open research*, 7:41.
- Black, C. N., Bot, M., Scheffer, P. G., Cuijpers, P., and Penninx, B. W. (2015). Is depression associated with increased oxidative stress? a systematic review and meta-analysis. *Psychoneuroendocrinology*, 51:164–175.
- Bo, S., Ghassami, A., and Mukherjee, D. (2024). A debiased estimator for the mediation functional in ultra-high-dimensional setting in the presence of interaction effects. *arXiv preprint arXiv:2412.08827*.
- Buccellato, F. R., D’Anca, M., Fenoglio, C., Scarpini, E., and Galimberti, D. (2021). Role of oxidative damage in alzheimer’s disease and neurodegeneration: From pathogenic mechanisms to biomarker discovery. *Antioxidants*, 10(9):1353.
- Cano, S. J., Posner, H. B., Moline, M. L., Hurt, S. W., Swartz, J., Hsu, T., and Hobart, J. C. (2010). The adas-cog in alzheimer’s disease clinical trials: psychometric evaluation of the sum and its parts. *Journal of Neurology, Neurosurgery & Psychiatry*, 81(12):1363–1368.
- Derkach, A., Pfeiffer, R. M., Chen, T.-H., and Sampson, J. N. (2019). High dimensional mediation analysis with latent variables. *Biometrics*, 75(3):745–756.
- Fan, J. and Gu, Y. (2023). Factor augmented sparse throughput deep relu neural networks for high dimensional regression. *Journal of the American Statistical Association*, pages 1–15.

- Fan, J. and Gu, Y. (2024). Factor augmented sparse throughput deep relu neural networks for high dimensional regression. *Journal of the American Statistical Association*, 119(548):2680–2694.
- Fan, J., Jana, S., Kulkarni, S., and Yin, Q. (2025). Factor informed double deep learning for average treatment effect estimation. *arXiv preprint arXiv:2508.17136*.
- Fan, J., Ke, Y., and Wang, K. (2020). Factor-adjusted regularized model selection. *Journal of Econometrics*, 216(1):71–85.
- Fan, J. and Liao, Y. (2022). Learning latent factors from diversified projections and its applications to over-estimated and weak factors. *Journal of the American Statistical Association*, 117(538):909–924.
- Fan, J., Liao, Y., and Mincheva, M. (2013). Large covariance estimation by thresholding principal orthogonal complements. *Journal of the Royal Statistical Society Series B: Statistical Methodology*, 75(4):603–680.
- Feng, Y. (2023). Optimal estimation of large-dimensional nonlinear factor models. *arXiv preprint arXiv:2311.07243*.
- Goodfellow, I., Bengio, Y., Courville, A., and Bengio, Y. (2016). *Deep learning*, volume 1. MIT press Cambridge.
- Greenberg, S. A. (2012). The geriatric depression scale (gds). *Best Practices in Nursing Care to Older Adults*, 4(1):1–2.
- Guerrero-López, A., Sevilla-Salcedo, C., Gómez-Verdejo, V., and Olmos, P. M. (2022). Multimodal hierarchical variational autoencoders with factor analysis latent space. *arXiv preprint arXiv:2207.09185*.
- Guo, X., Li, R., Liu, J., and Zeng, M. (2022). High-dimensional mediation analysis for selecting dna methylation loci mediating childhood trauma and cortisol stress reactivity. *Journal of the American Statistical Association*, 117(539):1110–1121.
- Guo, X., Li, R., Liu, J., and Zeng, M. (2023). Statistical inference for linear mediation models with high-dimensional mediators and application to studying stock reaction to covid-19 pandemic. *Journal of Econometrics*, 235(1):166–179.
- Guo, X., Li, R., Liu, J., and Zeng, M. (2024). Estimations and tests for generalized mediation models with high-dimensional potential mediators. *Journal of Business & Economic Statistics*, 42(1):243–256.
- Hinton, G. E. and Salakhutdinov, R. R. (2006). Reducing the dimensionality of data with neural networks. *science*, 313(5786):504–507.
- Imai, K., Keele, L., and Yamamoto, T. (2010). Identification, inference and sensitivity analysis for causal mediation effects. *Statistical Science*.
- Jiang, Z., Liu, Y., Klein, M. H., Aloui, A., Ren, Y., Li, K., Tarokh, V., and Carlson, D. (2023). Causal mediation analysis with multi-dimensional and indirectly observed mediators. *arXiv preprint arXiv:2306.07918*.
- Johnson, N. D., Wiener, H. W., Smith, A. K., Nishitani, S., Absher, D. M., Arnett, D. K., Aslibekyan, S., and Conneely, K. N. (2017). Non-linear patterns in age-related dna methylation may reflect cd4+ t cell differentiation. *Epigenetics*, 12(6):492–503.
- Jones, J., Ertefaie, A., and Strawderman, R. L. (2025). Causal mediation analysis: selection with asymptotically valid inference. *Journal of the Royal Statistical Society Series B: Statistical Methodology*, 87(3):678–700.
- Katerji, M., Filippova, M., and Duerksen-Hughes, P. (2019). Approaches and methods to measure oxidative stress in clinical samples: Research applications in the cancer field. *Oxidative medicine and cellular longevity*, 2019(1):1279250.

- Khemakhem, I., Kingma, D., Monti, R., and Hyvarinen, A. (2020). Variational autoencoders and nonlinear ica: A unifying framework. In *International conference on artificial intelligence and statistics*, pages 2207–2217. PMLR.
- Kingma, D. P. and Welling, M. (2013). Auto-encoding variational bayes. *arXiv preprint arXiv:1312.6114*.
- LeCun, Y., Bengio, Y., and Hinton, G. (2015). Deep learning. *nature*, 521(7553):436–444.
- Livingston, G., Huntley, J., Liu, K. Y., Costafreda, S. G., Selbæk, G., Alladi, S., Ames, D., Banerjee, S., Burns, A., Brayne, C., Fox, N. C., Ferri, C. P., Gitlin, L. N., Howard, R., Kales, H. C., Kivimäki, M., Larson, E. B., Nakasujja, N., Rockwood, K., Samus, Q., Shirai, K., Singh-Manoux, A., Schneider, L. S., Walsh, S., Yao, Y., Sommerlad, A., and Mukadam, N. (2024). Dementia prevention, intervention, and care: 2024 report of the *Lancet* standing commission. *The Lancet*, 404(10452):572–628.
- Lunnon, K., Smith, R., Hannon, E., De Jager, P. L., Srivastava, G., Volta, M., Troakes, C., Al-Sarraj, S., Burrage, J., Macdonald, R., et al. (2014). Methyloomic profiling implicates cortical deregulation of *ank1* in alzheimer’s disease. *Nature neuroscience*, 17(9):1164–1170.
- Miranda, S., Opazo, C., Larrondo, L. F., Muñoz, F. J., Ruiz, F., Leighton, F., and Inestrosa, N. C. (2000). The role of oxidative stress in the toxicity induced by amyloid  $\beta$ -peptide in alzheimer’s disease. *Progress in neurobiology*, 62(6):633–648.
- Mueller, S. G., Weiner, M. W., Thal, L. J., Petersen, R. C., Jack, C., Jagust, W., Trojanowski, J. Q., Toga, A. W., and Beckett, L. (2005). The alzheimer’s disease neuroimaging initiative. *Neuroimaging Clinics*, 15(4):869–877.
- Pandya, C. D., Howell, K. R., and Pillai, A. (2013). Antioxidants as potential therapeutics for neuropsychiatric disorders. *Progress in Neuro-Psychopharmacology and Biological Psychiatry*, 46:214–223.
- Pearl, J. (2001). Direct and indirect effects. *Probabilistic and Causal Inference: The Works of Judea Pearl*, page 373.
- Raghavan, N., Samtani, M. N., Farnum, M., Yang, E., Novak, G., Grundman, M., Narayan, V., DiBernardo, A., Initiative, A. D. N., et al. (2013). The adas-cog revisited: novel composite scales based on adas-cog to improve efficiency in mci and early ad trials. *Alzheimer’s & Dementia*, 9(1):S21–S31.
- Rahmenführer, J., De Bin, R., Benner, A., Ambroggi, F., Lusa, L., Boulesteix, A.-L., Migliavacca, E., Binder, H., Michiels, S., Sauerbrei, W., et al. (2023). Statistical analysis of high-dimensional biomedical data: a gentle introduction to analytical goals, common approaches and challenges. *BMC medicine*, 21(1):182.
- Rakshit, P. and Guo, Z. (2024). Statistical inference in high-dimensional poisson regression with applications to mediation analysis. *arXiv preprint arXiv:2410.20671*.
- Rubin, D. B. (1974). Estimating causal effects of treatments in randomized and nonrandomized studies. *Journal of educational Psychology*, 66(5):688.
- Tchetgen Tchetgen, E. J. and Shpitser, I. (2012). Semiparametric theory for causal mediation analysis: efficiency bounds, multiple robustness, and sensitivity analysis. *Annals of statistics*, 40(3):1816.
- Van Buuren, S. and Groothuis-Oudshoorn, K. (2011). mice: Multivariate imputation by chained equations in r. *Journal of statistical software*, 45:1–67.
- VanderWeele, T. (2015). *Explanation in causal inference: methods for mediation and interaction*. Oxford University Press.
- VanderWeele, T. and Vansteelandt, S. (2014). Mediation analysis with multiple mediators. *Epidemiologic methods*, 2(1):95–115.

- Vershinina, O., Bacalini, M., Zaikin, A., Franceschi, C., and Ivanchenko, M. (2021). Disentangling age-dependent dna methylation: deterministic, stochastic, and nonlinear. *Scientific reports*, 11(1):9201.
- Wang, W., Arora, R., Livescu, K., and Bilmes, J. (2015). On deep multi-view representation learning. In *International conference on machine learning*, pages 1083–1092. PMLR.
- Wörheide, M. A., Krumsiek, J., Kastenmüller, G., and Arnold, M. (2021). Multi-omics integration in biomedical research—a metabolomics-centric review. *Analytica chimica acta*, 1141:144–162.
- Xiu, D. and Shen, Z. (2024). Deep autoencoders for nonlinear factor models: Theory and applications. *Chicago Booth Research Paper*, (25-14).
- Xu, S., Liu, L., and Liu, Z. (2022). Deepmed: Semiparametric causal mediation analysis with debiased deep learning. *Advances in Neural Information Processing Systems*, 35:28238–28251.
- Zhang, L., Silva, T. C., Young, J. I., Gomez, L., Schmidt, M. A., Hamilton-Nelson, K. L., Kunkle, B. W., Chen, X., Martin, E. R., and Wang, L. (2020). Epigenome-wide meta-analysis of dna methylation differences in prefrontal cortex implicates the immune processes in alzheimer’s disease. *Nature communications*, 11(1):6114.
- Zhang, Q. (2022). High-dimensional mediation analysis with applications to causal gene identification. *Statistics in biosciences*, 14(3):432–451.
- Zhao, Y. and Luo, X. (2016). Pathway lasso: estimate and select sparse mediation pathways with high dimensional mediators. *arXiv preprint arXiv:1603.07749*.
- Zhao, Y. and Luo, X. (2021). Pathway lasso: pathway estimation and selection with high-dimensional mediators. *Statistics and its Interface*, 15(1):39.

# Appendix for “MediEncoder: Nonlinear Representation Learning for High-Dimensional Causal Mediation Analysis”

## A Related Work

**High-Dimensional Mediation Analysis.** Recent work extends causal mediation analysis to high-dimensional regimes where the number of mediators or covariates may exceed the sample size. Early approaches focus primarily on high-dimensional mediators, employing sparsity assumptions and variable selection techniques such as Lasso to estimate mediation effects (Zhao and Luo, 2016; Guo et al., 2022, 2023, 2024; Jones et al., 2025). Subsequent work incorporates interaction effects among treatment, mediators, and covariates, allowing for more flexible modeling of complex mechanisms (Rakshit and Guo, 2024). More recent developments consider settings where both mediators and covariates are high-dimensional and may interact, proposing estimation and inference procedures that account for their joint structure (Bo et al., 2024). Despite these advances, most existing methods rely on linear modeling assumptions and treat observed variables directly, which may be restrictive when the underlying mechanisms are nonlinear and only indirectly observed through noisy measurements.

**Factor Models.** Factor models provide a natural framework for representing high-dimensional data via a lower-dimensional set of latent variables. Classical linear factor models have been widely used in statistics and econometrics for dimension reduction (Bai and Ng, 2002, 2013; Fan et al., 2013, 2020; Fan and Liao, 2022). These ideas have also been incorporated into causal inference and mediation analysis to handle high-dimensional covariates or mediators by projecting them onto latent spaces (Derkach et al., 2019). However, existing approaches predominantly rely on linear factor structures, assuming observed variables are linear combinations of latent factors. In many scientific applications, particularly in biological and genomic settings, the mapping from latent processes to observed measurements is often nonlinear. Recent work has explored nonlinear extensions of factor models using neural networks to allow more flexible representations (Feng, 2023; Xiu and Shen, 2024; Fan et al., 2025), though their integration with mediation analysis remains limited. In parallel, factor-based methods have also been developed for high-dimensional average treatment effect (ATE) estimation under doubly robust frameworks. Fan et al. (2025) proposed a factor-informed AIPW estimator combining factor models and deep learning for high-dimensional causal inference. Their setting can be viewed as an ATE analogue of our problem, but still primarily relies on linear factor structures without considering nonlinear factor generation mechanisms.

**Autoencoders and More on Mediation Analysis.** Deep representation learning methods, especially autoencoders, provide a flexible approach for learning nonlinear low-dimensional representations of high-dimensional data (Hinton and Salakhutdinov, 2006; Goodfellow et al., 2016). They have been widely applied in large-scale settings for nonlinear dimension reduction and feature learning (LeCun et al., 2015; Khemakhem et al., 2020). Variational autoencoders further introduce probabilistic latent-variable models that enable structured and generative representations (Kingma and Welling, 2013). Related work on multi-view representation learning, including multi-view autoencoders and deep canonical correlation methods, aims to learn shared representations across multiple data modalities (Wang et al., 2015; Guerrero-López et al., 2022). Xu et al. (2022) develop a deep learning-based mediation estimator that is robust to model misspecification. However, their approach learns representations independently and does not explicitly model for high-dimensionality and latent factor structure. In particular, it does not consider a shared representation capturing the dependence between covariates and mediators, which is important in high-dimensional biological systems driven by associated latent factors. Jiang et al. (2023) propose a variational autoencoder-based mediation framework for indirectly observed mediators; however, their method does not accommodate latent and nonlinear structures in covariates, does not model the structural dependence between the latent representations of covariates and mediators, and does not allow treatment–covariate or treatment–mediator interactions. In addition, their estimation procedure may be sensitive to model misspecification.

## B Overview of Baseline Methods

We consider several baseline methods for estimating low-dimensional latent representations (factors) from high-dimensional covariates  $X$  and mediators  $M$ . These representations are subsequently used in downstream mediation effect estimation.

**Diversified Projection.** Diversified projection method (Fan and Liao, 2022; Fan and Gu, 2023) constructs a linear surrogate of latent factors using a projection matrix  $W \in \mathbb{R}^{p \times \tilde{p}}$  that satisfies boundedness and significance conditions. The estimated factors are obtained as

$$\hat{\mathbf{f}} = p^{-1}W^\top x,$$

which can be viewed as an affine approximation of the true latent factor  $f$ :

$$\hat{\mathbf{f}} = H\mathbf{f} + \xi, \quad \text{with } H = p^{-1}W^\top B.$$

Under mild conditions, the signal term  $Hf$  dominates the noise  $\xi$ , allowing  $\tilde{f}$  to serve as a consistent proxy for  $f$ . This approach avoids explicit estimation of the factor loading matrix and does not require precise knowledge of the factor dimension.

**Autoencoder.** Autoencoders (AE) learn nonlinear low-dimensional representations by jointly training an encoder  $g(\cdot)$  and a decoder  $h(\cdot)$ . Given input  $x$ , the latent representation is  $z = g(x)$  and the reconstruction is  $\hat{x} = h(z)$ . The model is trained by minimizing the reconstruction loss:

$$\min_{g,h} \sum_{i=1}^n \|x_i - h(g(x_i))\|_2^2.$$

In our setting, autoencoders are applied separately to  $X$  and  $M$  to obtain latent representations, which may fail to capture shared structure across modalities.

**Variational Autoencoder.** Variational autoencoders (VAE) extend autoencoders by introducing a probabilistic latent-variable model. The encoder defines a variational posterior  $q_\phi(z|x)$ , while the decoder specifies a likelihood  $p_\theta(x|z)$ . The model is trained by maximizing the evidence lower bound (ELBO), equivalently minimizing:

$$\mathcal{L}_{\text{VAE}} = \mathbb{E}_{q_\phi(z|x)} [\|x - \hat{x}\|_2^2] + \text{KL}(q_\phi(z|x) \| p(z)),$$

where  $p(z)$  is a prior distribution. Similar to AE, VAEs are typically applied independently to  $X$  and  $M$ , which may not capture their joint dependence structure.

**IMAVAE.** IMAVAE (Jiang et al., 2023) extends the VAE framework to mediation analysis with indirectly observed mediators by incorporating treatment and covariates as auxiliary variables. Let  $u = t$  or  $u = (w, t)$  denote the auxiliary input. The model jointly learns an encoder  $q_\phi(z|x, u)$ , decoder  $p_\theta(x|z)$ , and predictor  $g_\gamma(z, u)$  for the outcome. The objective function is:

$$\min_{\theta, \phi, \gamma} \left\{ \alpha \mathcal{L}_{\theta, \phi}(\hat{x}, x) - \beta \mathcal{L}_{\theta, \phi}(x, u) + \mathcal{L}_{\phi, S, \lambda, \gamma}(\hat{y}, y) \right\},$$

where  $\mathcal{L}_{\theta, \phi}(x, u)$  corresponds to the ELBO term,  $\mathcal{L}_{\theta, \phi}(\hat{x}, x)$  is the reconstruction loss, and  $\mathcal{L}_{\phi, S, \lambda, \gamma}(\hat{y}, y)$  is the prediction loss for the outcome. This framework enables learning latent mediator representations informed by treatment and covariates, but remains tied to a specific generative model.

## C Details of Algorithm 1

### C.1 Nuisance Function Estimation

- Estimate nuisance functions on  $\mathcal{I}_{\text{nu}}^{(k)}$ :

$$\begin{aligned}
\hat{\pi}_1^{(k)} &\in \arg \min_{g \in \mathcal{F}_\pi} \sum_{i \in \mathcal{I}_{\text{nu}}^{(k)}} \left[ -A_i \log g(\hat{\mathbf{f}}_{X,i}^{(k)}) - (1 - A_i) \log\{1 - g(\hat{\mathbf{f}}_{X,i}^{(k)})\} \right], \\
\hat{\mu}_1^{(k)} &\in \arg \min_{g \in \mathcal{F}_\mu} \sum_{\substack{i \in \mathcal{I}_{\text{nu}}^{(k)} \\ A_i=1}} \left[ Y_i - g(\hat{\mathbf{f}}_{X,i}^{(k)}, \hat{\mathbf{f}}_{M,i}^{(k)}) \right]^2, \\
\hat{\rho}^{(k)} &\in \arg \min_{g \in \mathcal{F}_\rho} \sum_{i \in \mathcal{I}_{\text{nu}}^{(k)}} \left[ -A_i \log g(\hat{\mathbf{f}}_{X,i}^{(k)}, \hat{\mathbf{f}}_{M,i}^{(k)}) - (1 - A_i) \log\{1 - g(\hat{\mathbf{f}}_{X,i}^{(k)}, \hat{\mathbf{f}}_{M,i}^{(k)})\} \right], \\
\hat{\mu}_{10}^{(k)} &\in \arg \min_{g \in \mathcal{F}_{\mu_{10}}} \sum_{\substack{i \in \mathcal{I}_{\text{nu}}^{(k)} \\ A_i=0}} \left[ \hat{\mu}_1^{(k)}(\hat{\mathbf{f}}_{X,i}^{(k)}, \hat{\mathbf{f}}_{M,i}^{(k)}) - g(\hat{\mathbf{f}}_{X,i}^{(k)}) \right]^2.
\end{aligned} \tag{C.1}$$

- Estimate the density ratio  $\pi_2(f_X, f_M) = p(f_M | A = 0, f_X)/p(f_M | A = 1, f_X)$  by Bayes' rule:

$$\hat{\pi}_2^{(k)}(u, v) = \frac{1 - \hat{\rho}^{(k)}(u, v)}{\hat{\rho}^{(k)}(u, v)} \frac{\hat{\pi}_1^{(k)}(u)}{1 - \hat{\pi}_1^{(k)}(u)}. \tag{C.2}$$

### C.2 Tuning Algorithm

The auxiliary regression  $\hat{m}_1^{(\lambda)}$  is used only to select the representation learning tuning parameter  $\lambda$  and is not used in the final influence function-based estimator. After  $\hat{\lambda}$  is selected, Algorithm 1 refits the coupled autoencoder on the fold-specific representation-training set and estimates the nuisance functions on a separate nuisance-estimation set.

## D More on Simulation Study

### D.1 Simulation Settings

The data generating process is as follows:

1. We generate latent covariates  $\mathbf{f}_X \in \mathbb{R}^{\bar{p}}$  from  $\mathbf{f}_X \sim \mathcal{U}(-1, 1)^{\bar{p}}$ . The treatment variable  $A$  is generated according to a logistic model based on  $\mathbf{f}_X$ :

$$\mathbb{P}(A = 1 | \mathbf{f}_X) = \frac{\exp(\mathbf{f}_X^\top \alpha)}{1 + \exp(\mathbf{f}_X^\top \alpha)}, \quad A \sim \text{Bernoulli}\left(\frac{\exp(\mathbf{f}_X^\top \alpha)}{1 + \exp(\mathbf{f}_X^\top \alpha)}\right),$$

where  $\alpha \in \mathbb{R}^{\bar{p}}$  is drawn once from  $\mathcal{U}(0, 2)^{\bar{p}}$ .

2. The latent mediators  $\mathbf{f}_M \in \mathbb{R}^{\bar{q}}$  are generated through a nonlinear transformation of  $\mathbf{f}_X$ , the treatment indicator  $A$ , and additive noise:

$$\mathbf{f}_M = (1 - A)(\boldsymbol{\delta}_0 \mathbf{f}_X^{\circ 2} + \mathbf{u}_{XM}) + A(\boldsymbol{\delta}_1 \mathbf{f}_X^{\circ 2} + \mathbf{u}'_{XM}), \quad \mathbf{u}_{XM}, \mathbf{u}'_{XM} \sim \mathcal{N}(0, \Sigma_U),$$

where  $\mathbf{f}_X^{\circ 2}$  denotes the element-wise square of  $\mathbf{f}_X$ ,  $\boldsymbol{\delta}_0, \boldsymbol{\delta}_1 \in \mathbb{R}^{\bar{q} \times \bar{p}}$  have entries drawn once from  $\mathcal{U}(0.5, 1.5)$ , and  $\Sigma_U = R_U \Lambda_U R_U^\top$ , where  $R_U \in \mathbb{R}^{\bar{q} \times \bar{q}}$  is an orthonormal matrix and  $\Lambda_U = \text{diag}(\lambda_1, \dots, \lambda_{\bar{q}})$  with  $\lambda_j \sim \mathcal{U}(1, 2)$ .

---

**Algorithm 2** Tuning  $\lambda = (\lambda_1, \lambda_2, \lambda_3)$  for MediEncoder

**Require:** Training indices  $\mathcal{I}_{\text{tr}}$ , validation indices  $\mathcal{I}_{\text{val}}$ , tuning grid  $\Lambda \subset [0, \infty)^3 \setminus \{(0, 0, 0)\}$ , representation class  $\mathcal{Z}_{\text{NN}}$ , auxiliary outcome-regression class  $\mathcal{F}_\mu^{\text{tun}}$

**Ensure:** Selected tuning parameter  $\hat{\lambda} = (\hat{\lambda}_1, \hat{\lambda}_2, \hat{\lambda}_3)$

1: Define the treated training and validation subsets

$$\mathcal{I}_{\text{tr},1} := \{i \in \mathcal{I}_{\text{tr}} : A_i = 1\}, \quad \mathcal{I}_{\text{val},1} := \{i \in \mathcal{I}_{\text{val}} : A_i = 1\}.$$

2: Assume  $|\mathcal{I}_{\text{tr},1}| > 0$  and  $|\mathcal{I}_{\text{val},1}| > 0$ ; otherwise, redraw the sample split.

3: **for** each  $\lambda = (\lambda_1, \lambda_2, \lambda_3) \in \Lambda$  **do**

4: Fit the coupled autoencoder on  $\mathcal{I}_{\text{tr}}$ :

$$\begin{aligned} \hat{z}_{XM}^{(\lambda)} &= \left( \hat{g}_X^{(\lambda)}, \hat{g}_M^{(\lambda)}, \hat{g}_{XM}^{(\lambda)}, \hat{h}_X^{(\lambda)}, \hat{h}_M^{(\lambda)} \right) \\ &\in \arg \min_{z_{XM} = (g_X, g_M, g_{XM}, h_X, h_M) \in \mathcal{Z}_{\text{NN}}} \frac{1}{|\mathcal{I}_{\text{tr}}|} \sum_{i \in \mathcal{I}_{\text{tr}}} \left[ \lambda_1 \|X_i - h_X(g_X(X_i))\|_2^2 + \lambda_2 \|M_i - h_M(g_M(M_i))\|_2^2 \right. \\ &\quad \left. + \lambda_3 \|g_M(M_i) - g_{XM}(A_i, g_X(X_i))\|_2^2 \right]. \end{aligned}$$

5: Compute learned representations for all  $i \in \mathcal{I}_{\text{tr}} \cup \mathcal{I}_{\text{val}}$ :

$$\hat{\mathbf{f}}_{X,i}^{(\lambda)} = \hat{g}_X^{(\lambda)}(X_i), \quad \hat{\mathbf{f}}_{M,i}^{(\lambda)} = \hat{g}_M^{(\lambda)}(M_i).$$

6: Fit an auxiliary treated-outcome regression on the training subset:

$$\hat{m}_1^{(\lambda)} \in \arg \min_{g \in \mathcal{F}_\mu^{\text{tun}}} \frac{1}{|\mathcal{I}_{\text{tr},1}|} \sum_{i \in \mathcal{I}_{\text{tr},1}} \left[ Y_i - g\left(\hat{\mathbf{f}}_{X,i}^{(\lambda)}, \hat{\mathbf{f}}_{M,i}^{(\lambda)}\right) \right]^2.$$

7: Compute the held-out validation prediction error:

$$\widehat{\text{PE}}(\lambda) = \frac{1}{|\mathcal{I}_{\text{val},1}|} \sum_{i \in \mathcal{I}_{\text{val},1}} \left[ Y_i - \hat{m}_1^{(\lambda)}\left(\hat{\mathbf{f}}_{X,i}^{(\lambda)}, \hat{\mathbf{f}}_{M,i}^{(\lambda)}\right) \right]^2.$$

8: **end for**

9: Select any minimizer

$$\hat{\lambda} = (\hat{\lambda}_1, \hat{\lambda}_2, \hat{\lambda}_3) \in \arg \min_{\lambda \in \Lambda} \widehat{\text{PE}}(\lambda).$$

10: **return**  $\hat{\lambda}$

---

3. The outcome variable  $Y$  is generated via a nonlinear equation:

$$\begin{aligned} Y &= (1 - A) \left( \sin(5\mathbf{f}_X)^\top \beta_0 + \log(1 + \exp(\mathbf{f}_X^\top \kappa_0)) + (\mathbf{f}_M \circ \mathbf{f}_X^{\circ 2})^\top \gamma_0 + \epsilon'_Y \right) \\ &\quad + A \left( \sin(5\mathbf{f}_X)^\top \beta_1 + \log(1 + \exp(\mathbf{f}_X^\top \kappa_1)) + (\mathbf{f}_M \circ \mathbf{f}_X^{\circ 2})^\top \gamma_1 + \epsilon_Y \right), \end{aligned}$$

where  $\beta_0, \beta_1, \kappa_0, \kappa_1 \in \mathbb{R}^{\bar{p}}$ ,  $\gamma_0, \gamma_1 \in \mathbb{R}^{\bar{q}}$ , each drawn once from  $\mathcal{U}(0.5, 1.5)$ , and  $\epsilon_Y, \epsilon'_Y \sim \mathcal{N}(0, \sigma_Y^2)$ .

4. We generate the observed high-dimensional covariates  $X \in \mathbb{R}^p$  and mediators  $M \in \mathbb{R}^q$  through nonlinear factor loadings with additive noise. Specifically, for each observed coordinate  $j = 1, \dots, p$  and  $k = 1, \dots, q$ , we generate

$$X_j = \phi_{X,j}(\mathbf{f}_X) + \mathbf{u}_{X,j}, \quad M_k = \phi_{M,k}(\mathbf{f}_M) + \mathbf{u}_{M,k},$$

where  $\mathbf{f}_X \in \mathbb{R}^{\bar{p}}$  and  $\mathbf{f}_M \in \mathbb{R}^{\bar{q}}$  denote the latent factors.

**Nonlinear loading families.** We consider nonlinear factor loadings for  $g_{X,j}(\cdot)$  and  $g_{M,k}(\cdot)$  in wavelet (see D.1.1 for more details) based on Haar atoms, and we use an additive structure over latent coordinates:

$$g_{X,j}(\mathbf{f}_X) = \sum_{i=1}^{\bar{p}} h_{X,ji}(\mathbf{f}_{X_i}), \quad g_{M,k}(\mathbf{f}_M) = \sum_{i=1}^{\bar{q}} h_{M,ki}(\mathbf{f}_{M_i}),$$

where the univariate functions  $h_{X,jm}(\cdot)$  and  $h_{M,km}(\cdot)$  are instantiated using the wavelet bases.

5. The idiosyncratic components satisfy

$$\mathbf{u}_X \sim \mathcal{N}(0, \sigma_X^2 I_p), \quad \mathbf{u}_M \sim \mathcal{N}(0, \sigma_M^2 I_q),$$

independently of the latent factors.

### D.1.1 Wavelet Loading

In the simulation experiment 5, the loading functions  $g_{X,j}(\cdot)$  and  $g_{M,k}(\cdot)$  are constructed using nonlinear basis expansions. Specifically, we consider nonlinear loadings based on wavelet which follows an additive structure over latent coordinates.

**Haar mother wavelet.** We adopt the standard Haar mother wavelet  $\psi : \mathbb{R} \rightarrow \mathbb{R}$ , defined by

$$\psi(t) = \begin{cases} 1, & 0 \leq t < 1, \\ -1, & 1 \leq t < 2, \\ 0, & \text{otherwise.} \end{cases}$$

This function satisfies

$$\int_{\mathbb{R}} \psi(t) dt = 0, \quad \|\psi\|_{L^2} = \sqrt{2}.$$

**Wavelet atoms.** For each wavelet atom  $\phi_\ell$ , we independently sample an integer-valued scale parameter  $r_\ell \sim \text{Unif}\{r_{\min}, \dots, r_{\max}\}$ . To ensure that the wavelet atoms overlap with the latent support, we sample a location  $t_\ell \sim \text{Unif}[x_{\min}, x_{\max}]$ , where  $[x_{\min}, x_{\max}]$  denotes the range of the latent variables. The corresponding translation parameter is then defined as  $s_\ell = \lfloor 2^{r_\ell} t_\ell \rfloor$ . Given the sampled pair  $(r_\ell, s_\ell)$ , the wavelet atom is  $\psi_{r_\ell, s_\ell}(t) = 2^{r_\ell/2} \psi(2^{r_\ell} t - s_\ell)$ .

**Additive nonlinear loading.** For each latent coordinate  $i$ , we select a collection of  $L$  wavelet atoms  $\{\phi_\ell(\cdot)\}_{\ell=1}^L \subset \{\psi_{r,s}(\cdot)\}$ . The loading functions are defined as

$$g_{X,j}(\mathbf{f}_X) = \sum_{i=1}^{\bar{p}} \sum_{\ell=1}^L \lambda_{X,ji\ell}^{\text{wavelet}} \phi_\ell(\mathbf{f}_{X_i}), \quad g_{M,k}(\mathbf{f}_M) = \sum_{i=1}^{\bar{q}} \sum_{\ell=1}^L \lambda_{M,ki\ell}^{\text{wavelet}} \phi_\ell(\mathbf{f}_{M_i}),$$

where  $\lambda_{X,jm\ell}^{\text{wavelet}} \sim \mathcal{N}\left(0, \frac{1}{L}\right)$ ,  $\lambda_{M,km\ell}^{\text{wavelet}} \sim \mathcal{N}\left(0, \frac{1}{L}\right)$ , drawn once at initialization.

## E Proof of Theorem 4.3

For notational simplicity, we present the analysis for a single fold (e.g.,  $k = 1$ , so  $|\mathcal{I}_4|$  is used for evaluation of  $\hat{\theta}_0^{\text{IF}}$  and write  $n = |\mathcal{I}_4|$  for simplicity). The arguments for the remaining folds follow analogously by permuting the roles of  $\mathcal{I}_1, \dots, \mathcal{I}_4$  (see Algorithm 1).

**Decomposition of  $\hat{\theta}_0^{\text{IF}} - \theta_0$ .** Our goal in this step is to decompose  $\hat{\theta}_0^{\text{IF}} - \theta_0$  as the leading influence-function term and the remainder terms. Although the Algorithm 1 estimates the auxiliary propensity  $\rho(\mathbf{f}_X, \mathbf{f}_M) := \mathbb{P}(A = 1 \mid \mathbf{f}_X, \mathbf{f}_M)$  rather than estimating the mediator density ratio directly, we keep the

notation  $\pi_2$  for readability in this part of the proof. Throughout the proof,  $\pi_2$  is understood as the Bayes-rule representation  $\pi_2(\mathbf{f}_X, \mathbf{f}_M) = \frac{1-\rho(\mathbf{f}_X, \mathbf{f}_M)}{\rho(\mathbf{f}_X, \mathbf{f}_M)} \cdot \frac{\pi_1(\mathbf{f}_X)}{1-\pi_1(\mathbf{f}_X)}$ .

We first claim that the estimator admits the decomposition

$$\hat{\theta}_0^{\text{IF}} - \theta_0 = \frac{1}{n} \sum_{i=1}^n \Psi_i + R_0 + R_1 + R_2 + R_3 + R_4,$$

where the oracle influence-function score

$$\begin{aligned} \Psi_i &:= \mu_{10}(\mathbf{f}_{X,i}) + \frac{A_i}{\pi_1(\mathbf{f}_{X,i})} \pi_2(\mathbf{f}_{X,i}, \mathbf{f}_{M,i}) (Y_i - \mu_1(\mathbf{f}_{X,i}, \mathbf{f}_{M,i})) \\ &\quad + \frac{1 - A_i}{1 - \pi_1(\mathbf{f}_{X,i})} (\mu_1(\mathbf{f}_{X,i}, \mathbf{f}_{M,i}) - \mu_{10}(\mathbf{f}_{X,i})) - \theta_0. \end{aligned}$$

The remainder terms collect the differences between the estimated nuisance quantities and their population counterparts. Specifically,

$$\begin{aligned} R_0 &= \frac{1}{n} \sum_{i=1}^n A_i \pi_2(\mathbf{f}_{X,i}, \mathbf{f}_{M,i}) \left( \frac{1}{\hat{\pi}_1(\hat{\mathbf{f}}_{X,i})} - \frac{1}{\pi_1(\mathbf{f}_{X,i})} \right) (Y_i - \mu_1(\mathbf{f}_{X,i}, \mathbf{f}_{M,i})), \\ R_1 &= \frac{1}{n} \sum_{i=1}^n A_i \frac{\hat{\pi}_2(\hat{\mathbf{f}}_{X,i}, \hat{\mathbf{f}}_{M,i}) - \pi_2(\mathbf{f}_{X,i}, \mathbf{f}_{M,i})}{\hat{\pi}_1(\hat{\mathbf{f}}_{X,i})} (Y_i - \mu_1(\mathbf{f}_{X,i}, \mathbf{f}_{M,i})), \\ R_2 &= \frac{1}{n} \sum_{i=1}^n \left[ \frac{1 - A_i}{1 - \hat{\pi}_1(\hat{\mathbf{f}}_{X,i})} - A_i \frac{\hat{\pi}_2(\hat{\mathbf{f}}_{X,i}, \hat{\mathbf{f}}_{M,i})}{\hat{\pi}_1(\hat{\mathbf{f}}_{X,i})} \right] (\hat{\mu}_1(\hat{\mathbf{f}}_{X,i}, \hat{\mathbf{f}}_{M,i}) - \mu_1(\mathbf{f}_{X,i}, \mathbf{f}_{M,i})), \\ R_3 &= \frac{1}{n} \sum_{i=1}^n (1 - A_i) (\mu_1(\mathbf{f}_{X,i}, \mathbf{f}_{M,i}) - \mu_{10}(\mathbf{f}_{X,i})) \left( \frac{1}{1 - \hat{\pi}_1(\hat{\mathbf{f}}_{X,i})} - \frac{1}{1 - \pi_1(\mathbf{f}_{X,i})} \right), \\ R_4 &= \frac{1}{n} \sum_{i=1}^n \frac{A_i - \hat{\pi}_1(\hat{\mathbf{f}}_{X,i})}{1 - \hat{\pi}_1(\hat{\mathbf{f}}_{X,i})} (\hat{\mu}_{10}(\hat{\mathbf{f}}_{X,i}) - \mu_{10}(\mathbf{f}_{X,i})). \end{aligned}$$

For readability, we suppress the arguments of all functions throughout the following derivation. For example, we write  $\hat{\pi}_1 = \hat{\pi}_1(\hat{\mathbf{f}}_{X,i})$ ,  $\pi_1 = \pi_1(\mathbf{f}_{X,i})$ ,  $\hat{\pi}_2 = \hat{\pi}_2(\hat{\mathbf{f}}_{X,i}, \hat{\mathbf{f}}_{M,i})$ ,  $\pi_2 = \pi_2(\mathbf{f}_{X,i}, \mathbf{f}_{M,i})$ , and similarly for  $\hat{\mu}_1$ ,  $\mu_1$  and  $\hat{\mu}_{10}$ ,  $\mu_{10}$ .

We now prove this decomposition step by step. By definition of  $\hat{\theta}_0^{\text{IF}}$ , we have

$$\hat{\theta}_0^{\text{IF}} - \theta_0 = \frac{1}{n} \sum_{i=1}^n \left[ \hat{\mu}_{10} + \frac{A_i}{\hat{\pi}_1} \hat{\pi}_2 (Y_i - \hat{\mu}_1) + \frac{1 - A_i}{1 - \hat{\pi}_1} (\hat{\mu}_1 - \hat{\mu}_{10}) \right] - \theta_0. \quad (\text{E.1})$$

Introduce

$$\begin{aligned} Z_{1,i} &:= \frac{A_i}{\hat{\pi}_1} \hat{\pi}_2 (Y_i - \hat{\mu}_1) - \frac{A_i}{\pi_1} \pi_2 (Y_i - \mu_1), \\ Z_{0,i} &:= \frac{1 - A_i}{1 - \hat{\pi}_1} (\hat{\mu}_1 - \hat{\mu}_{10}) - \frac{1 - A_i}{1 - \pi_1} (\mu_1 - \mu_{10}). \end{aligned}$$

Then (E.1) can be rewritten as

$$\hat{\theta}_0^{\text{IF}} - \theta_0 = \frac{1}{n} \sum_{i=1}^n \Psi_i + \frac{1}{n} \sum_{i=1}^n (\hat{\mu}_{10} - \mu_{10}) + \frac{1}{n} \sum_{i=1}^n Z_{1,i} + \frac{1}{n} \sum_{i=1}^n Z_{0,i}, \quad (\text{E.2})$$

where (E.2) is obtained by adding and subtracting  $\Psi_i$  and regrouping terms. We next expand  $Z_{1,i}$  in (E.2). By direct algebra,

$$Z_{1,i} = \frac{A_i}{\hat{\pi}_1} \hat{\pi}_2 (Y_i - \hat{\mu}_1) - \frac{A_i}{\pi_1} \pi_2 (Y_i - \mu_1)$$

$$\begin{aligned}
&= A_i \left[ \frac{\hat{\pi}_2}{\hat{\pi}_1} (Y_i - \hat{\mu}_1) - \frac{\pi_2}{\pi_1} (Y_i - \mu_1) \right] \\
&= A_i \left[ \frac{\hat{\pi}_2}{\hat{\pi}_1} (Y_i - \hat{\mu}_1) - \frac{\hat{\pi}_2}{\hat{\pi}_1} (Y_i - \mu_1) + \frac{\hat{\pi}_2}{\hat{\pi}_1} (Y_i - \mu_1) - \frac{\pi_2}{\pi_1} (Y_i - \mu_1) \right] \\
&= A_i \left[ \frac{\hat{\pi}_2}{\hat{\pi}_1} (\mu_1 - \hat{\mu}_1) + \left( \frac{\hat{\pi}_2}{\hat{\pi}_1} - \frac{\pi_2}{\pi_1} \right) (Y_i - \mu_1) \right] \\
&= A_i \frac{\hat{\pi}_2}{\hat{\pi}_1} (\mu_1 - \hat{\mu}_1) + A_i \left[ \frac{\hat{\pi}_2 - \pi_2}{\hat{\pi}_1} + \pi_2 \left( \frac{1}{\hat{\pi}_1} - \frac{1}{\pi_1} \right) \right] (Y_i - \mu_1) \\
&= A_i \frac{\hat{\pi}_2}{\hat{\pi}_1} (\mu_1 - \hat{\mu}_1) + A_i \frac{\hat{\pi}_2 - \pi_2}{\hat{\pi}_1} (Y_i - \mu_1) + A_i \pi_2 \left( \frac{1}{\hat{\pi}_1} - \frac{1}{\pi_1} \right) (Y_i - \mu_1).
\end{aligned}$$

We next expand  $Z_{0,i}$  in (E.2). Again, by direct algebra,

$$\begin{aligned}
Z_{0,i} &= \hat{\mu}_{10} - \mu_{10} + \frac{1 - A_i}{1 - \hat{\pi}_1} (\hat{\mu}_1 - \hat{\mu}_{10}) - \frac{1 - A_i}{1 - \pi_1} (\mu_1 - \mu_{10}) \\
&= \hat{\mu}_{10} - \mu_{10} + (1 - A_i) \left[ \frac{\hat{\mu}_1 - \hat{\mu}_{10}}{1 - \hat{\pi}_1} - \frac{\mu_1 - \mu_{10}}{1 - \pi_1} \right] \\
&= \hat{\mu}_{10} - \mu_{10} + (1 - A_i) \left[ \frac{\hat{\mu}_1 - \hat{\mu}_{10}}{1 - \hat{\pi}_1} - \frac{\mu_1 - \mu_{10}}{1 - \hat{\pi}_1} + \frac{\mu_1 - \mu_{10}}{1 - \hat{\pi}_1} - \frac{\mu_1 - \mu_{10}}{1 - \pi_1} \right] \\
&= \hat{\mu}_{10} - \mu_{10} + (1 - A_i) \left[ \frac{\hat{\mu}_1 - \hat{\mu}_{10} - \mu_1 + \mu_{10}}{1 - \hat{\pi}_1} + (\mu_1 - \mu_{10}) \left( \frac{1}{1 - \hat{\pi}_1} - \frac{1}{1 - \pi_1} \right) \right] \\
&= \hat{\mu}_{10} - \mu_{10} + (1 - A_i) \left[ \frac{\hat{\mu}_1 - \mu_1}{1 - \hat{\pi}_1} - \frac{\hat{\mu}_{10} - \mu_{10}}{1 - \hat{\pi}_1} + (\mu_1 - \mu_{10}) \left( \frac{1}{1 - \hat{\pi}_1} - \frac{1}{1 - \pi_1} \right) \right] \\
&= \hat{\mu}_{10} - \mu_{10} - \frac{1 - A_i}{1 - \hat{\pi}_1} (\hat{\mu}_{10} - \mu_{10}) + \frac{1 - A_i}{1 - \hat{\pi}_1} (\hat{\mu}_1 - \mu_1) \\
&\quad + (1 - A_i) (\mu_1 - \mu_{10}) \left( \frac{1}{1 - \hat{\pi}_1} - \frac{1}{1 - \pi_1} \right) \\
&= \left[ 1 - \frac{1 - A_i}{1 - \hat{\pi}_1} \right] (\hat{\mu}_{10} - \mu_{10}) + \frac{1 - A_i}{1 - \hat{\pi}_1} (\hat{\mu}_1 - \mu_1) \\
&\quad + (1 - A_i) (\mu_1 - \mu_{10}) \left( \frac{1}{1 - \hat{\pi}_1} - \frac{1}{1 - \pi_1} \right) \\
&= \frac{A_i - \hat{\pi}_1}{1 - \hat{\pi}_1} (\hat{\mu}_{10} - \mu_{10}) + \frac{1 - A_i}{1 - \hat{\pi}_1} (\hat{\mu}_1 - \mu_1) \\
&\quad + (1 - A_i) (\mu_1 - \mu_{10}) \left( \frac{1}{1 - \hat{\pi}_1} - \frac{1}{1 - \pi_1} \right).
\end{aligned}$$

Substituting the expansions of  $Z_{1,i}$  and  $Z_{0,i}$  into (E.2), we obtain

$$\begin{aligned}
\hat{\theta}_0^{\text{IF}} - \theta_0 &= \frac{1}{n} \sum_{i=1}^n \Psi_i \\
&\quad + \frac{1}{n} \sum_{i=1}^n A_i \frac{\hat{\pi}_2}{\hat{\pi}_1} (\mu_1 - \hat{\mu}_1) + \frac{1}{n} \sum_{i=1}^n A_i \frac{\hat{\pi}_2 - \pi_2}{\hat{\pi}_1} (Y_i - \mu_1) + \frac{1}{n} \sum_{i=1}^n A_i \pi_2 \left( \frac{1}{\hat{\pi}_1} - \frac{1}{\pi_1} \right) (Y_i - \mu_1) \\
&\quad + \frac{1}{n} \sum_{i=1}^n \frac{A_i - \hat{\pi}_1}{1 - \hat{\pi}_1} (\hat{\mu}_{10} - \mu_{10}) + \frac{1}{n} \sum_{i=1}^n \frac{1 - A_i}{1 - \hat{\pi}_1} (\hat{\mu}_1 - \mu_1) \\
&\quad + \frac{1}{n} \sum_{i=1}^n (1 - A_i) (\mu_1 - \mu_{10}) \left( \frac{1}{1 - \hat{\pi}_1} - \frac{1}{1 - \pi_1} \right)
\end{aligned}$$

$$\begin{aligned}
&= \frac{1}{n} \sum_{i=1}^n \Psi_i \\
&\quad + \frac{1}{n} \sum_{i=1}^n A_i \pi_2 \left( \frac{1}{\hat{\pi}_1} - \frac{1}{\pi_1} \right) (Y_i - \mu_1) \\
&\quad + \frac{1}{n} \sum_{i=1}^n A_i \frac{\hat{\pi}_2 - \pi_2}{\hat{\pi}_1} (Y_i - \mu_1) \\
&\quad + \frac{1}{n} \sum_{i=1}^n \left[ \frac{1 - A_i}{1 - \hat{\pi}_1} - A_i \frac{\hat{\pi}_2}{\hat{\pi}_1} \right] (\hat{\mu}_1 - \mu_1) \\
&\quad + \frac{1}{n} \sum_{i=1}^n (1 - A_i) (\mu_1 - \mu_{10}) \left( \frac{1}{1 - \hat{\pi}_1} - \frac{1}{1 - \pi_1} \right) \\
&\quad + \frac{1}{n} \sum_{i=1}^n \frac{A_i - \hat{\pi}_1}{1 - \hat{\pi}_1} (\hat{\mu}_{10} - \mu_{10}).
\end{aligned}$$

Comparing with the definitions of  $R_0, R_1, R_2, R_3, R_4$ , we obtain

$$\hat{\theta}_0^{\text{IF}} - \theta_0 = \frac{1}{n} \sum_{i=1}^n \Psi_i + R_0 + R_1 + R_2 + R_3 + R_4. \quad (\text{E.3})$$

**Reduction to the remainder terms.** To establish the asymptotic linearity of  $\hat{\theta}_0^{\text{IF}}$ , it suffices to show that  $\sqrt{n} R_j = o_p(1)$ ,  $j = 0, \dots, 4$ . Multiplying the decomposition in Equation (E.3) by  $\sqrt{n}$  yields

$$\begin{aligned}
\sqrt{n}(\hat{\theta}_0^{\text{IF}} - \theta_0) &= \frac{1}{\sqrt{n}} \sum_{i=1}^n \Psi_i + \sqrt{n} R_0 + \sqrt{n} R_1 + \sqrt{n} R_2 + \sqrt{n} R_3 + \sqrt{n} R_4 \\
&=: \frac{1}{\sqrt{n}} \sum_{i=1}^n \Psi_i + T_1 + T_2 + T_3 + T_4 + T_5.
\end{aligned}$$

Thus, it remains to show that  $T_j = o_p(1)$  for  $j = 1, \dots, 5$ , in which case

$$\sqrt{n}(\hat{\theta}_0^{\text{IF}} - \theta_0) = \frac{1}{\sqrt{n}} \sum_{i=1}^n \Psi_i + o_p(1).$$

We now write the remainder terms explicitly:

$$\begin{aligned}
T_1 &= \frac{1}{\sqrt{n}} \sum_{i=1}^n A_i \pi_2(\mathbf{f}_{X,i}, \mathbf{f}_{M,i}) \left( \frac{1}{\hat{\pi}_1(\hat{\mathbf{f}}_{X,i})} - \frac{1}{\pi_1(\mathbf{f}_{X,i})} \right) (Y_i - \mu_1(\mathbf{f}_{X,i}, \mathbf{f}_{M,i})), \\
T_2 &= \frac{1}{\sqrt{n}} \sum_{i=1}^n A_i \frac{\hat{\pi}_2(\hat{\mathbf{f}}_{X,i}, \hat{\mathbf{f}}_{M,i}) - \pi_2(\mathbf{f}_{X,i}, \mathbf{f}_{M,i})}{\hat{\pi}_1(\hat{\mathbf{f}}_{X,i})} (Y_i - \mu_1(\mathbf{f}_{X,i}, \mathbf{f}_{M,i})), \\
T_3 &= \frac{1}{\sqrt{n}} \sum_{i=1}^n \left[ \frac{1 - A_i}{1 - \hat{\pi}_1(\hat{\mathbf{f}}_{X,i})} - A_i \frac{\hat{\pi}_2(\hat{\mathbf{f}}_{X,i}, \hat{\mathbf{f}}_{M,i})}{\hat{\pi}_1(\hat{\mathbf{f}}_{X,i})} \right] (\hat{\mu}_1(\hat{\mathbf{f}}_{X,i}, \hat{\mathbf{f}}_{M,i}) - \mu_1(\mathbf{f}_{X,i}, \mathbf{f}_{M,i})), \\
T_4 &= \frac{1}{\sqrt{n}} \sum_{i=1}^n (1 - A_i) (\mu_1(\mathbf{f}_{X,i}, \mathbf{f}_{M,i}) - \mu_{10}(\mathbf{f}_{X,i})) \left( \frac{1}{1 - \hat{\pi}_1(\hat{\mathbf{f}}_{X,i})} - \frac{1}{1 - \pi_1(\mathbf{f}_{X,i})} \right), \\
T_5 &= \frac{1}{\sqrt{n}} \sum_{i=1}^n \frac{A_i - \hat{\pi}_1(\hat{\mathbf{f}}_{X,i})}{1 - \hat{\pi}_1(\hat{\mathbf{f}}_{X,i})} (\hat{\mu}_{10}(\hat{\mathbf{f}}_{X,i}) - \mu_{10}(\mathbf{f}_{X,i})).
\end{aligned}$$

Before proceeding with the analysis, we define the following sigma-algebras:

$$\mathcal{G}_n^{T_1} := \sigma(\{\mathbf{f}_{X,i}, \mathbf{f}_{M,i}, \mathbf{u}_{X,i}, \mathbf{u}_{M,i} : i \in \mathcal{I}_4\}, \hat{\pi}_1),$$

$$\begin{aligned}
\mathcal{G}_n^{T_2} &:= \sigma\left(\{\mathbf{f}_{X,i}, \mathbf{f}_{M,i}, \mathbf{u}_{X,i}, \mathbf{u}_{M,i} : i \in \mathcal{I}_4\}, \hat{\pi}_1, \hat{\rho}\right), \\
\mathcal{G}_n^{T_3} &:= \sigma\left(\{\mathbf{f}_{X,i}, \mathbf{f}_{M,i}, \mathbf{u}_{X,i}, \mathbf{u}_{M,i} : i \in \mathcal{I}_4\}, \hat{\pi}_1, \hat{\rho}, \hat{\mu}_1\right), \\
\mathcal{G}_n^{T_4} = \mathcal{G}_n^{T_5} &:= \sigma\left(\{\mathbf{f}_{X,i}, \mathbf{f}_{M,i}, \mathbf{u}_{X,i}, \mathbf{u}_{M,i} : i \in \mathcal{I}_4\}, \hat{\pi}_1, \hat{\mu}_{10}\right).
\end{aligned}$$

**Analysis of  $T_1$ .** We consider a single fold  $\mathcal{I}_4$  for evaluation and  $|\mathcal{I}_4| = n$ , and all summations below are taken over  $i \in \mathcal{I}_4$ . We first study the conditional expectation of  $T_1$ :

$$\begin{aligned}
\mathbb{E}[T_1 \mid \mathcal{G}_n^{T_1}] &= \mathbb{E}\left[\frac{1}{\sqrt{n}} \sum_{i \in \mathcal{I}_4} A_i \pi_2(\mathbf{f}_{X,i}, \mathbf{f}_{M,i}) \left(\frac{1}{\hat{\pi}_1(\hat{\mathbf{f}}_{X,i})} - \frac{1}{\pi_1(\mathbf{f}_{X,i})}\right) (Y_i - \mu_1(\mathbf{f}_{X,i}, \mathbf{f}_{M,i})) \mid \mathcal{G}_n^{T_1}\right] \\
&= \frac{1}{\sqrt{n}} \sum_{i \in \mathcal{I}_4} \pi_2(\mathbf{f}_{X,i}, \mathbf{f}_{M,i}) \left(\frac{1}{\hat{\pi}_1(\hat{\mathbf{f}}_{X,i})} - \frac{1}{\pi_1(\mathbf{f}_{X,i})}\right) \mathbb{E}[A_i (Y_i - \mu_1(\mathbf{f}_{X,i}, \mathbf{f}_{M,i})) \mid \mathcal{G}_n^{T_1}] \\
&= \frac{1}{\sqrt{n}} \sum_{i \in \mathcal{I}_4} \pi_2(\mathbf{f}_{X,i}, \mathbf{f}_{M,i}) \left(\frac{1}{\hat{\pi}_1(\hat{\mathbf{f}}_{X,i})} - \frac{1}{\pi_1(\mathbf{f}_{X,i})}\right) \\
&\quad \cdot \mathbb{E}[A_i \mathbb{E}[Y_i - \mu_1(\mathbf{f}_{X,i}, \mathbf{f}_{M,i}) \mid A_i = 1, \mathbf{f}_{X,i}, \mathbf{f}_{M,i}] \mid \mathcal{G}_n^{T_1}] \\
&= 0.
\end{aligned}$$

Therefore,  $\mathbb{E}[T_1 \mid \mathcal{G}_n^{T_1}] = 0$ . We next study the conditional variance of  $T_1$ . Using conditional independence across observations given  $\mathcal{G}_n^{T_1}$ , we have:

$$\begin{aligned}
\text{Var}(T_1 \mid \mathcal{G}_n^{T_1}) &= \frac{1}{n} \sum_{i \in \mathcal{I}_4} \text{Var}\left(A_i \pi_2(\mathbf{f}_{X,i}, \mathbf{f}_{M,i}) \left(\frac{1}{\hat{\pi}_1(\hat{\mathbf{f}}_{X,i})} - \frac{1}{\pi_1(\mathbf{f}_{X,i})}\right) (Y_i - \mu_1(\mathbf{f}_{X,i}, \mathbf{f}_{M,i})) \mid \mathcal{G}_n^{T_1}\right) \\
&\leq \frac{1}{n} \sum_{i \in \mathcal{I}_4} \pi_2(\mathbf{f}_{X,i}, \mathbf{f}_{M,i})^2 \left(\frac{1}{\hat{\pi}_1(\hat{\mathbf{f}}_{X,i})} - \frac{1}{\pi_1(\mathbf{f}_{X,i})}\right)^2 \\
&\quad \cdot \mathbb{E}\left[A_i (Y_i - \mu_1(\mathbf{f}_{X,i}, \mathbf{f}_{M,i}))^2 \mid \mathcal{G}_n^{T_1}\right] \\
&\leq C \frac{1}{n} \sum_{i \in \mathcal{I}_4} \left(\frac{1}{\hat{\pi}_1(\hat{\mathbf{f}}_{X,i})} - \frac{1}{\pi_1(\mathbf{f}_{X,i})}\right)^2 \\
&= C \frac{1}{n} \sum_{i \in \mathcal{I}_4} \left|\frac{\pi_1(\mathbf{f}_{X,i}) - \hat{\pi}_1(\hat{\mathbf{f}}_{X,i})}{\hat{\pi}_1(\hat{\mathbf{f}}_{X,i}) \pi_1(\mathbf{f}_{X,i})}\right|^2 \\
&\leq C \frac{1}{n} \sum_{i \in \mathcal{I}_4} (\hat{\pi}_1(\hat{\mathbf{f}}_{X,i}) - \pi_1(\mathbf{f}_{X,i}))^2 \\
&= C \left\| \hat{\pi}_1(\hat{\mathbf{f}}_X) - \pi_1(\mathbf{f}_X) \right\|_{L_2(P_n)}^2 \\
&= C \left\| \hat{\pi}_1(\hat{\mathbf{f}}_X) - \pi_1 \circ v_X^{-1}(\hat{\mathbf{f}}_X) + \pi_1 \circ v_X^{-1}(\hat{\mathbf{f}}_X) - \pi_1(\mathbf{f}_X) \right\|_{L_2(P_n)}^2 \\
&\leq C \left( \left\| \hat{\pi}_1(\hat{\mathbf{f}}_X) - \pi_1 \circ v_X^{-1}(\hat{\mathbf{f}}_X) \right\|_{L_2(P_n)} + \left\| \pi_1 \circ v_X^{-1}(\hat{\mathbf{f}}_X) - \pi_1(\mathbf{f}_X) \right\|_{L_2(P_n)} \right)^2 \\
&\leq C \left\| \hat{\pi}_1(\hat{\mathbf{f}}_X) - \pi_1 \circ v_X^{-1}(\hat{\mathbf{f}}_X) \right\|_{L_2(P_n)}^2 + C \left\| \pi_1 \circ v_X^{-1}(\hat{\mathbf{f}}_X) - \pi_1(\mathbf{f}_X) \right\|_{L_2(P_n)}^2.
\end{aligned}$$

The last inequality follows from Young's inequality, equivalently  $(a + b)^2 \leq 2a^2 + 2b^2$ . The second inequality above uses  $A_i \leq 1$ , boundedness of  $\pi_2$ ,  $\pi_1$  and  $\hat{\pi}_1$ , and the bounded conditional second moment in Assumption 4.1. It remains to bound the first empirical  $L_2(P_n)$  term. We first add and subtract its population counterpart:

$$\left\| \hat{\pi}_1(\hat{\mathbf{f}}_X) - \pi_1 \circ v_X^{-1}(\hat{\mathbf{f}}_X) \right\|_{L_2(P_n)}^2$$

$$\begin{aligned}
&= \|\hat{\pi}_1 - \pi_1 \circ v_X^{-1}\|_{L_2(P)}^2 + \left\{ \|\hat{\pi}_1(\hat{\mathbf{f}}_X) - \pi_1 \circ v_X^{-1}(\hat{\mathbf{f}}_X)\|_{L_2(P_n)}^2 - \|\hat{\pi}_1 - \pi_1 \circ v_X^{-1}\|_{L_2(P)}^2 \right\} \\
&= O_p(\delta_{n,\pi_1}^2 + n^{-1/2}),
\end{aligned}$$

where the first term follows from the population  $L_2$  rate in Theorem 4.3, and the second term is obtained via Lemma E.1 applied to the empirical average over the evaluation fold. Combining the above bounds, we obtain  $\text{Var}(T_1 | \mathcal{G}_n^{T_1}) = O_p(\delta_{n,\pi_1}^2 + n^{-1/2} + \delta_{n,f}^2) = o_p(1)$ . Together with  $\mathbb{E}[T_1 | \mathcal{G}_n^{T_1}] = 0$ , Chebyshev's inequality gives, for any  $\varepsilon > 0$ ,

$$\mathbb{P}(|T_1| > \varepsilon | \mathcal{G}_n^{T_1}) \leq \frac{\text{Var}(T_1 | \mathcal{G}_n^{T_1})}{\varepsilon^2} = o_p(1).$$

Since  $0 \leq \mathbb{P}(|T_1| > \varepsilon | \mathcal{G}_n^{T_1}) \leq 1$ , the dominated convergence argument gives  $\mathbb{P}(|T_1| > \varepsilon) = \mathbb{E}[\mathbb{P}(|T_1| > \varepsilon | \mathcal{G}_n^{T_1})] \rightarrow 0$ . Hence  $T_1 = o_p(1)$ .

**Analysis of  $T_2$ .** Recall that the density ratio  $\hat{\pi}_2$  is represented as  $\hat{\pi}_2(\hat{\mathbf{f}}_X, \hat{\mathbf{f}}_M) = \frac{1 - \hat{\rho}(\hat{\mathbf{f}}_X, \hat{\mathbf{f}}_M)}{\hat{\rho}(\hat{\mathbf{f}}_X, \hat{\mathbf{f}}_M)} \cdot \frac{\hat{\pi}_1(\hat{\mathbf{f}}_X)}{1 - \hat{\pi}_1(\hat{\mathbf{f}}_X)}$ . We first study the conditional expectation of  $T_2$  given  $\mathcal{G}_n^{T_2}$ :

$$\begin{aligned}
\mathbb{E}[T_2 | \mathcal{G}_n^{T_2}] &= \mathbb{E} \left[ \frac{1}{\sqrt{n}} \sum_{i \in \mathcal{I}_4} A_i \frac{\hat{\pi}_2(\hat{\mathbf{f}}_{X,i}, \hat{\mathbf{f}}_{M,i}) - \pi_2(\mathbf{f}_{X,i}, \mathbf{f}_{M,i})}{\hat{\pi}_1(\hat{\mathbf{f}}_{X,i})} (Y_i - \mu_1(\mathbf{f}_{X,i}, \mathbf{f}_{M,i})) \middle| \mathcal{G}_n^{T_2} \right] \\
&= \frac{1}{\sqrt{n}} \sum_{i \in \mathcal{I}_4} \frac{\hat{\pi}_2(\hat{\mathbf{f}}_{X,i}, \hat{\mathbf{f}}_{M,i}) - \pi_2(\mathbf{f}_{X,i}, \mathbf{f}_{M,i})}{\hat{\pi}_1(\hat{\mathbf{f}}_{X,i})} \mathbb{E}[A_i (Y_i - \mu_1(\mathbf{f}_{X,i}, \mathbf{f}_{M,i})) | \mathcal{G}_n^{T_2}] \\
&= \frac{1}{\sqrt{n}} \sum_{i \in \mathcal{I}_4} \frac{\hat{\pi}_2(\hat{\mathbf{f}}_{X,i}, \hat{\mathbf{f}}_{M,i}) - \pi_2(\mathbf{f}_{X,i}, \mathbf{f}_{M,i})}{\hat{\pi}_1(\hat{\mathbf{f}}_{X,i})} \\
&\quad \cdot \mathbb{E}[A_i \mathbb{E}[Y_i - \mu_1(\mathbf{f}_{X,i}, \mathbf{f}_{M,i}) | A_i = 1, \mathbf{f}_{X,i}, \mathbf{f}_{M,i}] | \mathcal{G}_n^{T_2}] \\
&= 0.
\end{aligned}$$

We next study the conditional variance of  $T_2$ :

$$\begin{aligned}
\text{Var}(T_2 | \mathcal{G}_n^{T_2}) &= \frac{1}{n} \sum_{i \in \mathcal{I}_4} \text{Var} \left( A_i \frac{\hat{\pi}_2(\hat{\mathbf{f}}_{X,i}, \hat{\mathbf{f}}_{M,i}) - \pi_2(\mathbf{f}_{X,i}, \mathbf{f}_{M,i})}{\hat{\pi}_1(\hat{\mathbf{f}}_{X,i})} (Y_i - \mu_1(\mathbf{f}_{X,i}, \mathbf{f}_{M,i})) \middle| \mathcal{G}_n^{T_2} \right) \\
&\leq \frac{1}{n} \sum_{i \in \mathcal{I}_4} \left( \frac{\hat{\pi}_2(\hat{\mathbf{f}}_{X,i}, \hat{\mathbf{f}}_{M,i}) - \pi_2(\mathbf{f}_{X,i}, \mathbf{f}_{M,i})}{\hat{\pi}_1(\hat{\mathbf{f}}_{X,i})} \right)^2 \mathbb{E}[A_i (Y_i - \mu_1(\mathbf{f}_{X,i}, \mathbf{f}_{M,i}))^2 | \mathcal{G}_n^{T_2}] \\
&\leq C \frac{1}{n} \sum_{i \in \mathcal{I}_4} (\hat{\pi}_2(\hat{\mathbf{f}}_{X,i}, \hat{\mathbf{f}}_{M,i}) - \pi_2(\mathbf{f}_{X,i}, \mathbf{f}_{M,i}))^2.
\end{aligned}$$

The second inequality uses  $A_i \leq 1$ , positivity of  $\hat{\pi}_1$ , and the bounded conditional second moment in Assumption 4.1. Now, using the ratio representation of  $\pi_2$  together with the uniform boundedness of  $(\pi_1, \hat{\pi}_1, \rho, \hat{\rho})$ , we obtain

$$\begin{aligned}
&\left| \hat{\pi}_2(\hat{\mathbf{f}}_{X,i}, \hat{\mathbf{f}}_{M,i}) - \pi_2(\mathbf{f}_{X,i}, \mathbf{f}_{M,i}) \right| \\
&\leq C \left( \left| \hat{\rho}(\hat{\mathbf{f}}_{X,i}, \hat{\mathbf{f}}_{M,i}) - \rho \circ v^{-1}(\hat{\mathbf{f}}_{X,i}, \hat{\mathbf{f}}_{M,i}) \right| + \left| \hat{\pi}_1(\hat{\mathbf{f}}_{X,i}) - \pi_1 \circ v_X^{-1}(\hat{\mathbf{f}}_{X,i}) \right| \right. \\
&\quad \left. + \left| \rho \circ v^{-1}(\hat{\mathbf{f}}_{X,i}, \hat{\mathbf{f}}_{M,i}) - \rho(\mathbf{f}_{X,i}, \mathbf{f}_{M,i}) \right| + \left| \pi_1 \circ v_X^{-1}(\hat{\mathbf{f}}_{X,i}) - \pi_1(\mathbf{f}_{X,i}) \right| \right),
\end{aligned}$$

where we use that the maps  $x \mapsto (1-x)/x$  and  $x \mapsto x/(1-x)$  are Lipschitz. Therefore, we obtain

$$\begin{aligned}
&\frac{1}{n} \sum_{i \in \mathcal{I}_4} (\hat{\pi}_2(\hat{\mathbf{f}}_{X,i}, \hat{\mathbf{f}}_{M,i}) - \pi_2(\mathbf{f}_{X,i}, \mathbf{f}_{M,i}))^2 \\
&\leq C \left\| \hat{\rho}(\hat{\mathbf{f}}_X, \hat{\mathbf{f}}_M) - \rho \circ v^{-1}(\hat{\mathbf{f}}_X, \hat{\mathbf{f}}_M) \right\|_{L_2(P_n)}^2 + C \left\| \hat{\pi}_1(\hat{\mathbf{f}}_X) - \pi_1 \circ v_X^{-1}(\hat{\mathbf{f}}_X) \right\|_{L_2(P_n)}^2
\end{aligned}$$

$$\begin{aligned}
& + C \left\| \rho \circ v^{-1}(\hat{\mathbf{f}}_X, \hat{\mathbf{f}}_M) - \rho(\mathbf{f}_X, \mathbf{f}_M) \right\|_{L_2(P_n)}^2 + C \left\| \pi_1 \circ v_X^{-1}(\hat{\mathbf{f}}_X) - \pi_1(\mathbf{f}_X) \right\|_{L_2(P_n)}^2 \\
& = O_p(\delta_{n,\rho}^2 + n^{-1/2}) + O_p(\delta_{n,\pi_1}^2 + n^{-1/2}) + O_p(\delta_{n,f}^2) + O_p(\delta_{n,f}^2) \\
& = O_p(\delta_{n,\rho}^2 + \delta_{n,\pi_1}^2 + \delta_{n,f}^2 + n^{-1/2}).
\end{aligned}$$

where the inequality follows  $(a + b + c + d)^2 \leq C(a^2 + b^2 + c^2 + d^2)$ . The first two rates follow by adding and subtracting their population  $L_2(P)$  counterparts, using the nuisance rates in Theorem 4.3, and applying Lemma E.1. The last two rates follow from the Lipschitz continuity of  $\rho$  and  $\pi_1$  together with the factor-recovery rate in Theorem 4.3. Combining the above bounds, we obtain  $\text{Var}(T_2 \mid \mathcal{G}_n^{T_2}) = O_p(\delta_{n,\rho}^2 + \delta_{n,\pi_1}^2 + \delta_{n,f}^2 + n^{-1/2}) = o_p(1)$ . Together with  $\mathbb{E}[T_2 \mid \mathcal{G}_n^{T_2}] = 0$ , Chebyshev's inequality gives, for any  $\varepsilon > 0$ ,

$$\mathbb{P}(|T_2| > \varepsilon \mid \mathcal{G}_n^{T_2}) \leq \frac{\text{Var}(T_2 \mid \mathcal{G}_n^{T_2})}{\varepsilon^2} = o_p(1).$$

Hence  $T_2 = o_p(1)$  by the similar argument as in proof of  $T_1$ .

**Analysis of  $T_3$ .** Consider  $T_3$ , which can be expressed as

$$\begin{aligned}
T_3 &= \frac{1}{\sqrt{n}} \sum_{i \in \mathcal{I}_4} \frac{(1 - A_i) - A_i \frac{1 - \hat{\rho}(\hat{\mathbf{f}}_{X,i}, \hat{\mathbf{f}}_{M,i})}{\hat{\rho}(\hat{\mathbf{f}}_{X,i}, \hat{\mathbf{f}}_{M,i})}}{1 - \hat{\pi}_1(\hat{\mathbf{f}}_{X,i})} (\hat{\mu}_1(\hat{\mathbf{f}}_{X,i}, \hat{\mathbf{f}}_{M,i}) - \mu_1(\mathbf{f}_{X,i}, \mathbf{f}_{M,i})) \\
&= \frac{1}{\sqrt{n}} \sum_{i \in \mathcal{I}_4} \frac{(1 - A_i) - A_i \frac{1 - \rho(\mathbf{f}_{X,i}, \mathbf{f}_{M,i})}{\rho(\mathbf{f}_{X,i}, \mathbf{f}_{M,i})}}{1 - \pi_1(\mathbf{f}_{X,i})} (\hat{\mu}_1(\hat{\mathbf{f}}_{X,i}, \hat{\mathbf{f}}_{M,i}) - \mu_1(\mathbf{f}_{X,i}, \mathbf{f}_{M,i})) \\
&\quad + \frac{1}{\sqrt{n}} \sum_{i \in \mathcal{I}_4} \left[ \frac{(1 - A_i) - A_i \frac{1 - \hat{\rho}(\hat{\mathbf{f}}_{X,i}, \hat{\mathbf{f}}_{M,i})}{\hat{\rho}(\hat{\mathbf{f}}_{X,i}, \hat{\mathbf{f}}_{M,i})}}{1 - \hat{\pi}_1(\hat{\mathbf{f}}_{X,i})} - \frac{(1 - A_i) - A_i \frac{1 - \rho(\mathbf{f}_{X,i}, \mathbf{f}_{M,i})}{\rho(\mathbf{f}_{X,i}, \mathbf{f}_{M,i})}}{1 - \pi_1(\mathbf{f}_{X,i})} \right] \\
&\quad \cdot (\hat{\mu}_1(\hat{\mathbf{f}}_{X,i}, \hat{\mathbf{f}}_{M,i}) - \mu_1(\mathbf{f}_{X,i}, \mathbf{f}_{M,i})) \\
&=: T_{31} + T_{32}.
\end{aligned}$$

We first study  $T_{31}$ . Then

$$\begin{aligned}
\mathbb{E}[T_{31} \mid \mathcal{G}_n^{T_3}] &= \frac{1}{\sqrt{n}} \sum_{i \in \mathcal{I}_4} \frac{\hat{\mu}_1(\hat{\mathbf{f}}_{X,i}, \hat{\mathbf{f}}_{M,i}) - \mu_1(\mathbf{f}_{X,i}, \mathbf{f}_{M,i})}{1 - \pi_1(\mathbf{f}_{X,i})} \\
&\quad \cdot \mathbb{E} \left[ (1 - A_i) - A_i \frac{1 - \rho(\mathbf{f}_{X,i}, \mathbf{f}_{M,i})}{\rho(\mathbf{f}_{X,i}, \mathbf{f}_{M,i})} \mid \mathcal{G}_n^{T_3} \right] \\
&= \frac{1}{\sqrt{n}} \sum_{i \in \mathcal{I}_4} \frac{\hat{\mu}_1(\hat{\mathbf{f}}_{X,i}, \hat{\mathbf{f}}_{M,i}) - \mu_1(\mathbf{f}_{X,i}, \mathbf{f}_{M,i})}{1 - \pi_1(\mathbf{f}_{X,i})} \\
&\quad \cdot \mathbb{E} \left[ \mathbb{E} \left[ (1 - A_i) - A_i \frac{1 - \rho(\mathbf{f}_{X,i}, \mathbf{f}_{M,i})}{\rho(\mathbf{f}_{X,i}, \mathbf{f}_{M,i})} \mid \mathbf{f}_{X,i}, \mathbf{f}_{M,i} \right] \mid \mathcal{G}_n^{T_3} \right] \\
&= \frac{1}{\sqrt{n}} \sum_{i \in \mathcal{I}_4} \frac{\hat{\mu}_1(\hat{\mathbf{f}}_{X,i}, \hat{\mathbf{f}}_{M,i}) - \mu_1(\mathbf{f}_{X,i}, \mathbf{f}_{M,i})}{1 - \pi_1(\mathbf{f}_{X,i})} \cdot 0 \\
&= 0,
\end{aligned}$$

where

$$\begin{aligned}
\mathbb{E} \left[ (1 - A_i) - A_i \frac{1 - \rho(\mathbf{f}_{X,i}, \mathbf{f}_{M,i})}{\rho(\mathbf{f}_{X,i}, \mathbf{f}_{M,i})} \mid \mathbf{f}_{X,i}, \mathbf{f}_{M,i} \right] &= 1 - \rho(\mathbf{f}_{X,i}, \mathbf{f}_{M,i}) - \rho(\mathbf{f}_{X,i}, \mathbf{f}_{M,i}) \frac{1 - \rho(\mathbf{f}_{X,i}, \mathbf{f}_{M,i})}{\rho(\mathbf{f}_{X,i}, \mathbf{f}_{M,i})} \\
&= 0.
\end{aligned}$$

Therefore,  $\mathbb{E}[T_{31} \mid \mathcal{G}_n^{T_3}] = 0$ . Next, Given  $\mathcal{G}_n^{T_3}$ ,

$$\text{Var}(T_{31} \mid \mathcal{G}_n^{T_3}) \leq C \frac{1}{n} \sum_{i \in \mathcal{I}_4} (\hat{\mu}_1(\hat{\mathbf{f}}_{X,i}, \hat{\mathbf{f}}_{M,i}) - \mu_1(\mathbf{f}_{X,i}, \mathbf{f}_{M,i}))^2$$

$$\begin{aligned}
&= C \left\| \hat{\mu}_1(\hat{\mathbf{f}}_X, \hat{\mathbf{f}}_M) - \mu_1(\mathbf{f}_X, \mathbf{f}_M) \right\|_{L_2(P_n)}^2 \\
&\leq C \left\| \hat{\mu}_1(\hat{\mathbf{f}}_X, \hat{\mathbf{f}}_M) - \mu_1 \circ v^{-1}(\hat{\mathbf{f}}_X, \hat{\mathbf{f}}_M) \right\|_{L_2(P_n)}^2 + C \left\| \mu_1 \circ v^{-1}(\hat{\mathbf{f}}_X, \hat{\mathbf{f}}_M) - \mu_1(\mathbf{f}_X, \mathbf{f}_M) \right\|_{L_2(P_n)}^2 \\
&= O_p(\delta_{n,\mu_1}^2 + n^{-1/2}) + O_p(\delta_{n,f}^2) \\
&= O_p(\delta_{n,\mu_1}^2 + \delta_{n,f}^2 + n^{-1/2}) = o_p(1).
\end{aligned}$$

Together with  $\mathbb{E}[T_{31} \mid \mathcal{G}_n^{T_3}] = 0$ , Chebyshev's inequality and the same dominated-convergence argument as in the proof of  $T_1$  imply  $T_{31} = o_p(1)$ .

We next study  $T_{32}$ . Recall that

$$T_{32} = \frac{1}{\sqrt{n}} \sum_{i \in \mathcal{I}_4} Z_{1,i} Z_{2,i},$$

where

$$\begin{aligned}
Z_{1,i} &:= \frac{(1 - A_i) - A_i \frac{1 - \hat{\rho}(\hat{\mathbf{f}}_{X,i}, \hat{\mathbf{f}}_{M,i})}{\hat{\rho}(\hat{\mathbf{f}}_{X,i}, \hat{\mathbf{f}}_{M,i})}}{1 - \hat{\pi}_1(\hat{\mathbf{f}}_{X,i})} - \frac{(1 - A_i) - A_i \frac{1 - \rho(\mathbf{f}_{X,i}, \mathbf{f}_{M,i})}{\rho(\mathbf{f}_{X,i}, \mathbf{f}_{M,i})}}{1 - \pi_1(\mathbf{f}_{X,i})}, \\
Z_{2,i} &:= \hat{\mu}_1(\hat{\mathbf{f}}_{X,i}, \hat{\mathbf{f}}_{M,i}) - \mu_1(\mathbf{f}_{X,i}, \mathbf{f}_{M,i}).
\end{aligned}$$

By Cauchy–Schwarz,

$$|T_{32}| \leq \frac{1}{\sqrt{n}} \left( \sum_{i \in \mathcal{I}_4} Z_{1,i}^2 \right)^{1/2} \left( \sum_{i \in \mathcal{I}_4} Z_{2,i}^2 \right)^{1/2} = \sqrt{n} \left( \frac{1}{n} \sum_{i \in \mathcal{I}_4} Z_{1,i}^2 \right)^{1/2} \left( \frac{1}{n} \sum_{i \in \mathcal{I}_4} Z_{2,i}^2 \right)^{1/2}.$$

By positivity and Lipschitz continuity of the maps  $x \mapsto (1 - x)/x$  and  $x \mapsto 1/(1 - x)$ ,

$$\begin{aligned}
|Z_{1,i}| &\leq C \left| \hat{\rho}(\hat{\mathbf{f}}_{X,i}, \hat{\mathbf{f}}_{M,i}) - \rho \circ v^{-1}(\hat{\mathbf{f}}_{X,i}, \hat{\mathbf{f}}_{M,i}) \right| + C \left| \rho \circ v^{-1}(\hat{\mathbf{f}}_{X,i}, \hat{\mathbf{f}}_{M,i}) - \rho(\mathbf{f}_{X,i}, \mathbf{f}_{M,i}) \right| \\
&\quad + C \left| \hat{\pi}_1(\hat{\mathbf{f}}_{X,i}) - \pi_1 \circ v_X^{-1}(\hat{\mathbf{f}}_{X,i}) \right| + C \left| \pi_1 \circ v_X^{-1}(\hat{\mathbf{f}}_{X,i}) - \pi_1(\mathbf{f}_{X,i}) \right|.
\end{aligned}$$

Therefore, using  $(a + b + c + d)^2 \leq C(a^2 + b^2 + c^2 + d^2)$ , Lemma E.1, and Assumptions in Theorem 4.3, we have:

$$\begin{aligned}
\left( \frac{1}{n} \sum_{i \in \mathcal{I}_4} Z_{1,i}^2 \right)^{1/2} &\leq C \left\| \hat{\rho}(\hat{\mathbf{f}}_X, \hat{\mathbf{f}}_M) - \rho \circ v^{-1}(\hat{\mathbf{f}}_X, \hat{\mathbf{f}}_M) \right\|_{L_2(P_n)} \\
&\quad + C \left\| \rho \circ v^{-1}(\hat{\mathbf{f}}_X, \hat{\mathbf{f}}_M) - \rho(\mathbf{f}_X, \mathbf{f}_M) \right\|_{L_2(P_n)} \\
&\quad + C \left\| \hat{\pi}_1(\hat{\mathbf{f}}_X) - \pi_1 \circ v_X^{-1}(\hat{\mathbf{f}}_X) \right\|_{L_2(P_n)} \\
&\quad + C \left\| \pi_1 \circ v_X^{-1}(\hat{\mathbf{f}}_X) - \pi_1(\mathbf{f}_X) \right\|_{L_2(P_n)} \\
&= O_p(\delta_{n,\rho} + n^{-1/2}) + O_p(\delta_{n,f}) + O_p(\delta_{n,\pi_1} + n^{-1/2}) + O_p(\delta_{n,f}) \\
&= O_p(\delta_{n,\rho} + \delta_{n,\pi_1} + \delta_{n,f} + n^{-1/2}).
\end{aligned}$$

Similarly,

$$\begin{aligned}
\left( \frac{1}{n} \sum_{i \in \mathcal{I}_4} Z_{2,i}^2 \right)^{1/2} &\leq C \left\| \hat{\mu}_1(\hat{\mathbf{f}}_X, \hat{\mathbf{f}}_M) - \mu_1 \circ v^{-1}(\hat{\mathbf{f}}_X, \hat{\mathbf{f}}_M) \right\|_{L_2(P_n)} \\
&\quad + C \left\| \mu_1 \circ v^{-1}(\hat{\mathbf{f}}_X, \hat{\mathbf{f}}_M) - \mu_1(\mathbf{f}_X, \mathbf{f}_M) \right\|_{L_2(P_n)}
\end{aligned}$$

$$\begin{aligned}
&= O_p(\delta_{n,\mu_1} + n^{-1/2}) + O_p(\delta_{n,f}) \\
&= O_p(\delta_{n,\mu_1} + \delta_{n,f} + n^{-1/2}),
\end{aligned}$$

again by Lemma E.1. Combining the above bounds gives

$$\begin{aligned}
|T_{32}| &= O_p \left[ \sqrt{n}(\delta_{n,\rho} + \delta_{n,\pi_1} + \delta_{n,f} + n^{-1/2})(\delta_{n,\mu_1} + \delta_{n,f} + n^{-1/2}) \right] \\
&= o_p(1),
\end{aligned}$$

Combining the results for  $T_{31}$  and  $T_{32}$ , we conclude  $T_3 = o_p(1)$ .

**Analysis of  $T_4$ .** We first study the conditional expectation of  $T_4$  given  $\mathcal{G}_n^{T_4}$ :

$$\begin{aligned}
\mathbb{E}[T_4 | \mathcal{G}_n^{T_4}] &= \frac{1}{\sqrt{n}} \sum_{i \in \mathcal{I}_4} \left( \frac{1}{1 - \hat{\pi}_1(\hat{\mathbf{f}}_{X,i})} - \frac{1}{1 - \pi_1(\mathbf{f}_{X,i})} \right) \\
&\quad \cdot \mathbb{E}[(1 - A_i)(\mu_1(\mathbf{f}_{X,i}, \mathbf{f}_{M,i}) - \mu_{10}(\mathbf{f}_{X,i})) | \mathcal{G}_n^{T_4}] \\
&= \frac{1}{\sqrt{n}} \sum_{i \in \mathcal{I}_4} \left( \frac{1}{1 - \hat{\pi}_1(\hat{\mathbf{f}}_{X,i})} - \frac{1}{1 - \pi_1(\mathbf{f}_{X,i})} \right) \\
&\quad \cdot \mathbb{E}[\mathbb{E}[(1 - A_i)(\mu_1(\mathbf{f}_{X,i}, \mathbf{f}_{M,i}) - \mu_{10}(\mathbf{f}_{X,i})) | A_i, \mathbf{f}_{X,i}] | \mathcal{G}_n^{T_4}] \\
&= 0.
\end{aligned}$$

The last equality follows from the definition  $\mu_{10}(\mathbf{f}_X) = \mathbb{E}[\mu_1(\mathbf{f}_X, \mathbf{f}_M) | A = 0, \mathbf{f}_X]$ , which implies

$$\begin{aligned}
&\mathbb{E}[(1 - A_i)(\mu_1(\mathbf{f}_{X,i}, \mathbf{f}_{M,i}) - \mu_{10}(\mathbf{f}_{X,i})) | A_i, \mathbf{f}_{X,i}] \\
&= (1 - A_i) \mathbb{E}[\mu_1(\mathbf{f}_{X,i}, \mathbf{f}_{M,i}) - \mu_{10}(\mathbf{f}_{X,i}) | A_i, \mathbf{f}_{X,i}] = 0.
\end{aligned}$$

We next study the conditional variance:

$$\begin{aligned}
\text{Var}(T_4 | \mathcal{G}_n^{T_4}) &\leq \frac{1}{n} \sum_{i \in \mathcal{I}_4} \mathbb{E} \left[ (1 - A_i)(\mu_1(\mathbf{f}_{X,i}, \mathbf{f}_{M,i}) - \mu_{10}(\mathbf{f}_{X,i}))^2 \left( \frac{1}{1 - \hat{\pi}_1(\hat{\mathbf{f}}_{X,i})} - \frac{1}{1 - \pi_1(\mathbf{f}_{X,i})} \right)^2 \middle| \mathcal{G}_n^{T_4} \right] \\
&\leq C \frac{1}{n} \sum_{i \in \mathcal{I}_4} \left( \frac{1}{1 - \hat{\pi}_1(\hat{\mathbf{f}}_{X,i})} - \frac{1}{1 - \pi_1(\mathbf{f}_{X,i})} \right)^2 \\
&\leq C \frac{1}{n} \sum_{i \in \mathcal{I}_4} (\hat{\pi}_1(\hat{\mathbf{f}}_{X,i}) - \pi_1(\mathbf{f}_{X,i}))^2 \\
&= C \left\| \hat{\pi}_1(\hat{\mathbf{f}}_X) - \pi_1(\mathbf{f}_X) \right\|_{L_2(P_n)}^2 \\
&\leq C \left\| \hat{\pi}_1(\hat{\mathbf{f}}_X) - \pi_1 \circ v_X^{-1}(\hat{\mathbf{f}}_X) \right\|_{L_2(P_n)}^2 + C \left\| \pi_1 \circ v_X^{-1}(\hat{\mathbf{f}}_X) - \pi_1(\mathbf{f}_X) \right\|_{L_2(P_n)}^2 \\
&= O_p(\delta_{n,\pi_1}^2 + n^{-1/2}) + O_p(\delta_{n,f}^2) \\
&= O_p(\delta_{n,\pi_1}^2 + \delta_{n,f}^2 + n^{-1/2}) = o_p(1).
\end{aligned}$$

The second inequality uses  $1 - A_i \leq 1$ , boundedness of  $\pi_1$  and  $\hat{\pi}_1$ , and the bounded conditional second moment in Assumption 4.1. Together with  $\mathbb{E}[T_4 | \mathcal{G}_n^{T_4}] = 0$ , Chebyshev's inequality and the same bounded-convergence-in-probability argument as in the proof of  $T_1$  imply  $T_4 = o_p(1)$ .

**Analysis of  $T_5$ .** Consider  $T_5$ , which can be expressed as

$$\begin{aligned}
T_5 &= \frac{1}{\sqrt{n}} \sum_{i \in \mathcal{I}_4} \frac{A_i - \hat{\pi}_1(\hat{\mathbf{f}}_{X,i})}{1 - \hat{\pi}_1(\hat{\mathbf{f}}_{X,i})} (\hat{\mu}_{10}(\hat{\mathbf{f}}_{X,i}) - \mu_{10}(\mathbf{f}_{X,i})) \\
&= \frac{1}{\sqrt{n}} \sum_{i \in \mathcal{I}_4} \frac{A_i - \pi_1(\mathbf{f}_{X,i})}{1 - \pi_1(\mathbf{f}_{X,i})} (\hat{\mu}_{10}(\hat{\mathbf{f}}_{X,i}) - \mu_{10}(\mathbf{f}_{X,i}))
\end{aligned}$$

$$\begin{aligned}
& + \frac{1}{\sqrt{n}} \sum_{i \in \mathcal{I}_4} \left[ \frac{A_i - \hat{\pi}_1(\hat{\mathbf{f}}_{X,i})}{1 - \hat{\pi}_1(\hat{\mathbf{f}}_{X,i})} - \frac{A_i - \pi_1(\mathbf{f}_{X,i})}{1 - \pi_1(\mathbf{f}_{X,i})} \right] \\
& \quad \cdot (\hat{\mu}_{10}(\hat{\mathbf{f}}_{X,i}) - \mu_{10}(\mathbf{f}_{X,i})) \\
& =: T_{51} + T_{52}.
\end{aligned}$$

We first study  $T_{51}$ . Then

$$\begin{aligned}
\mathbb{E}[T_{51} \mid \mathcal{G}_n^{T_5}] &= \frac{1}{\sqrt{n}} \sum_{i \in \mathcal{I}_4} \frac{\hat{\mu}_{10}(\hat{\mathbf{f}}_{X,i}) - \mu_{10}(\mathbf{f}_{X,i})}{1 - \pi_1(\mathbf{f}_{X,i})} \mathbb{E}[A_i - \pi_1(\mathbf{f}_{X,i}) \mid \mathcal{G}_n^{T_5}] \\
&= \frac{1}{\sqrt{n}} \sum_{i \in \mathcal{I}_4} \frac{\hat{\mu}_{10}(\hat{\mathbf{f}}_{X,i}) - \mu_{10}(\mathbf{f}_{X,i})}{1 - \pi_1(\mathbf{f}_{X,i})} \mathbb{E}[\mathbb{E}[A_i - \pi_1(\mathbf{f}_{X,i}) \mid \mathbf{f}_{X,i}] \mid \mathcal{G}_n^{T_5}] \\
&= 0.
\end{aligned}$$

We next study the conditional variance:

$$\begin{aligned}
\text{Var}(T_{51} \mid \mathcal{G}_n^{T_5}) &\leq C \frac{1}{n} \sum_{i \in \mathcal{I}_4} (\hat{\mu}_{10}(\hat{\mathbf{f}}_{X,i}) - \mu_{10}(\mathbf{f}_{X,i}))^2 \\
&= C \left\| \hat{\mu}_{10}(\hat{\mathbf{f}}_X) - \mu_{10}(\mathbf{f}_X) \right\|_{L_2(P_n)}^2 \\
&\leq C \left\| \hat{\mu}_{10}(\hat{\mathbf{f}}_X) - \mu_{10} \circ v_X^{-1}(\hat{\mathbf{f}}_X) \right\|_{L_2(P_n)}^2 + C \left\| \mu_{10} \circ v_X^{-1}(\hat{\mathbf{f}}_X) - \mu_{10}(\mathbf{f}_X) \right\|_{L_2(P_n)}^2 \\
&= O_p(\delta_{n,\mu_{10}}^2 + n^{-1/2}) + O_p(\delta_{n,f}^2) \\
&= O_p(\delta_{n,\mu_{10}}^2 + \delta_{n,f}^2 + n^{-1/2}) = o_p(1).
\end{aligned}$$

Together with  $\mathbb{E}[T_{51} \mid \mathcal{G}_n^{T_5}] = 0$ , Chebyshev's inequality and the same bounded-convergence-in-probability argument as in the proof of  $T_1$  imply  $T_{51} = o_p(1)$ .

We next study  $T_{52}$ . Let  $Z_{1,i} := \frac{A_i - \hat{\pi}_1(\hat{\mathbf{f}}_{X,i})}{1 - \hat{\pi}_1(\hat{\mathbf{f}}_{X,i})} - \frac{A_i - \pi_1(\mathbf{f}_{X,i})}{1 - \pi_1(\mathbf{f}_{X,i})}$ , and  $Z_{2,i} := \hat{\mu}_{10}(\hat{\mathbf{f}}_{X,i}) - \mu_{10}(\mathbf{f}_{X,i})$ . Then, we write

$$T_{52} = \frac{1}{\sqrt{n}} \sum_{i \in \mathcal{I}_4} Z_{1,i} Z_{2,i}.$$

By Cauchy–Schwarz,

$$|T_{52}| \leq \frac{1}{\sqrt{n}} \left( \sum_{i \in \mathcal{I}_4} Z_{1,i}^2 \right)^{1/2} \left( \sum_{i \in \mathcal{I}_4} Z_{2,i}^2 \right)^{1/2} = \sqrt{n} \left( \frac{1}{n} \sum_{i \in \mathcal{I}_4} Z_{1,i}^2 \right)^{1/2} \left( \frac{1}{n} \sum_{i \in \mathcal{I}_4} Z_{2,i}^2 \right)^{1/2}.$$

By positivity and Lipschitz continuity of the map  $x \mapsto (A_i - x)/(1 - x)$  on the relevant range,

$$\begin{aligned}
|Z_{1,i}| &\leq C \left| \hat{\pi}_1(\hat{\mathbf{f}}_{X,i}) - \pi_1(\mathbf{f}_{X,i}) \right| \\
&\leq C \left| \hat{\pi}_1(\hat{\mathbf{f}}_{X,i}) - \pi_1 \circ v_X^{-1}(\hat{\mathbf{f}}_{X,i}) \right| + C \left| \pi_1 \circ v_X^{-1}(\hat{\mathbf{f}}_{X,i}) - \pi_1(\mathbf{f}_{X,i}) \right|.
\end{aligned}$$

Therefore,

$$\begin{aligned}
\left( \frac{1}{n} \sum_{i \in \mathcal{I}_4} Z_{1,i}^2 \right)^{1/2} &\leq C \left\| \hat{\pi}_1(\hat{\mathbf{f}}_X) - \pi_1 \circ v_X^{-1}(\hat{\mathbf{f}}_X) \right\|_{L_2(P_n)} + C \left\| \pi_1 \circ v_X^{-1}(\hat{\mathbf{f}}_X) - \pi_1(\mathbf{f}_X) \right\|_{L_2(P_n)} \\
&= O_p(\delta_{n,\pi_1} + n^{-1/2}) + O_p(\delta_{n,f}) \\
&= O_p(\delta_{n,\pi_1} + \delta_{n,f} + n^{-1/2}).
\end{aligned}$$

Similarly,

$$|Z_{2,i}| \leq \left| \hat{\mu}_{10}(\hat{\mathbf{f}}_{X,i}) - \mu_{10} \circ v_X^{-1}(\hat{\mathbf{f}}_{X,i}) \right| + \left| \mu_{10} \circ v_X^{-1}(\hat{\mathbf{f}}_{X,i}) - \mu_{10}(\mathbf{f}_{X,i}) \right|,$$

and hence

$$\begin{aligned} \left( \frac{1}{n} \sum_{i \in \mathcal{I}_4} Z_{2,i}^2 \right)^{1/2} &\leq C \left\| \hat{\mu}_{10}(\hat{\mathbf{f}}_X) - \mu_{10} \circ v_X^{-1}(\hat{\mathbf{f}}_X) \right\|_{L_2(\mathbb{P}_n)} + C \left\| \mu_{10} \circ v_X^{-1}(\hat{\mathbf{f}}_X) - \mu_{10}(\mathbf{f}_X) \right\|_{L_2(\mathbb{P}_n)} \\ &= O_p(\delta_{n,\mu_{10}} + n^{-1/2}) + O_p(\delta_{n,f}) \\ &= O_p(\delta_{n,\mu_{10}} + \delta_{n,f} + n^{-1/2}). \end{aligned}$$

Combining the above bounds gives

$$|T_{52}| = O_p \left[ \sqrt{n}(\delta_{n,\pi_1} + \delta_{n,f} + n^{-1/2})(\delta_{n,\mu_{10}} + \delta_{n,f} + n^{-1/2}) \right] = o_p(1).$$

we obtain  $T_{52} = o_p(1)$ . Together with  $T_{51} = o_p(1)$ , this implies  $T_5 = o_p(1)$ .

**Asymptotics.** Combining the bounds for  $T_1, \dots, T_5$ , we obtain

$$\sqrt{n}(\hat{\theta}_0^{\text{IF}} - \theta_0) = \frac{1}{\sqrt{n}} \sum_{i=1}^n \Psi_i + o_p(1).$$

Since  $\mathbb{E}[\Psi_i] = 0$  and  $\text{Var}(\Psi_i) = \sigma_{\text{eff}}^2 < \infty$  by the central limit theorem,

$$\frac{1}{\sqrt{n}} \sum_{i=1}^n \Psi_i \xrightarrow{d} \mathcal{N}(0, \sigma_{\text{eff}}^2).$$

Applying Slutsky's theorem yields

$$\sqrt{n}(\hat{\theta}_0^{\text{IF}} - \theta_0) \xrightarrow{d} \mathcal{N}(0, \sigma_{\text{eff}}^2).$$

**Lemma E.1.** Suppose  $f : \mathcal{X} \rightarrow [-B, B]$  where  $\mathcal{X} \subseteq \mathbb{R}^d$ . Let  $X_1, \dots, X_n \sim P$  for some probability measure  $P$  on  $\mathcal{X}$ . Define  $L_2(\mathbb{P}_n)$  and  $L_2(P)$  norm of  $f$  as:

$$\|f\|_n := \|f\|_{L_2(\mathbb{P}_n)} = \sqrt{\frac{1}{n} \sum_i f^2(X_i)}, \quad \|f\|_2 = \|f\|_{L_2(P)} = \sqrt{\int f^2(x) dP(x)}.$$

Then, we have:

$$\mathbb{P}(|\|f\|_n - \|f\|_2| > t) \leq \frac{B^2}{nt^2}.$$

As a consequence,  $|\|f\|_n - \|f\|_2| = O_p(n^{-1/2})$ .

## F Proof of Lemma E.1

From definition we have:

$$|\|f\|_n - \|f\|_2| = \frac{|\|f\|_n^2 - \|f\|_2^2|}{\|f\|_n + \|f\|_2} \leq \frac{|\|f\|_n^2 - \|f\|_2^2|}{\|f\|_2}$$

As a consequence, we have:

$$\begin{aligned} \mathbb{P}(|\|f\|_n - \|f\|_2| > t) &\leq \mathbb{P}(|\|f\|_n^2 - \|f\|_2^2| > t\|f\|_2) \\ &= \mathbb{P} \left( \left| \frac{1}{n} \sum_{i=1}^n (f^2(X_i) - \mathbb{E}[f^2(X)]) \right| > t\|f\|_2 \right) \end{aligned}$$

$$\begin{aligned}
&\leq \frac{\text{var}(f^2(X))}{nt^2\|f\|_2^2} \\
&\leq \frac{\mathbb{E}(f^4(X))}{nt^2\|f\|_2^2} \\
&\leq \frac{B^2\mathbb{E}(f^2(X))}{nt^2\|f\|_2^2} = \frac{B^2}{nt^2}.
\end{aligned}$$

The last inequality follows from the fact that  $\|f\|_\infty \leq B$ . This completes the proof.

## G Proof of Theorem 4.7

The proof mostly follows using a similar argument as in the proof of Theorem 1 of [Fan and Gu \(2023\)](#). We highlight the key parts here. As the proof for  $\hat{\pi}_1$  and  $\hat{\rho}$  are analogous, we skip the latter for brevity and present the proof of the other three nuisances here.

### G.1 Rate for $\hat{\mu}_1$ under the transformed factor representation

Recall our notation  $\mathbf{f} = (\mathbf{f}_X, \mathbf{f}_M)$  denotes the unobserved factors, and  $\hat{\mathbf{f}} = (\hat{\mathbf{f}}_X, \hat{\mathbf{f}}_M)$  denotes the estimated factors, i.e.  $\hat{\mathbf{f}}_X = \hat{g}_X(X)$  and  $\hat{\mathbf{f}}_M = \hat{g}_M(M)$ . By the regression model, we have:

$$Y_i = \mu_1(\mathbf{f}_i) + \epsilon_i$$

where  $\mathbb{E}[\epsilon_i \mid \mathbf{f}_i, \mathbf{u}_{X,i}, \mathbf{u}_{M,i}, A] = 0$  and  $\epsilon_i$  is sub-gaussian random variable. As  $\hat{\mathbf{f}}$  is a function of  $(\mathbf{f}, \mathbf{u}_X, \mathbf{u}_M)$ , and the encoder is estimated from a separate dataset, it is immediate that  $\mathbb{E}[\epsilon \mid \hat{\mathbf{f}}, A] = 0$ . We use the notation  $\eta = \mu_1 \circ \nu^{-1}$ . As per Theorem 4.7,  $\eta$  is bounded, Lipschitz, and moreover  $\eta \in \mathcal{H}(d_\eta, \ell_\eta, \mathcal{P})$  with DAS  $\gamma_\eta^*$ . Let  $\mathcal{I}_1 = \{i \in \mathcal{I}_{\text{nuis}} : A_i = 1\}$ . As per our assumption,

$$\|\hat{\mathbf{f}} - \nu(\mathbf{f})\|_{L_2(P_1)} = O_p(\delta_{n,f}),$$

Let  $\mathcal{G}_{\eta,n} := \mathcal{G}(L_\eta, d_\eta, 1, N_\eta, M_\eta, B_\eta)$  be a collection of truncated ReLU network class used to estimate  $\eta_1$ , where  $d_\eta = \tilde{p} + \tilde{q}$  be the input dimension,  $L_\eta$  is the depth,  $N_\eta$  is the width,  $M_\eta$  is the truncation level, and  $B_\eta$  is the weight bound. We take  $M_\eta$  larger than  $\|\eta\|_\infty$ . The estimator  $\hat{\eta}_1$  is defined as:

$$\hat{\eta} \in \arg \min_{g \in \mathcal{G}_{\eta,n}} \frac{1}{n_1} \sum_{i \in \mathcal{I}_1} \left\{ Y_i - g(\hat{\mathbf{f}}_i) \right\}^2.$$

By Theorem 4 of [Fan and Gu \(2024\)](#), since  $\eta \in \mathcal{H}(d_\eta, \ell_\eta, \mathcal{P})$  and is supported on a bounded domain, there exist constants  $C_1, C_2, C_3, C_4 > 0$ , depending only on the HCM parameters, such that for any integer  $N_\mu \geq 2$ , there exists a ReLU network

$$\eta^\dagger \in \mathcal{G}(C_1, d_\eta, 1, C_2 N_\eta, \infty, C_3 N_\eta^{C_4})$$

satisfying

$$\|\eta^\dagger - \eta\|_\infty \leq C N_\eta^{-2\gamma_\eta^*}. \quad (\text{A.2})$$

After truncation at level  $M_\eta$ , the approximation error does not increase, provided  $M_\eta > \|\eta\|_\infty$ . Therefore, by enlarging constants, we may regard  $\eta^\dagger \in \mathcal{G}_{\eta,n}$  and retain the same approximation bound. Consequently,

$$\|\eta^\dagger - \eta\|_\infty^2 \leq C N_\eta^{-4\gamma_\eta^*}. \quad (\text{G.1})$$

However, our estimator is evaluated at the learned representation  $\hat{\mathbf{f}}$ , whereas the target is  $\mu_1(\mathbf{f}) = \eta(\nu(\mathbf{f}))$ . Thus, the relevant oracle error is

$$\|\eta^\dagger(\hat{\mathbf{f}}) - \eta(\nu(\mathbf{f}))\|_{L_2(P_1)}^2.$$

Using  $(a + b)^2 \leq 2a^2 + 2b^2$ , we have

$$\mathbb{E}_1 \left[ \left\{ \eta^\dagger(\hat{\mathbf{f}}) - \eta(\nu(\mathbf{f})) \right\}^2 \right] \leq 2\mathbb{E}_1 \left[ \left\{ \eta^\dagger(\hat{\mathbf{f}}) - \eta(\hat{\mathbf{f}}) \right\}^2 \right] + 2\mathbb{E}_1 \left[ \left\{ \eta(\hat{\mathbf{f}}) - \eta(\nu(\mathbf{f})) \right\}^2 \right].$$

The first term is controlled by the uniform approximation bound:

$$\mathbb{E}_1 \left[ \left\{ \eta^\dagger(\hat{\mathbf{f}}) - \eta(\hat{\mathbf{f}}) \right\}^2 \right] \leq \|\eta^\dagger - \eta\|_\infty^2 \leq CN_\eta^{-4\gamma_\eta^*}.$$

For the second term, since  $\eta$  is Lipschitz,

$$\mathbb{E}_1 \left[ \left\{ \eta(\hat{\mathbf{f}}) - \eta(\nu(\mathbf{f})) \right\}^2 \right] \leq L_\eta^2 \mathbb{E}_1 \|\hat{\mathbf{f}} - \nu(\mathbf{f})\|_2^2 = O_p(\delta_{n,f}^2).$$

Therefore,

$$\|\eta^\dagger(\hat{\mathbf{f}}) - \eta(\nu(\mathbf{f}))\|_{L_2(P_1)}^2 = O_p \left( N_\eta^{-4\gamma_\eta^*} + \delta_{n,f}^2 \right). \quad (\text{G.2})$$

Next, we bound the stochastic error. For any  $g \in \mathcal{G}_{\eta,n}$ , define  $r_g(i) := g(\hat{\mathbf{f}}_i) - \eta(\nu(\mathbf{f}_i))$ . In particular,

$$r_{\hat{\eta}}(i) = \hat{\eta}(\hat{\mathbf{f}}_i) - \eta(\nu(\mathbf{f}_i)), \quad r_{\eta^\dagger}(i) = \eta^\dagger(\hat{\mathbf{f}}_i) - \eta(\nu(\mathbf{f}_i)).$$

Since  $Y_i = \eta(\nu(\mathbf{f}_i)) + \varepsilon_i$ , the empirical loss can be written as

$$\frac{1}{n_1} \sum_{i \in \mathcal{I}_1} \{Y_i - g(\hat{\mathbf{f}}_i)\}^2 = \frac{1}{n_1} \sum_{i \in \mathcal{I}_1} \{\varepsilon_i - r_g(i)\}^2.$$

By the empirical-risk minimizing property of  $\hat{\eta}$ ,

$$\frac{1}{n_1} \sum_{i \in \mathcal{I}_1} \{\varepsilon_i - r_{\hat{\eta}_1}(i)\}^2 \leq \frac{1}{n_1} \sum_{i \in \mathcal{I}_1} \{\varepsilon_i - r_{\eta^\dagger}(i)\}^2.$$

Expanding both sides and canceling the common term  $n^{-1} \sum_i \varepsilon_i^2$ , we obtain the basic inequality

$$\begin{aligned} \|r_{\hat{\eta}_1}\|_{n,1}^2 &\leq \|r_{\eta^\dagger}\|_{n,1}^2 + \frac{2}{n_1} \sum_{i \in \mathcal{I}_1} \varepsilon_i \left\{ \hat{\eta}_1(\hat{\mathbf{f}}_i) - \eta^\dagger(\hat{\mathbf{f}}_i) \right\}, \\ &\leq \|r_{\eta^\dagger}\|_{n,1}^2 + 2 \sup_{g \in \mathcal{G}_{\eta,n}} \left| \frac{1}{n_1} \sum_{i \in \mathcal{I}_1} \varepsilon_i \left\{ g(\hat{\mathbf{f}}_i) - \eta^\dagger(\hat{\mathbf{f}}_i) \right\} \right|, \end{aligned} \quad (\text{G.3})$$

where

$$\|h\|_{n,1}^2 := \frac{1}{n_1} \sum_{i \in \mathcal{I}_1} h_i^2.$$

Thus, it remains to control the supremum of the empirical process. By Lemma 4 of [Fan and Gu \(2024\)](#), the suprema can be bounded in terms of the pseudo-dimension of the network class. Let  $V_n = \text{Pdim}(\mathcal{G}_{\eta,n})$  denotes the pseudo-dimension of  $\mathcal{G}_{\eta,n}$ . Then with probability at least  $1 - e^{-t}$ ,

$$\left| \frac{1}{n_1} \sum_{i \in \mathcal{I}_1} \varepsilon_i \left\{ g(\hat{\mathbf{f}}_i) - \eta^\dagger(\hat{\mathbf{f}}_i) \right\} \right| \leq C \left( \|g(\hat{\mathbf{f}}) - \eta^\dagger(\hat{\mathbf{f}})\|_{n,1} + \sqrt{\frac{V_n \log n_1}{n_1}} \right) \sqrt{\frac{V_n \log n_1}{n_1} + \frac{t}{n}}$$

simultaneously for all  $g \in \mathcal{G}_{\eta,n}$ . Applying this inequality to  $g = \hat{\eta}$  gives

$$\begin{aligned} \left| \frac{1}{n_1} \sum_{i \in \mathcal{I}_1} \varepsilon_i \left\{ \hat{\eta}_1(\hat{\mathbf{f}}_i) - \eta^\dagger(\hat{\mathbf{f}}_i) \right\} \right| &\leq C \left( \|\hat{\eta}_1(\hat{\mathbf{f}}) - \eta^\dagger(\hat{\mathbf{f}})\|_{n,1} + \sqrt{\frac{V_n \log n_1}{n_1}} \right) \sqrt{\frac{V_n \log n_1}{n_1} + \frac{t}{n}} \\ &\leq C \left( \|r_{\hat{\eta}_1}\|_{n,1} + \|r_{\eta^\dagger}\|_{n,1} + \sqrt{\frac{V_n \log n_1}{n_1}} \right) \sqrt{\frac{V_n \log n_1}{n_1} + \frac{t}{n}} \end{aligned}$$

where the last line follows from the fact that:

$$\|\widehat{\eta}_1(\widehat{\mathbf{f}}) - \eta^\dagger(\widehat{\mathbf{f}})\|_{n,1} \leq \|r_{\widehat{\eta}_1}\|_{n,1} + \|r_{\eta^\dagger}\|_{n,1}.$$

This, along with Equation (G.3) yields:

$$\|r_{\widehat{\eta}_1}\|_{n,1}^2 \leq \|r_{\eta^\dagger}\|_{n,1}^2 + C \left( \|r_{\widehat{\eta}_1}\|_{n,1} + \|r_{\eta^\dagger}\|_{n,1} + \sqrt{\frac{V_n \log n_1}{n_1}} \right) \sqrt{\frac{V_n \log n_1}{n_1} + \frac{t}{n}}.$$

We then apply Young's inequality and change sides to obtain:

$$\|r_{\widehat{\eta}_1}\|_{n,1}^2 \leq C \left( \|r_{\eta^\dagger}\|_{n,1}^2 + \frac{V_n \log n_1}{n_1} + \frac{t}{n} \right).$$

Conditional on the representation-learning fold,  $r_{\eta^\dagger}$  is a fixed bounded function of the nuisance-fold observation. Therefore, by Bernstein's inequality applied to the fixed oracle  $r_{\eta^\dagger}$ ,

$$\|r_{\eta^\dagger}\|_{n,1}^2 \leq C \|r_{\eta^\dagger}\|_{L_2(P_1)}^2 + C \frac{t}{n}$$

with probability at least  $1 - e^{-t}$ . This, along with the previous equation, yields with probability  $\geq 1 - 2e^{-t}$ :

$$\|r_{\widehat{\eta}_1}\|_{n,1}^2 \lesssim \left( \|r_{\eta^\dagger}\|_{L_2(P_1)}^2 + \frac{V_n \log n_1}{n_1} + \frac{t}{n} \right) \quad (\text{G.4})$$

It remains to bound  $V_\mu = \text{Pdim}(\mathcal{G}_{\mu,n})$ . By Theorem 7 of Bartlett et al. (2019), we have:

$$V_n \leq CW_\eta L_\eta \log W_\eta \leq C_1 N_\eta^2 L_\eta^2 \log(N_\eta^2 L_\eta).$$

Choosing  $L_\eta \asymp 1$  and  $N_\eta \asymp n^{1/(4\gamma_\eta^*+2)}$ , we conclude from Equation (G.2) and (G.4):

$$\|r_{\widehat{\eta}_1}\|_{n,1}^2 = O_p \left( n^{-\frac{2\gamma_\eta^*}{2\gamma_\eta^*+1}} (\log n)^a + \delta_{n,f}^2 \right).$$

Finally, applying the empirical-to-population norm comparison, as in Lemma 3 and the last step of the proof of Theorem 1 of Fan and Gu (2024), gives the same bound for the population norm:

$$\|r_{\widehat{\eta}_1}\|_{L_2(P_1)}^2 = O_p \left( n^{-\frac{2\gamma_\eta^*}{2\gamma_\eta^*+1}} (\log n)^a + \delta_{n,f}^2 \right).$$

**Remark G.1.** As  $n_1 \sim n$  (by positivity assumption  $\mathbb{P}(A=1) > 0$ ) we use  $n$  instead of  $n_1$  in the rate.

## G.2 Rate for $\widehat{\pi}_1$ under the transformed factor representation

We now prove the rate for the treatment propensity nuisance  $\pi_1(\mathbf{f}_X) := \mathbb{P}(A=1 | \mathbf{f}_X)$ . Define as before, the relevant nuisance parameter,

$$\eta := \pi_1 \circ \nu^{-1}, \quad \eta(\nu(\mathbf{f}_X)) = \pi_1(\mathbf{f}_X).$$

Let  $\mathcal{I}_\pi = \mathcal{I}_{\text{nuis}}$  be the nuisance-estimation fold and write  $n = |\mathcal{I}_\pi|$  for simplicity. Assume

$$\|\widehat{\mathbf{f}}_X - \nu(\mathbf{f}_X)\|_{L_2(P)} = O_p(\delta_{n,f}). \quad (\text{B.1})$$

From our assumption in Theorem 4.3, the propensity score is uniformly bounded away from 0 and 1, i.e., for some  $\kappa \in (0, 1/2)$ ,

$$\kappa \leq \eta(\nu(\mathbf{f}_X)) \leq 1 - \kappa$$

almost surely. We restrict the neural-network estimators to take values in  $[\kappa/2, 1 - \kappa/2]$  by clipping. This does not affect the rate. Suppose  $\eta$  admits a bounded Lipschitz HCM extension to a compact set containing

both  $\nu(\mathbf{f}_X)$  and  $\hat{\mathbf{f}}_X$  with probability tending to one. Let  $\eta \in \mathcal{H}(d_\eta, \ell_\eta, \mathcal{P})$  with DAS  $\gamma_\eta^*$ , where  $d_\eta = \tilde{p}$  is the input dimension. Let

$$\mathcal{G}_{\eta,n} := \mathcal{G}(L_\eta, d_\eta, 1, N_\eta, M_\eta, B_\eta)$$

be the clipped ReLU network class. As per Line 7 of Algorithm 1

$$\hat{\eta} \in \arg \min_{g \in \mathcal{G}_{\eta,n}} \frac{1}{n} \sum_{i \in \mathcal{I}_\pi} \ell(A_i, g(\hat{\mathbf{f}}_{X,i})) := \arg \min_{g \in \mathcal{G}_{\eta,n}} \mathbb{P}_n(\ell(A, g(\hat{\mathbf{f}}_X)))$$

where

$$\ell(a, u) := -a \log u - (1-a) \log(1-u), \quad u \in [\kappa/2, 1 - \kappa/2].$$

As in the previous subsection, we can use the approximation theorem (e.g., Theorem 4 of Fan and Gu (2024)), there exists

$$\eta^\dagger \in \mathcal{G}(C_1, d_\eta, 1, C_2 N_\eta, \infty, C_3 N_\eta^{C_4})$$

such that

$$\|\eta^\dagger - \eta\|_\infty \leq C N_\eta^{-2\gamma_\eta^*}.$$

After clipping, we may take  $\eta^\dagger \in \mathcal{G}_{\eta,n}$  and retain

$$\|\eta^\dagger - \eta\|_\infty^2 \leq C N_\eta^{-4\gamma_\eta^*}. \quad (\text{G.5})$$

As in the proof for  $\hat{\mu}_1$ , the relevant oracle error is

$$\|\eta^\dagger(\hat{\mathbf{f}}_X) - \eta(\nu(\mathbf{f}_X))\|_{L_2(P)}^2.$$

Using the same decomposition as in the previous subsection, and the Lipschitzness of  $\eta$ ,

$$\|\eta^\dagger(\hat{\mathbf{f}}_X) - \eta(\nu(\mathbf{f}_X))\|_{L_2(P)}^2 \lesssim \|\eta^\dagger - \eta\|_\infty^2 + \|\hat{\mathbf{f}}_X - \nu(\mathbf{f}_X)\|_{L_2(P)}^2.$$

Therefore,

$$\|\eta^\dagger(\hat{\mathbf{f}}_X) - \eta(\nu(\mathbf{f}_X))\|_{L_2(P)}^2 = O_p\left(N_\eta^{-4\gamma_\eta^*} + \delta_{n,f}^2\right). \quad (\text{G.6})$$

By empirical risk minimization,

$$\mathbb{P}_n \ell(A, \hat{\eta}(\hat{\mathbf{f}}_X)) \leq \mathbb{P}_n \ell(A, \eta^\dagger(\hat{\mathbf{f}}_X)).$$

Adding and subtracting population risks gives

$$\begin{aligned} P\{\ell(A, \hat{\eta}(\hat{\mathbf{f}}_X)) - \ell(A, \eta(\nu(\mathbf{f}_X)))\} &\leq P\{\ell(A, \eta^\dagger(\hat{\mathbf{f}}_X)) - \ell(A, \eta(\nu(\mathbf{f}_X)))\} \\ &\quad + (P - \mathbb{P}_n)\{\ell(A, \hat{\eta}(\hat{\mathbf{f}}_X)) - \ell(A, \eta^\dagger(\hat{\mathbf{f}}_X))\}. \end{aligned} \quad (\text{G.7})$$

Since  $\hat{\mathbf{f}}_X$  is a function of  $(\mathbf{f}_X, \mathbf{u}_X)$  and  $A$  is independent of  $\mathbf{u}_X$ ,

$$\mathbb{P}(A = 1 \mid \nu(\mathbf{f}_X), \hat{\mathbf{f}}_X) = \pi_1(\mathbf{f}_X) = \eta(\nu(\mathbf{f}_X)).$$

Hence, for any  $g \in \mathcal{G}_{\eta,n}$ ,

$$P\{\ell(A, g(\hat{\mathbf{f}}_X)) - \ell(A, \eta(\nu(\mathbf{f}_X)))\} = \mathbb{E} \left[ \text{KL}\{\text{Bern}(\eta(\nu(\mathbf{f}_X))) \parallel \text{Bern}(g(\hat{\mathbf{f}}_X))\} \right].$$

By overlap and clipping, this KL divergence is equivalent to squared error:

$$c_\kappa \{g(\hat{\mathbf{f}}_X) - \eta(\nu(\mathbf{f}_X))\}^2 \leq \text{KL}\{\cdot, \cdot\} \leq C_\kappa \{g(\hat{\mathbf{f}}_X) - \eta(\nu(\mathbf{f}_X))\}^2.$$

Therefore, applying the lower bound to  $\hat{\eta}$  and the upper bound to  $\eta^\dagger$ , (G.7) yields

$$\begin{aligned} \|\hat{\eta}(\hat{\mathbf{f}}_X) - \eta(\nu(\mathbf{f}_X))\|_{L_2(P)}^2 &\lesssim \|\eta^\dagger(\hat{\mathbf{f}}_X) - \eta(\nu(\mathbf{f}_X))\|_{L_2(P)}^2 \\ &\quad + (P - \mathbb{P}_n)\{\ell(A, \hat{\eta}(\hat{\mathbf{f}}_X)) - \ell(A, \eta^\dagger(\hat{\mathbf{f}}_X))\}. \end{aligned} \quad (\text{G.8})$$

The logistic loss is Lipschitz on  $[\kappa/2, 1 - \kappa/2]$  since

$$|\partial_u \ell(a, u)| \leq \frac{2}{\kappa}.$$

Thus, by the contraction inequality and the pseudo-dimension bound used in Lemma 4 of [Fan and Gu \(2024\)](#), if

$$V_n := \text{Pdim}(\mathcal{G}_{\eta, n}),$$

then with probability at least  $1 - e^{-t}$ ,

$$\begin{aligned} & (P - \mathbb{P}_n)\{\ell(A, \hat{\eta}(\mathbf{f}_X)) - \ell(A, \eta^\dagger(\mathbf{f}_X))\} \\ & \leq \zeta \|\hat{\eta}(\mathbf{f}_X) - \eta(\nu(\mathbf{f}_X))\|_{L_2(P)}^2 + C_\zeta \|\eta^\dagger(\mathbf{f}_X) - \eta(\nu(\mathbf{f}_X))\|_{L_2(P)}^2 + C_\zeta \left( \frac{V_n \log n}{n} + \frac{t}{n} \right). \end{aligned}$$

Choosing  $\zeta$  small enough and combining this with [\(G.8\)](#), we obtain

$$\|\hat{\eta}(\mathbf{f}_X) - \eta(\nu(\mathbf{f}_X))\|_{L_2(P)}^2 \lesssim \|\eta^\dagger(\mathbf{f}_X) - \eta(\nu(\mathbf{f}_X))\|_{L_2(P)}^2 + \frac{V_n \log n}{n} + \frac{t}{n}.$$

Using [\(G.6\)](#),

$$\|\hat{\eta}(\mathbf{f}_X) - \eta(\nu(\mathbf{f}_X))\|_{L_2(P)}^2 = O_p \left( N_\eta^{-4\gamma_\eta^*} + \delta_{n, f}^2 + \frac{V_n \log n}{n} \right). \quad (\text{G.9})$$

Finally, as in the proof for  $\hat{\mu}_1$ ,

$$V_n \lesssim (L_\eta^2 N_\eta^2 + d_\eta L_\eta N_\eta) \log(L_\eta N_\eta d_\eta).$$

Taking  $L_\eta \asymp 1$  and balancing

$$N_\eta^{-4\gamma_\eta^*} \quad \text{and} \quad \frac{N_\eta^2 \log N_\eta \log n}{n}$$

gives

$$N_\eta \asymp n^{1/(4\gamma_\eta^*+2)}$$

up to logarithmic factors. Therefore,

$$\|\hat{\eta}(\mathbf{f}_X) - \eta(\nu(\mathbf{f}_X))\|_{L_2(P)}^2 = O_p \left( n^{-2\gamma_\eta^*/(2\gamma_\eta^*+1)} (\log n)^a + \delta_{n, f}^2 \right).$$

Equivalently,

$$\|\hat{\pi}_1(\mathbf{f}_X) - \pi_1(\mathbf{f}_X)\|_{L_2(P)}^2 = O_p \left( n^{-2\gamma_\eta^*/(2\gamma_\eta^*+1)} (\log n)^a + \delta_{n, f}^2 \right).$$

### G.3 Rate for $\hat{\mu}_{10}$ under the transformed factor representation

We now prove the rate for  $\mu_{10}(\mathbf{f}_X) := \mathbb{E}[\mu_1(\mathbf{f}_X, \mathbf{f}_M) \mid A = 0, \mathbf{f}_X]$ . Define the relevant nuisance parameter  $\eta := \mu_{10} \circ \nu_X^{-1}$  so that  $\eta(\nu_X(\mathbf{f}_X)) = \mu_{10}(\mathbf{f}_X)$ . Let us also define

$$\mathcal{I}_0 := \{i \in \mathcal{I}_{\text{nuis}} : A_i = 0\}, \quad n_0 := |\mathcal{I}_0|.$$

The estimator  $\hat{\eta}$  is obtained by regressing the generated outcome  $\hat{\mu}_1(\mathbf{f}_{X,i}, \mathbf{f}_{M,i})$  on  $\mathbf{f}_{X,i}$ :

$$\hat{\eta} \in \arg \min_{g \in \mathcal{G}_{\eta, n}} \frac{1}{n_0} \sum_{i \in \mathcal{I}_0} \left\{ \hat{\mu}_1(\mathbf{f}_{X,i}, \mathbf{f}_{M,i}) - g(\mathbf{f}_{X,i}) \right\}^2.$$

Assume

$$\|\mathbf{f}_X - \nu_X(\mathbf{f}_X)\|_{L_2(P_0)} = O_p(\delta_{n, f}),$$

where  $P_0$  denotes the distribution conditional on  $A = 0$ . Assume also that  $\eta$  admits a bounded Lipschitz HCM extension to a compact set containing both  $\nu_X(\mathbf{f}_X)$  and  $\widehat{\mathbf{f}}_X$  with probability tending to one, and  $\eta \in \mathcal{H}(d_\eta, \ell_\eta, \mathcal{P})$  with DAS  $\gamma_\eta^*$ . As before, let

$$\mathcal{G}_{\eta,n} := \mathcal{G}(L_\eta, d_\eta, 1, N_\eta, M_\eta, B_\eta)$$

be the truncated ReLU class. By Theorem 4 of [Fan and Gu \(2024\)](#), there exists

$$\eta^\dagger \in \mathcal{G}(C_1, d_\eta, 1, C_2 N_\eta, \infty, C_3 N_\eta^{C_4})$$

such that

$$\|\eta^\dagger - \eta\|_\infty \leq C N_\eta^{-2\gamma_\eta^*}.$$

After truncation, we may regard  $\eta^\dagger \in \mathcal{G}_{\eta,n}$  and retain

$$\|\eta^\dagger - \eta\|_\infty^2 \leq C N_\eta^{-4\gamma_\eta^*}.$$

As in the proof of  $\widehat{\mu}_1$ , the relevant oracle error is

$$\|\eta^\dagger(\widehat{\mathbf{f}}_X) - \eta(\nu_X(\mathbf{f}_X))\|_{L_2(P_0)}^2.$$

Using the same decomposition as before and Lipschitzness of  $\eta$ ,

$$\|\eta^\dagger(\widehat{\mathbf{f}}_X) - \eta(\nu_X(\mathbf{f}_X))\|_{L_2(P_0)}^2 = O_p\left(N_\eta^{-4\gamma_\eta^*} + \delta_{n,f}^2\right). \quad (\text{G.10})$$

Now, for  $i \in \mathcal{I}_0$ , define

$$\begin{aligned} \xi_i &:= \mu_1(\mathbf{f}_{X,i}, \mathbf{f}_{M,i}) - \mu_{10}(\mathbf{f}_{X,i}), \\ \Delta_i &:= \widehat{\mu}_1(\widehat{\mathbf{f}}_{X,i}, \widehat{\mathbf{f}}_{M,i}) - \mu_1(\mathbf{f}_{X,i}, \mathbf{f}_{M,i}). \end{aligned}$$

Then the generated outcome satisfies

$$\widehat{\mu}_1(\widehat{\mathbf{f}}_{X,i}, \widehat{\mathbf{f}}_{M,i}) = \eta(\nu_X(\mathbf{f}_{X,i})) + \xi_i + \Delta_i.$$

Here  $\xi_i$  is the intrinsic second-stage regression noise, while  $\Delta_i$  is the first-stage error from estimating  $\mu_1$ . By independent of  $(\mathbf{f}_X, \mathbf{f}_M)$  with  $(\mathbf{u}_X, \mathbf{u}_M)$ , we have:

$$\mathbb{E}[\xi_i \mid \mathbf{f}_{X,i}, \mathbf{u}_{X,i}, A_i = 0] = 0,$$

so that, conditional on the representation-learning fold,

$$\mathbb{E}[\xi_i \mid \widehat{\mathbf{f}}_{X,i}, A_i = 0] = 0.$$

For any  $g \in \mathcal{G}_{\eta,n}$ , define

$$r_g(i) := g(\widehat{\mathbf{f}}_{X,i}) - \eta(\nu_X(\mathbf{f}_{X,i})).$$

By empirical risk minimization,

$$\frac{1}{n_0} \sum_{i \in \mathcal{I}_0} \{\xi_i + \Delta_i - r_{\widehat{\eta}}(i)\}^2 \leq \frac{1}{n_0} \sum_{i \in \mathcal{I}_0} \{\xi_i + \Delta_i - r_{\eta^\dagger}(i)\}^2.$$

Expanding both sides and canceling common terms gives

$$\|r_{\widehat{\eta}}\|_{n,0}^2 \leq \|r_{\eta^\dagger}\|_{n,0}^2 + \frac{2}{n_0} \sum_{i \in \mathcal{I}_0} \xi_i \left\{ \widehat{\eta}(\widehat{\mathbf{f}}_{X,i}) - \eta^\dagger(\widehat{\mathbf{f}}_{X,i}) \right\} + \frac{2}{n_0} \sum_{i \in \mathcal{I}_0} \Delta_i \left\{ \widehat{\eta}(\widehat{\mathbf{f}}_{X,i}) - \eta^\dagger(\widehat{\mathbf{f}}_{X,i}) \right\}. \quad (\text{G.11})$$

The first stochastic term is handled exactly as in the proof of  $\widehat{\mu}_1$ , using Lemma 4 of [Fan and Gu \(2024\)](#). The second term is new and comes from the generated outcome.

By Cauchy's inequality and Young's inequality,

$$\begin{aligned} \left| \frac{2}{n_0} \sum_{i \in \mathcal{I}_0} \Delta_i \left\{ \widehat{\eta}(\widehat{\mathbf{f}}_{X,i}) - \eta^\dagger(\widehat{\mathbf{f}}_{X,i}) \right\} \right| &\leq 2 \|\Delta\|_{n,0} \|\widehat{\eta}(\widehat{\mathbf{f}}_X) \eta^\dagger(\widehat{\mathbf{f}}_X)\|_{n,0} \\ &\leq \zeta \|r_{\widehat{\eta}}\|_{n,0}^2 + C_\zeta \|r_{\eta^\dagger}\|_{n,0}^2 + C_\zeta \|\Delta\|_{n,0}^2. \end{aligned}$$

Combining this with (G.11), and applying the same empirical process bound as in the proof of  $\widehat{\mu}_1$ , we obtain

$$\|r_{\widehat{\eta}}\|_{n,0}^2 \lesssim \|r_{\eta^\dagger}\|_{n,0}^2 + \frac{V_n \log n}{n} + \|\Delta\|_{n,0}^2 + \frac{t}{n},$$

where

$$V_n := \text{Pdim}(\mathcal{G}_{\eta,n}).$$

By Bernstein's inequality for the fixed oracle and the already established rate for  $\widehat{\mu}_1$  under  $P_0$ ,

$$\|\Delta\|_{n,0}^2 = O_p(r_{\mu_1,0,n}^2),$$

where

$$r_{\mu_1,0,n}^2 := \|\widehat{\mu}_1(\widehat{\mathbf{f}}_X, \widehat{\mathbf{f}}_M) - \mu_1(\mathbf{f}_X, \mathbf{f}_M)\|_{L_2(P_0)}^2.$$

Therefore,

$$\|\widehat{\eta}(\widehat{\mathbf{f}}_X) - \eta(\nu_X(\mathbf{f}_X))\|_{L_2(P_0)}^2 = O_p \left( N_\eta^{-4\gamma_\eta^*} + \delta_{n,f}^2 + \frac{V_n \log n}{n} + r_{\mu_1,0,n}^2 \right). \quad (\text{G.12})$$

Finally, as before,

$$V_n \lesssim (L_\eta^2 N_\eta^2 + d_\eta L_\eta N_\eta) \log(L_\eta N_\eta d_\eta).$$

Taking  $L_\eta \asymp 1$  and balancing

$$N_\eta^{-4\gamma_\eta^*} \quad \text{and} \quad \frac{N_\eta^2 \log N_\eta \log n}{n}$$

gives

$$N_\eta \asymp n^{1/(4\gamma_\eta^*+2)}$$

up to logarithmic factors. Hence,

$$\|\widehat{\eta}(\widehat{\mathbf{f}}_X) - \eta(\nu_X(\mathbf{f}_X))\|_{L_2(P_0)}^2 = O_p \left( n^{-2\gamma_\eta^*/(2\gamma_\eta^*+1)} (\log n)^a + \delta_{n,f}^2 + r_{\mu_1,0,n}^2 \right).$$

Equivalently,

$$\|\widehat{\mu}_{10}(\widehat{\mathbf{f}}_X) - \mu_{10}(\mathbf{f}_X)\|_{L_2(P_0)}^2 = O_p \left( n^{-2\gamma_\eta^*/(2\gamma_\eta^*+1)} (\log n)^a + \delta_{n,f}^2 + r_{\mu_1,0,n}^2 \right).$$

## H A sufficient condition for factor recovery

**Proposition H.1** (Sufficient condition for factor recovery). *Let*

$$\begin{aligned} \mathcal{L}_\lambda(z_{XM}) = \mathbb{E} \left[ \lambda_1 \|X - h_X(g_X(X))\|_2^2 + \lambda_2 \|M - h_M(g_M(M))\|_2^2 \right. \\ \left. + \lambda_3 \|g_M(M) - g_{XM}(A, g_X(X))\|_2^2 \right] \end{aligned}$$

denote the population MediEncoder objective, where  $z = (g_X, g_M, g_{XM}, h_X, h_M) \in \mathcal{Z}$ . Let

$$\mathcal{L}_\lambda^* := \inf_{z \in \mathcal{Z}} \mathcal{L}_\lambda(z).$$

Let  $\mathcal{V}$  be a class of maps  $\nu = (\nu_X, \nu_M) : \mathbb{R}^{\bar{p}+\bar{q}} \rightarrow \mathbb{R}^{\bar{p}+\bar{q}}$  such that each  $\nu \in \mathcal{V}$  admits a Lipschitz left inverse on the support of  $(\mathbf{f}_X, \mathbf{f}_M)$ . Assume that the representation class contains oracle encoders  $g_X^*$  and  $g_M^*$ , together with a transformation  $\nu^* = (\nu_X^*, \nu_M^*) \in \mathcal{V}$ , such that

$$\|g_X^*(X) - \nu_X^*(\mathbf{f}_X)\|_{L_2(P)} \leq \delta_{X,\text{app}}, \quad \|g_M^*(M) - \nu_M^*(\mathbf{f}_M)\|_{L_2(P)} \leq \delta_{M,\text{app}}.$$

Assume further that the population objective satisfies the quotient-stability condition

$$d_{\mathcal{V}}^2(z) \leq C\{\mathcal{L}_\lambda(z) - \mathcal{L}_\lambda^*\} + C(\delta_{X,\text{app}}^2 + \delta_{M,\text{app}}^2), \quad (\text{H.1})$$

where, for  $z \in \mathcal{Z}$ ,

$$d_{\mathcal{V}}^2(z) := \inf_{\nu \in \mathcal{V}} \left\{ \|g_X(X) - \nu_X(\mathbf{f}_X)\|_{L_2(P)}^2 + \|g_M(M) - \nu_M(\mathbf{f}_M)\|_{L_2(P)}^2 \right\}.$$

Suppose the fitted MediEncoder  $\hat{z} = (\hat{g}_X, \hat{g}_M, \hat{g}_{XM}, \hat{h}_X, \hat{h}_M)$  satisfies the excess-risk bound

$$\mathcal{L}_\lambda(\hat{z}) - \mathcal{L}_\lambda^* = O_p(r_n^2). \quad (\text{H.2})$$

Then there exists a possibly  $n$ -dependent transformation  $\nu_n = (\nu_{X,n}, \nu_{M,n}) \in \mathcal{V}$  such that

$$\|\hat{g}_X(X) - \nu_{X,n}(\mathbf{f}_X)\|_{L_2(P)} + \|\hat{g}_M(M) - \nu_{M,n}(\mathbf{f}_M)\|_{L_2(P)} = O_p(r_n + \delta_{X,\text{app}} + \delta_{M,\text{app}}).$$

In particular, if  $r_n + \delta_{X,\text{app}} + \delta_{M,\text{app}} = o(n^{-1/4})$ , then the factor-recovery condition

$$\|\hat{\mathbf{f}} - \nu_n(\mathbf{f})\|_{L_2(P)} = o_p(n^{-1/4})$$

holds, where

$$\hat{\mathbf{f}} := (\hat{g}_X(X), \hat{g}_M(M)), \quad \nu_n(\mathbf{f}) := (\nu_{X,n}(\mathbf{f}_X), \nu_{M,n}(\mathbf{f}_M)).$$

**Remark H.2.** Condition (H.1) is the natural analog of a curvature condition for autoencoder-based representations. A fixed encoder is generally not identifiable from reconstruction loss, since invertible reparametrizations of the bottleneck coordinates can be absorbed by the decoder. The distance  $d_{\mathcal{V}}$  therefore measures recovery only up to the equivalence class of Lipschitz left-invertible transformations, which is precisely the level of recovery required by Theorem 4.3. The terms  $\delta_{X,\text{app}}$  and  $\delta_{M,\text{app}}$  represent the approximation errors, which depend on the expressibility of the underlying function class used for the encoders.

## I Proof of Proposition H

By condition (H.1) and (H.2), we have:

$$d_{\mathcal{V}}^2(\hat{z}) \leq C\{\mathcal{L}_\lambda(\hat{z}) - \mathcal{L}_\lambda^*\} + C(\delta_{X,\text{app}}^2 + \delta_{M,\text{app}}^2) = O_p(r_n^2 + \delta_{X,\text{app}}^2 + \delta_{M,\text{app}}^2).$$

Therefore,

$$d_{\mathcal{V}}(\hat{z}) = O_p(r_n + \delta_{X,\text{app}} + \delta_{M,\text{app}}).$$

By the definition of  $d_{\mathcal{V}}$ , for every  $\varepsilon > 0$  there exists  $\nu_\varepsilon = (\nu_{X,\varepsilon}, \nu_{M,\varepsilon}) \in \mathcal{V}$  such that

$$\begin{aligned} & \|\hat{g}_X(X) - \nu_{X,\varepsilon}(\mathbf{f}_X)\|_{L_2(P)}^2 + \|\hat{g}_M(M) - \nu_{M,\varepsilon}(\mathbf{f}_M)\|_{L_2(P)}^2 \\ & \leq d_{\mathcal{V}}^2(\hat{z}) + \varepsilon. \end{aligned}$$

Taking, for instance,  $\varepsilon = n^{-1}$  and writing  $\nu_n := \nu_{1/n}$  gives

$$\|\hat{g}_X(X) - \nu_{X,n}(\mathbf{f}_X)\|_{L_2(P)}^2 + \|\hat{g}_M(M) - \nu_{M,n}(\mathbf{f}_M)\|_{L_2(P)}^2 = O_p(r_n^2 + \delta_{X,\text{app}}^2 + \delta_{M,\text{app}}^2).$$

Taking square roots and using  $\sqrt{x+y+z} \leq \sqrt{x} + \sqrt{y} + \sqrt{z}$  yields

$$\left( \|\hat{g}_X(X) - \nu_{X,n}(\mathbf{f}_X)\|_{L_2(P)}^2 + \|\hat{g}_M(M) - \nu_{M,n}(\mathbf{f}_M)\|_{L_2(P)}^2 \right)^{1/2} = O_p(r_n + \delta_{X,\text{app}} + \delta_{M,\text{app}}).$$

Consequently,

$$\|\hat{g}_X(X) - \nu_{X,n}(\mathbf{f}_X)\|_{L_2(P)} + \|\hat{g}_M(M) - \nu_{M,n}(\mathbf{f}_M)\|_{L_2(P)} = O_p(r_n + \delta_{X,\text{app}} + \delta_{M,\text{app}}),$$

where the last step follows because the sum of two nonnegative terms is bounded by  $\sqrt{2}$  times their Euclidean norm.

Finally, by the definition of

$$\hat{\mathbf{f}} := (\hat{g}_X(X), \hat{g}_M(M)), \quad \nu_n(\mathbf{f}) := (\nu_{X,n}(\mathbf{f}_X), \nu_{M,n}(\mathbf{f}_M)),$$

we obtain

$$\|\hat{\mathbf{f}} - \nu_n(\mathbf{f})\|_{L_2(P)} = O_p(r_n + \delta_{X,\text{app}} + \delta_{M,\text{app}}).$$

Thus, if  $r_n + \delta_{X,\text{app}} + \delta_{M,\text{app}} = o(n^{-1/4})$ , then

$$\|\hat{\mathbf{f}} - \nu_n(\mathbf{f})\|_{L_2(P)} = o_p(n^{-1/4}),$$

which is the desired factor-recovery condition.

## J Additional Real Data Details

We apply our proposed method to investigate how depressive symptoms influence cognitive decline in Alzheimer’s disease, and whether this relationship is mediated by DNA methylation. Understanding this pathway is important because prior studies have established associations between depression and cognitive impairment, but the biological mechanisms—particularly epigenetic mediation—remain less clear. Here, we present the detailed data preprocessing procedure.

**Dataset.** We conduct our analysis using data from the Alzheimer’s Disease Neuroimaging Initiative (ADNI), a longitudinal, multi-center observational study designed to validate biomarkers for Alzheimer’s disease (AD) clinical trials (Mueller et al., 2005). The dataset is accessible via <https://adni.loni.usc.edu/>. Our treatment variable  $A$  is the Geriatric Depression Scale (GDS), a self-reported measure ranging from 0 to 15, with higher values indicating more severe depressive symptoms. We binarize GDS using the clinically standard threshold (e.g.,  $\text{GDS} > 5$  indicates depression). The outcome  $Y$  is the Alzheimer’s Disease Assessment Scale–Cognitive Subscale (ADAS-Cog), ranging from 0 to 85, where higher scores reflect greater cognitive impairment (Cano et al., 2010; Raghavan et al., 2013).

**Preprocessing.** We include clinically relevant covariates such as demographic and health-related variables, denoted by  $X$ . Missing values in  $X$  are imputed using `mice` (Van Buuren and Groothuis-Oudshoorn, 2011). To enhance model flexibility, we construct higher-order polynomial features and interaction terms, resulting in a covariate dimension of  $\dim(X) = 171$ . The mediator  $M$  consists of DNA methylation measurements obtained using the Illumina HumanMethylationEPIC BeadChip array. We preprocess the methylation data using the `minfi` package (Aryee et al., 2014), and we select CpG sites that have been reported to be significantly associated with Alzheimer’s disease in large-scale epigenome-wide association studies (EWAS), including a meta-analysis of Braak stage and re-analysis studies of publicly available GEO datasets (Zhang et al., 2020; Lunnon et al., 2014; Battram et al., 2022).

based on missingness and variability, retaining only those with no missing values. This yields  $\dim(M) = 3,206$  mediators. After preprocessing, we retain  $n = 649$  subjects with complete data across all variables.

**Choice of  $\tilde{p}$  and  $\tilde{q}$ .** We apply our proposed estimation procedure to estimate the natural indirect effect (NIE), natural direct effect (NDE), and total effect (TE). The projection dimensions  $(\tilde{p}, \tilde{q})$  are selected based on principal component analysis (PCA) where  $\tilde{p} = 5$  and  $\tilde{q} = 40$  number of coordinates is able to explain 80% variance.

## K More on Simulation and Ablation Study

All experiments were conducted in a cluster computing environment on a CPU compute node. The computational environment used Python 3.10.12 with 32 CPU cores. A typical full experimental run with 500 replications took approximately 84 hours to complete. Tables 3–9 and Tables 4–10 report the performance of different methods and ablation study compared with MediEncoder across varying sample sizes and covariate/mediator dimensions. The ablation study further evaluates the performance of MediEncoder after removing the alignment component in the loss function (3.1).

$n$	Estimator	SD	RMSE	CI Length	Coverage
100	Projection	37.471	37.839	146.884	0.980
	Autoencoder	42.495	44.101	166.575	0.965
	VAE	0.571	0.580	2.239	0.965
	IMAVAE	0.574	1.234	2.250	0.637
	MediEncoder	0.503	0.528	1.974	0.963
300	Projection	1.589	1.890	6.228	0.930
	Autoencoder	1.255	1.363	4.918	0.950
	VAE	0.391	0.401	1.533	0.950
	IMAVAE	0.439	0.644	1.759	0.830
	MediEncoder	0.402	0.419	1.575	0.955
800	Projection	0.402	0.549	1.577	0.880
	Autoencoder	0.379	0.435	1.487	0.920
	VAE	0.335	0.335	1.314	0.940
	IMAVAE	0.372	0.411	1.459	0.927
	MediEncoder	0.277	0.299	1.085	0.935
1200	Projection	0.280	0.428	1.099	0.820
	Autoencoder	0.383	0.457	1.502	0.915
	VAE	0.322	0.327	1.262	0.925
	IMAVAE	0.335	0.360	1.312	0.950
	MediEncoder	0.267	0.290	1.047	0.940
2000	Projection	0.265	0.411	1.040	0.780
	Autoencoder	0.321	0.415	1.257	0.865
	VAE	0.337	0.338	1.321	0.945
	IMAVAE	0.340	0.349	1.333	0.953
	MediEncoder	0.275	0.299	1.079	0.935
3000	Projection	0.269	0.370	1.055	0.845
	Autoencoder	0.328	0.412	1.288	0.880
	VAE	0.321	0.340	1.257	0.925
	IMAVAE	0.322	0.334	1.251	0.943
	MediEncoder	0.253	0.278	0.992	0.945

Table 3: Estimator performance comparison by sample size under the nonlinear wavelet DGP with  $p = 800$ ,  $q = 200$ ,  $\sigma_X = 2$ ,  $\sigma_M = 1$ ,  $\sigma_Y = 1$ ,  $\bar{p} = \bar{q} = 5$ ,  $\hat{p} = \hat{q} = 7$ , and  $B = 500$  replications.

	SD		RMSE		CI Length	
	$\lambda_3 = 0$	Tuning	$\lambda_3 = 0$	Tuning	$\lambda_3 = 0$	Tuning
100	0.594	0.503	0.596	0.528	2.330	1.974
300	0.410	0.402	0.414	0.419	1.605	1.575
800	0.360	0.277	0.359	0.299	1.413	1.085
1200	0.285	0.267	0.287	0.290	1.118	1.047
2000	0.358	0.275	0.356	0.299	1.403	1.079
3000	0.297	0.253	0.296	0.278	1.165	0.992

Table 4: Ablation study on the alignment term ( $\lambda_3$ ) in **MediEncoder** with  $p + q = 1000$ ,  $\sigma_X = 2$ ,  $\sigma_M = 1$ ,  $\sigma_Y = 1$ ,  $B = 500$ ,  $\bar{p} = \bar{q} = 5$ , and  $\tilde{p} = \tilde{q} = 7$ .

$n$	Estimator	SD	RMSE	CI Length	Coverage
100	Projection	14.190	14.631	55.626	0.942
	Autoencoder	24.003	24.196	94.09	0.945
	VAE	0.549	0.561	2.153	0.953
	IMAVAE	0.591	1.500	2.325	0.885
	MediEncoder	0.644	0.665	2.525	0.962
300	Projection	1.831	2.011	7.175	0.951
	Autoencoder	1.533	1.672	6.011	0.955
	VAE	0.412	0.423	1.616	0.952
	IMAVAE	0.442	0.733	1.740	0.875
	MediEncoder	0.366	0.388	1.435	0.945
800	Projection	0.390	0.537	1.528	0.871
	Autoencoder	0.482	0.572	1.889	0.913
	VAE	0.341	0.340	1.336	0.945
	IMAVAE	0.389	0.451	1.524	0.755
	MediEncoder	0.278	0.297	1.091	0.945
1200	Projection	0.319	0.439	1.251	0.855
	Autoencoder	0.415	0.465	1.626	0.915
	VAE	0.329	0.332	1.290	0.935
	IMAVAE	0.341	0.390	1.337	0.927
	MediEncoder	0.269	0.288	1.056	0.925
2000	Projection	0.262	0.410	1.021	0.771
	Autoencoder	0.365	0.469	1.410	0.875
	VAE	0.343	0.339	1.333	0.944
	IMAVAE	0.357	0.376	1.399	0.755
	MediEncoder	0.283	0.296	1.108	0.945
3000	Projection	0.262	0.368	1.027	0.862
	Autoencoder	0.331	0.396	1.294	0.885
	VAE	0.331	0.343	1.294	0.930
	IMAVAE	0.344	0.349	1.350	0.947
	MediEncoder	0.270	0.290	1.059	0.955

Table 5: Estimator performance comparison by sample size under the nonlinear wavelet DGP with  $p = 2000$ ,  $q = 1000$ ,  $\sigma_X = 2$ ,  $\sigma_M = 1$ ,  $\sigma_Y = 1$ ,  $\bar{p} = \bar{q} = 5$ ,  $\tilde{p} = \tilde{q} = 7$ , and  $B = 500$  replications.

	SD		RMSE		CI Length	
	$\lambda_3 = 0$	Tuning	$\lambda_3 = 0$	Tuning	$\lambda_3 = 0$	Tuning
100	0.544	0.644	0.548	0.665	2.134	2.525
300	0.416	0.366	0.420	0.388	1.629	1.435
800	0.371	0.278	0.371	0.297	1.453	1.091
1200	0.306	0.269	0.305	0.288	1.199	1.056
2000	0.336	0.283	0.335	0.296	1.318	1.108
3000	0.307	0.270	0.306	0.290	1.203	1.059

Table 6: Ablation study on the alignment term ( $\lambda_3$ ) in **MediEncoder** with  $p + q = 3000$ ,  $\sigma_X = 2$ ,  $\sigma_M = 1$ ,  $\sigma_Y = 1$ ,  $B = 500$ ,  $\bar{p} = \bar{q} = 5$ , and  $\tilde{p} = \tilde{q} = 7$ .

$n$	Estimator	SD	RMSE	CI Length	Coverage
100	Projection	14.559	15.367	57.072	0.939
	Autoencoder	50.642	51.505	198.441	0.954
	VAE	0.734	0.733	2.879	0.985
	IMAVAE	0.760	1.103	2.697	0.910
	MediEncoder	0.579	0.588	2.270	0.967
300	Projection	1.308	1.518	5.128	0.895
	Autoencoder	2.729	2.770	10.696	0.970
	VAE	0.438	0.449	1.717	0.954
	IMAVAE	0.405	0.554	1.508	0.858
	MediEncoder	0.390	0.394	1.528	0.967
800	Projection	0.322	0.499	1.263	0.781
	Autoencoder	0.444	0.524	1.739	0.914
	VAE	0.331	0.331	1.299	0.941
	IMAVAE	0.383	0.411	1.500	0.818
	MediEncoder	0.336	0.335	1.319	0.958
1200	Projection	0.285	0.412	1.116	0.805
	Autoencoder	0.417	0.489	1.636	0.925
	VAE	0.341	0.341	1.336	0.935
	IMAVAE	0.330	0.356	1.294	0.830
	MediEncoder	0.291	0.293	1.141	0.950
2000	Projection	0.269	0.418	1.053	0.784
	Autoencoder	0.336	0.449	1.318	0.870
	VAE	0.340	0.340	1.333	0.953
	IMAVAE	0.366	0.376	1.435	0.825
	MediEncoder	0.326	0.325	1.278	0.925
3000	Projection	0.245	0.350	0.962	0.835
	Autoencoder	0.345	0.427	1.353	0.885
	VAE	0.334	0.345	1.310	0.944
	IMAVAE	0.341	0.343	1.337	0.865
	MediEncoder	0.270	0.280	1.059	0.975

Table 7: Estimator performance comparison by sample size under the nonlinear wavelet DGP with  $p = 2500$ ,  $q = 2500$ ,  $\sigma_X = 1.5$ ,  $\sigma_M = 1$ ,  $\sigma_Y = 1$ ,  $\bar{p} = \bar{q} = 5$ ,  $\tilde{p} = \tilde{q} = 7$ , and  $B = 500$  replications.

	SD		RMSE		CI Length	
	$\lambda_3 = 0$	Tuning	$\lambda_3 = 0$	Tuning	$\lambda_3 = 0$	Tuning
100	0.722	0.579	0.720	0.588	2.831	2.270
300	0.414	0.390	0.414	0.394	1.624	1.528
800	0.353	0.336	0.360	0.335	1.382	1.319
1200	0.328	0.291	0.329	0.293	1.285	1.141
2000	0.368	0.326	0.386	0.325	1.441	1.278
3000	0.340	0.270	0.341	0.280	1.331	1.059

Table 8: Ablation study on the alignment term ( $\lambda_3$ ) in MediEncoder with  $p + q = 5000$ ,  $\sigma_X = 1.5$ ,  $\sigma_M = 1$ ,  $\sigma_Y = 1$ ,  $B = 500$ ,  $\bar{p} = \bar{q} = 5$ , and  $\tilde{p} = \tilde{q} = 7$ .

$n$	Estimator	SD	RMSE	CI Length	Coverage
100	Projection	15.814	16.352	61.992	0.950
	Autoencoder	59.019	59.821	231.348	0.954
	VAE	1.227	1.228	4.810	0.966
	IMAVAE	0.537	1.248	2.104	0.892
	MediEncoder	0.565	0.572	2.214	0.934
300	Projection	2.736	2.945	10.725	0.985
	Autoencoder	2.213	2.275	8.675	0.955
	VAE	0.414	0.414	1.621	0.945
	IMAVAE	0.380	0.568	1.490	0.880
	MediEncoder	0.389	0.406	1.525	0.973
800	Projection	0.401	0.570	1.572	0.847
	Autoencoder	0.509	0.600	1.995	0.912
	VAE	0.329	0.349	1.290	0.925
	IMAVAE	0.398	0.443	1.561	0.795
	MediEncoder	0.358	0.358	1.402	0.966
1200	Projection	0.310	0.424	1.216	0.854
	Autoencoder	0.437	0.493	1.711	0.912
	VAE	0.330	0.330	1.292	0.940
	IMAVAE	0.339	0.366	1.328	0.900
	MediEncoder	0.322	0.323	1.537	0.952
2000	Projection	0.281	0.417	1.100	0.820
	Autoencoder	0.342	0.431	1.342	0.902
	VAE	0.332	0.338	1.301	0.955
	IMAVAE	0.380	0.387	1.491	0.861
	MediEncoder	0.324	0.325	1.269	0.958
3000	Projection	0.255	0.351	0.999	0.841
	Autoencoder	0.352	0.422	1.378	0.897
	VAE	0.336	0.337	1.317	0.930
	IMAVAE	0.367	0.367	1.439	0.837
	MediEncoder	0.277	0.277	1.085	0.950

Table 9: Estimator performance comparison by sample size under the nonlinear wavelet DGP with  $p = 5000$ ,  $q = 5000$ ,  $\sigma_X = 1.5$ ,  $\sigma_M = 1$ ,  $\sigma_Y = 1$ ,  $\bar{p} = \bar{q} = 5$ ,  $\tilde{p} = \tilde{q} = 7$ , and  $B = 500$  replications.

	<b>SD</b>		<b>RMSE</b>		<b>CI Length</b>	
	$\lambda_3 = 0$	Tuning	$\lambda_3 = 0$	Tuning	$\lambda_3 = 0$	Tuning
100	0.666	0.565	0.663	0.572	2.610	2.214
300	0.440	0.389	0.442	0.406	1.725	1.525
800	0.372	0.358	0.391	0.358	1.458	1.402
1200	0.357	0.322	0.363	0.323	1.401	1.537
2000	0.392	0.324	0.408	0.325	1.536	1.269
3000	0.343	0.277	0.352	0.277	1.345	1.085

Table 10: Ablation study on the alignment term ( $\lambda_3$ ) in `MediEncoder` with  $p + q = 10000$ ,  $\sigma_X = 1.5$ ,  $\sigma_M = 1$ ,  $\sigma_Y = 1$ ,  $B = 500$ ,  $\bar{p} = \bar{q} = 5$ , and  $\tilde{p} = \tilde{q} = 7$ .